VOLUME 48, NUMBER 3, SEPTEMBER 2025

HADRONIC JOURNAL Volume 48, Number 3, September 2025

HADRONIC JOURNAL

Founded in 1978 by Prof. R. M. Santilli at Harvard University. Some of the past Editors include Professors S. L. Adler, A. 0. Barut, L. C. Biedenharn, N. N. Bogoliubov, M. Froissart, J.Lohmus, S. Okubo, Nobel Laureate Ilya Prigogine, M. L. Tomber, J. P.Vigier, J. Wess, Nobel Laureate Chen Ning Yang.

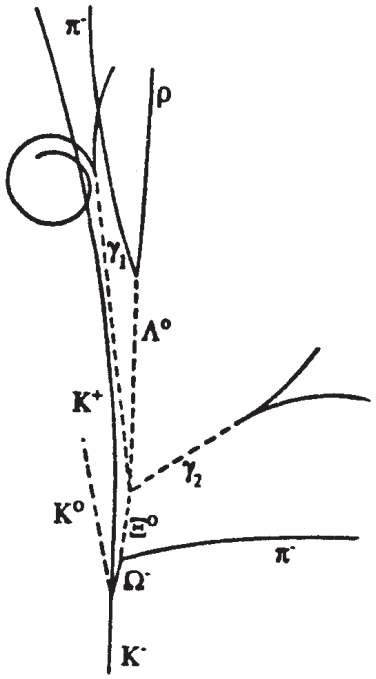

EDITORIAL BOARD

A.O.ANIMALU
A. K. ARINGAZIN
A. A. BHALEKAR
S. J. DHOBLE
J. DUNNING-DAVIES
T. L. GILL
L. P. HORWITZ
S. L. KALLA
S. I. KRUGLOV
J. LISSNER
M. NISHIOKA
R. F. O'CONNELL
Z. OZIEWICZ*
E. RECAMI*
M. SALEEM
S. SILVESTROV
H. M. SRIVASTAVA
E. TRELL
R.I. TSONCHEV
QI-REN ZHANG
C.A.WOLF
YI-ZHONG ZHUO

*In memoriam

FOUNDER and Editor In Chief
R. M. SANTILLI

HADRONIC PRESS, INC.

HADRONIC JOURNAL

Established in 1978 by Prof. R. M. Santilli at Harvard University Hadronic Journal and Algebras, Groups and Geometries have been regularly published since 1978 without publication charges and are among the few remaining independent refereed journals.

This Journal publishes advances research papers and Ph. D. theses in any field of mathematics without publication charges.

For subscription, format and any other information please visit the website
http://www.hadronicpress.com

HADRONIC PRESS INC.
35246 U. S. 19 North Suite 215
Palm Harbor, FL 34684, U.S.A.
http://www.hadronicpress.com
Email: info@hadronicpress.com
Phone: +1-727-946-0427

HADRONIC JOURNAL

Founder and Editor in Chief
RUGGERO MARIA SANTILLI
The Institute for Basic Research
35246 U. S. 19 North Suite 215, Palm Harbor, FL 34684, U.S.A.
Email: resarch@i-b-r.org; TEL: +1-727-688-3992

A. O. ANIMALU, University of Nigeria, Department of Physics, Nsukka, Nigeria animalu@nmc.edu.ng
A.K. ARINGAZIN, Department of Theoretical Physics, Institute for Basic Research Eurasian National University Astana 010008, Kazakhstan aringazin@mail.kz
A.A. BHALEKAR, Department of Chemistry, R.T.M. Nagpur University, Nagpur, 440033 India anabha@hotmail.com
S.J. DHOBLE, Department of Physics R.T.M. Nagpur University Nagpur, 440033 India sjdhoble@rediffmail.com
J. DUNNING-DAVIES, Department of Physics (Retired) University of Hull Hull, HU6 7RX England j.dunning-davies@hull.ac.uk
T. L. GILL, Howard University Research Center ComSERC Washington, DC 20059, USA tgill@howard.edu
L. P. HORWITZ, Department of Physics Tel Aviv Univ., Ramat Aviv, Israel horwitz@taunivm.tau.ac.il
S.L. KALLA, Department of Mathematics Vyas Institute of Higher Education Jodhpur, 342008, India shyamkalla@gmail.com
S.I. KRUGLOV, University of Toronto at Scarborough, Physical and Environmental Sciences Dept., 1265 Military Trail, Toronto, Ontario, Canada M1C 1A4 skrouglo@utm.utoronto.ca
J. LISSNER, Alumnus Foukzon Laboratory Center for Mathematical Sciences Technion-Israel Institute of Technology Haifa, 3200003, Israel
M. NISHIOKA, Yamaguchi University Department of Physics, Yamaguchi 753, Japan
R. F. O'CONNELL, Louisiana State University Department of Physics, Baton Rouge, LA 70803
Z.OZIEWICZ,* Universidad National Autonoma de Mexico, Faculdad de Estudios Superiores C.P. 54714, Cuautitlan Izcalli Aparto Postal # 25, Mexico **** In memoriam***
E. RECAMI, Universita' de Bergamo, Facolta' di Ingeneria, Viale Marconi 5, 1-24044 Dalmine (BG) Italy **** In memoriam***
M. SALEEM, University of the Punjab Center for High Energy Phys., Lahore, Pakistan dms@lhr.paknet.com.pk
S. SILVESTROV, School of Education, Culture and Communication (UKK) Malardalen University Box 883, 71610 Västerås, Sweden sergei.silvestrov@mdh.se
H. M. SRIVASTAVA, Department of Mathematics and Statistics, University of Victoria, Victoria, B. C. V8W 3P4, Canada, hmsri@uvvm.uvic.ca
E. TRELL, Faculty of Health Sciences, University of Linkoping, Se-581 83, Linkoping, Sweden erik.trell@gmail.com
R.I. TSONCHEV, Facultad de Fisica, Universidad Autonoma de Zacatecas, P. O. C-580, Zacatecas 98068, zac, Mexico rumen@ahobon.reduaz.ms
QI-REN ZHANG, Peking University, Department of Technical Phys., Beijing 100871, China zhangqr@sun.ihep.ac.cn
C.A. WOLF, Department of Physics, Massachusetts College of Liberal Arts, North Adams, Ma 01247 cwolf@mcla.mass.edu
YI-ZHONG ZHUO, Institute of Atomic Energy P.O. Box 275 (18) Beijing 102413, China zhuoyz@mipsa.ciae.ac.cn

HADRONIC JOURNAL

VOLUME 48, NUMBER 3, SEPTEMBER 2025

METHODS FOR EXPERIMENTAL VERIFICATION OF ISODUAL LIGHT, 247

Pietro Foralosso
The Institute for Basic Research
Palm Harbor, FL 34684

VARIATIONAL FORMULATIONS FOR A HYDROGEN NUCLEAR FUSION CHEMICAL REACTION INCLUDING AN EULERIAN CONTEXT, 265

Fabio Silva Botelho
Department of Mathematics
Federal University of Santa Catarina - UFSC
Florianópolis, SC, Brazil

DIRECT OBSERVATION OF UNUSUAL PROPERTIES OF STRONG INTERACTIONS INACCESSIBLE BY ACCELERATOR, 307

V.G. Plekhanov
Fonoriton Sci. Lab.
Garon Ltd, Tallinn 11413, Estonia

A VARIATIONAL FORMULATION FOR A TWO PHASE MODEL IN SUPERCONDUCTIVITY AND A RESPECTIVE NUMERICAL EXAMPLE, 341

Fabio Silva Botelho
Department of Mathematics
Federal University of Santa Catarina - UFSC
Florianópolis, SC, Brazil

HADRONIC JOURNAL 48, 247 - 264 (2025)
DOI 10.29083/HJ.48.03.2025/SC247

METHODS FOR EXPERIMENTAL VERIFICATION OF ISODUAL LIGHT

Pietro Foralosso
The Institute for Basic Research
Palm Harbor, FL 34684
peterfoss1979@yahoo.com

Received May 15, 2025
Revised June 16, 2025

Abstract

In this paper, we review the mathematical and physical foundation of the 1997 R. M. Santilli's paper on the hypothesis that light emitted by antimatter is an anti-Hermitean image of ordinary light, called by the author "isodual light," thus having all characteristics opposite to those of ordinary light, including negative energy and expected repulsion by a matter gravitational field; we review evidence obtained via Santilli telescopes with concave lenses of film traces that appear to be caused by galactic light with negative energy; and we propose a new method for producing isodual light in laboratory for subsequent measurements of the effects of isodual light on targets.

Copyright © 2025 by Hadronic Press, Inc., Palm Harbor, FL 34684, USA

1 Introduction

Since the time of Dirac's prediction of antiparticles and their detection, the theory of antimatter has been essentially developed at the level of second quantization.

This occurrence has created an unbalance between the theories of matter and antimatter at the classical and first quantization levels, as well as a number of shortcomings, such as the inability for the classical theory of antimatter to have a quantized formulation which is the correct charge (or PTC) conjugate of that of matter.

In order to resolve these shortcomings, in 1995 Santilli proposed a new anti-isomorphic image of conventional mathematics [2] characterized by the map of the conventional unit called isodual map, or isoduality:

$$+1 \to 1^d = -1^t = -1 \tag{1}$$

It should be noted that the change of the basic unit implies a simple, yet unique and non-trivial change of the totality of conventional mathematics, including numbers, angles, functions transforms, vector and metric spaces, algebras and geometries, etc.

This new map and isodual mathematics provide a novel classical representation of anti-matter not just on the charge conjugation level but also at gravitational level with the prediction of anti-gravity defined as the reversal of the sign of the curvature tensor for massive antiparticles in the field of matter with subsequent predictions of relevance in a number of fields [1]:

Prediction 1: Massive stable isodual particles (anti-matter made of positrons and anti-protons, such as the anti-hydrogen) experience anti-gravity (repulsive gravity) in the field of matter and ordinary gravity in the field of anti-matter.

The implications at cosmological level are profounds since this prediction suggests that galaxies made of matter naturally repel and isolate themselves from galaxies made of anti-matter except from rare instances where anti-matter objects possess too high kinetic energy to be effectively swerved away from each other and they subsequently impact against each other.

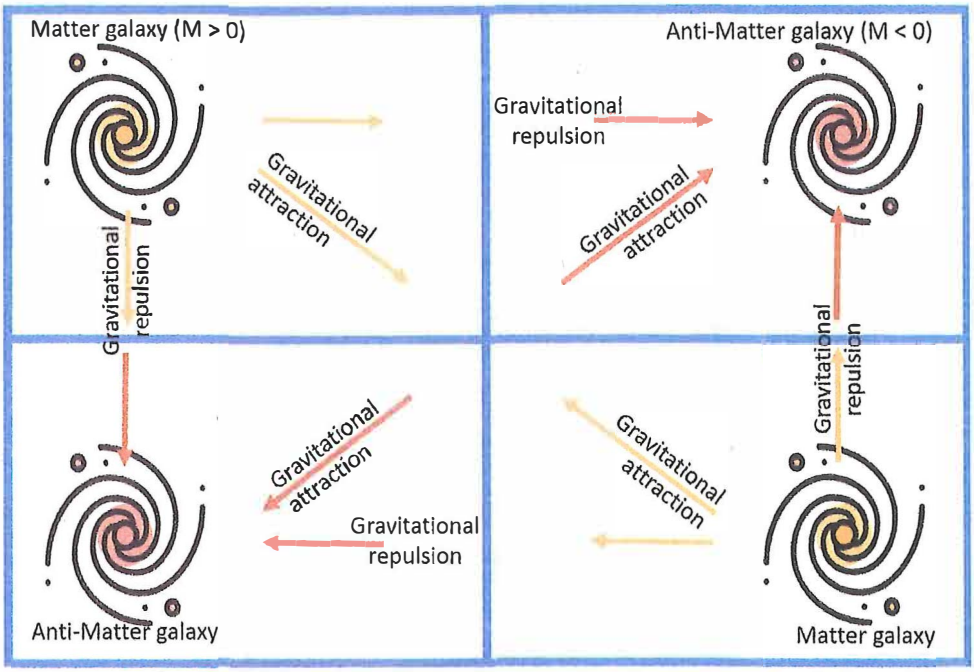

Image 1: An interpretation of matter and anti-matter gravitational interactions showing how it is possible for the two to remain gravitationally segregated.

One candidate particle for testing this prediction in a laboratory setting would be to measure the gravitational deflection of a horizontal positron beam with low enough kinetic energy so that the deflection upward or downward caused by earth gravity would be apparent at the end of the flight tube [10].

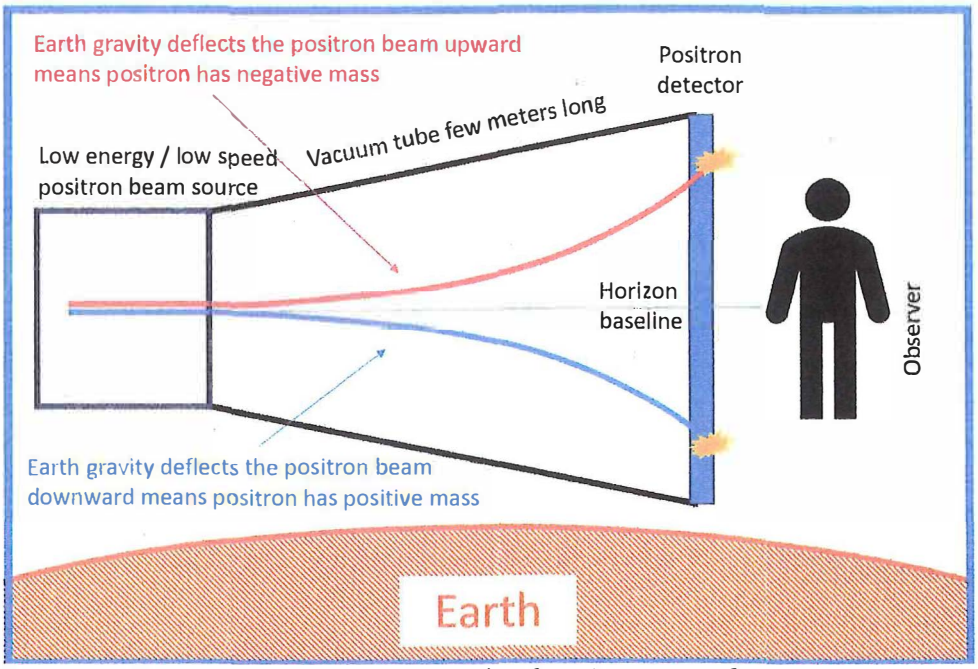

Image 2: Testing the negative mass of isolated positrons by measuring their gravitational deflection on a horizontal flight within a sufficiently shielded vacuum tube.

Prediction 2: Bound states of massive stable particles and their isoduals (such as the positronium) experience ordinary gravity in both fields of matter and anti-matter.

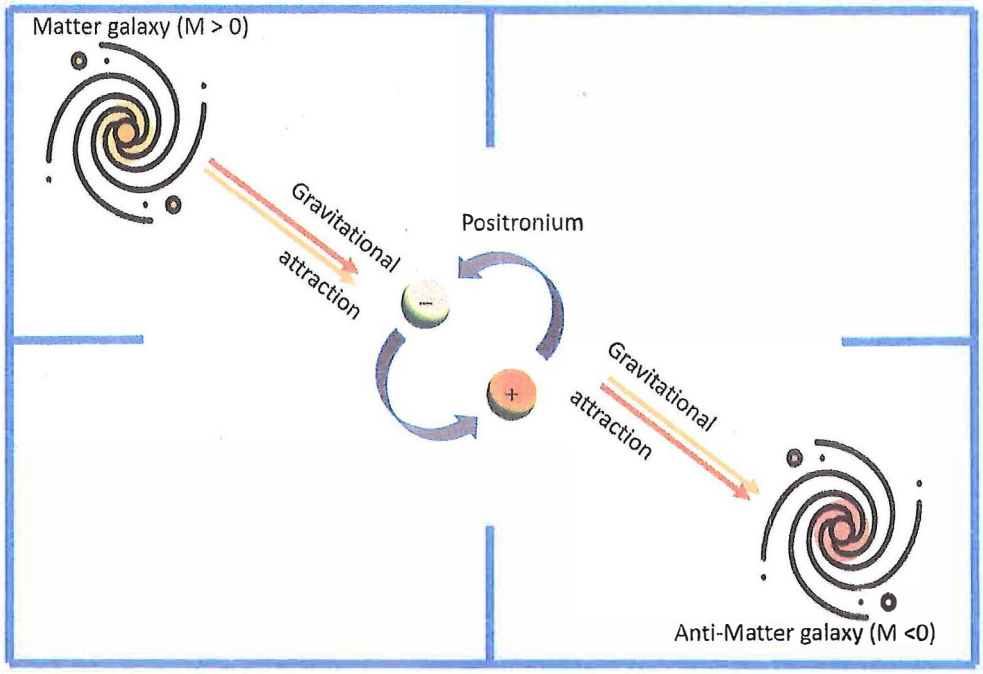

Image 3: Graphical interpretation of the positronium and the effects of gravity and anti-gravity fields being both attractive

We should hereby clarify the nature of the positronium as an isoself dual particle since it is evidently invariant under the isodual map interchanges $e \rightarrow e^d, e^d \rightarrow e$.

As such it possesses a positive spectrum E_n as referred to our spacetime, as well as exhibiting a negative spectrum when studied in the isodual spacetime.

The total state of positronium in our spacetime ($\hbar = 1$) is given by $I\,Pos > = I\,e > \times I\,e >^d$ and subsequent Schrodinger equation: [3]

$$i\frac{\partial}{\partial t} IPos > = (p_k \times p^k/2m)\, Ie > \times Ie >^d + Ie > (p_k \times p^k/2m)^d \times^d Ie >^d + V(r) \times Ie > \times Ie >^d = E_n\, IPos >,\ E_n > 0 \quad (2)$$

With a conjugate expression in isodual space-time here omitted for brevity.

This isodual interpretation of the positronium recovers the available information on electromagnetic and weak interactions of antiparticles.

When annihilating the positronium will yield one iso photon and one isodual counterpart:

$$Pos. = (e\,, e^d)_{IQM} \rightarrow \gamma + \gamma^d \qquad (3)$$

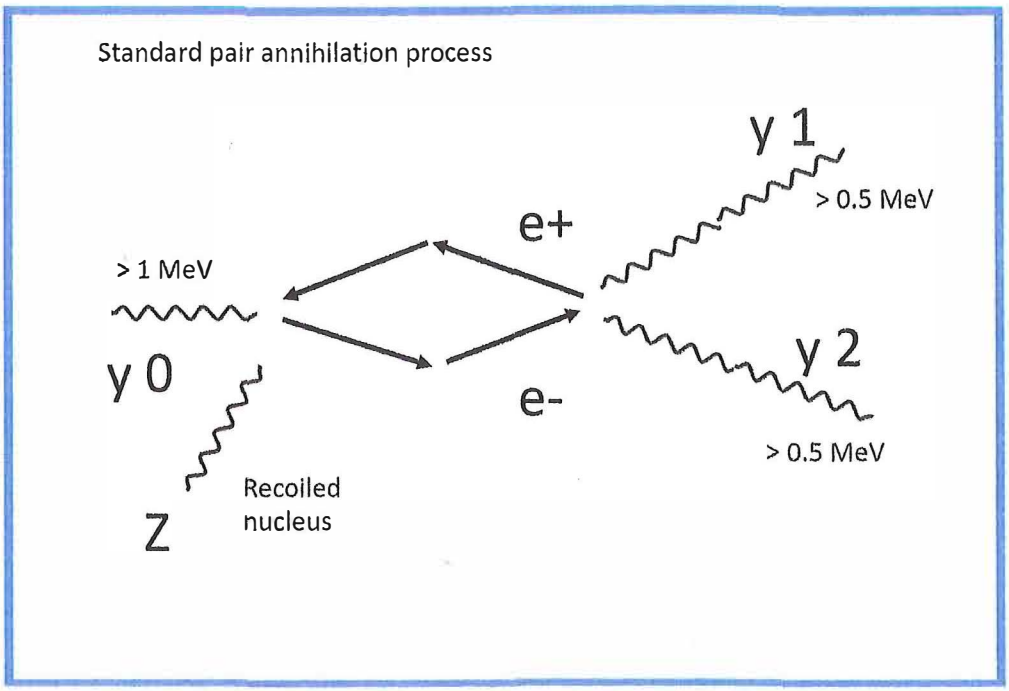

Image 4: Standard pair annihilation process with generation of 2 gamma rays both with positive energy

Prediction 3: Antimatter produces isodual photons who experience antigravity in the field of matter and anti-gravity in the field of anti-gravity.

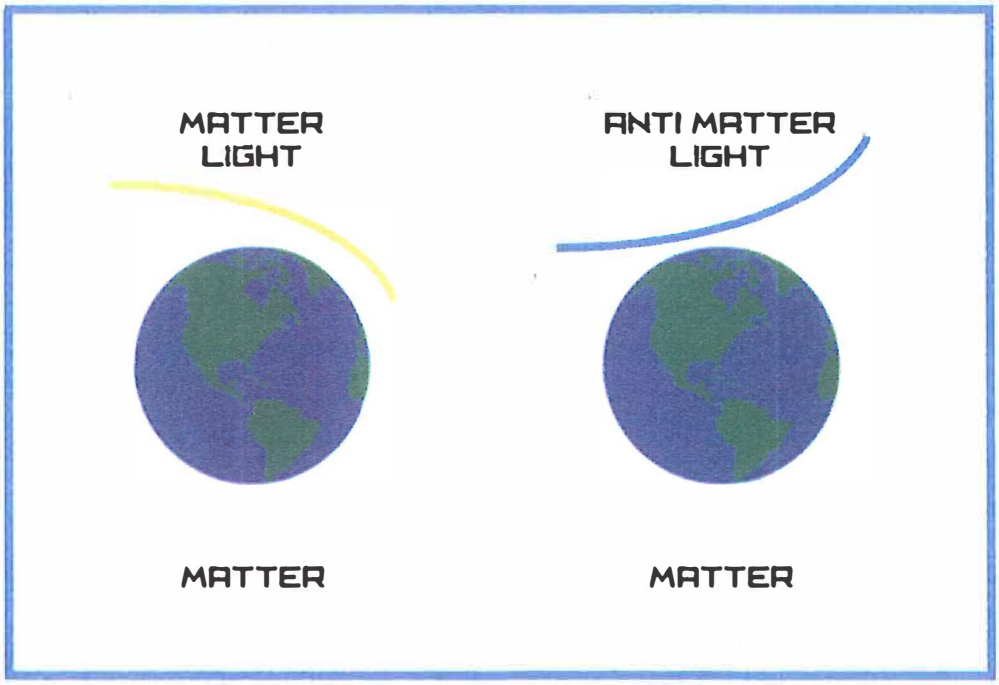

Image 5: Graphical interpretation of isodual light deflection by a gravitational field

To explain this last point we shall compare the photon and isodual photon plane wave and energy equations [3] / (2.3.59 …).

For a conventional photon we have:

$$\psi(t,r) = N \times e^{i\times(k\times r - E\times t)}, N \in R \tag{4A}$$

$$\psi(x) = N \times e^{i\times k_\mu \times x^\mu} \tag{4B}$$

$$E = h \times \nu \tag{4C}$$

Whilst the isodual photon has:

$$\psi^d(t^d,r^d) = N^d \times^d e_d^{\,i^d\times^d(k^d\times^d r^d - E^d\times^d t^d)}, N^d \in R^d \tag{5A}$$

$$\psi^d(x^d) = N^d \times^d e_d^{\,i^d\times^d k_\mu^d \times^d x^{d\mu}} \tag{5B}$$

$$E^d = h^d \times^d \nu^d \tag{5C}$$

To note that both types of photons travel in vacuum with the same absolute speed |c| for which we can verify: $k_\mu^d \times^d k^{d\mu} \equiv k_\mu \times k^\mu = 0$, and since the term i is isoselfdual then the exponents of the wave representations remain invariant thus confirming lack of contradiction between charge conjugation and isoduality.

Despite the above identities, there is a fundamental difference when describing particles in the basic $\mathcal{R}$ field (like gr, sec, cm) as opposed to an anti particle mapped into the isodual field $\mathcal{R}^d$ for which negative units of reference must be considered thus yielding $gr^d = -gr, sec^d = -sec, cm^d = -cm$, etc.

Through this transformation we then have that a negative energy particle moving backward in time remains causal in our frame of reference as our normally observed positive energy particles moving forward in time.
Therefore the energy of the normal photon above becomes:

$$E = h \times \nu > 0_{\mathcal{R}} \tag{4D}$$

Whilst the isodual photon is expressed as:

$$E^d = h^d \times^d \nu^d < 0_{\mathcal{R}^d} \tag{5D}$$

Thus verifying repulsion of the isodual photons in matter gravitational fields.

2 Additional experimental verification of anti-matter light

During recent years experiments were conducted to test isodual light theory by observing the night sky by means of specially conceived telescopes featuring concave lenses, and subsequent observations of dark streaks on the camera sensor [4], [5].

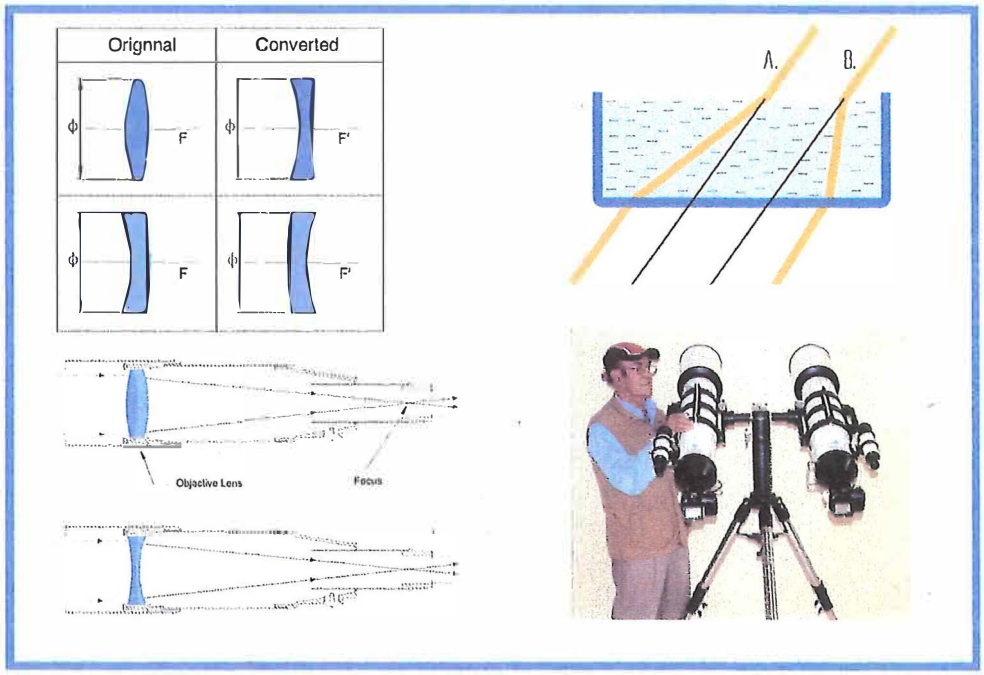

Image 6: Experimental setup for detection of anti-matter light by means of concave lenses as opposed to convex ones because of the negative angle of refraction.

The experimental results seem to extend prediction 3 to the following reformulation:

Prediction 4: In addition to experiencing anti-gravity in the domain of matter, the isolight also experiences negative coefficient of refraction as well as negative energy as referred to the domain of regular matter.

3 Theorical framework of isodual light production

We shall recall in equation (3) how the annihilation of positronium would yield one photon γ along with an anti-photon γ^d .

The energy content of isodual photon γ^d would appear to be positive as seen in the domain of matter, since all experiments involving electron positron annihilation indeed show experimental observation of said photon pairs (on

average) and also account for two positive electron masses as opposed to just one positive electron mass (energy) and one negative positron mass (energy).

This fact would also appear to be in conflict with observations with Galileo-Santilli's telescopes where isodual light appears to have negative energy content per prediction 4.

We here present, apparently for the first time, a resolution of said conflicts by proposing that the positron electron annihilation process is in fact the annihilation of 2 electrons and 2 positrons, with equation (3) now being rewritten as follow:

$$Pos. = (e\,, e^d)_{IQM} = e + e^d = e + a_e + e^d + a_{e^d} = 2\,e + 2\,e^d \rightarrow 2\,\gamma + 2\,\gamma^d \qquad (6)$$

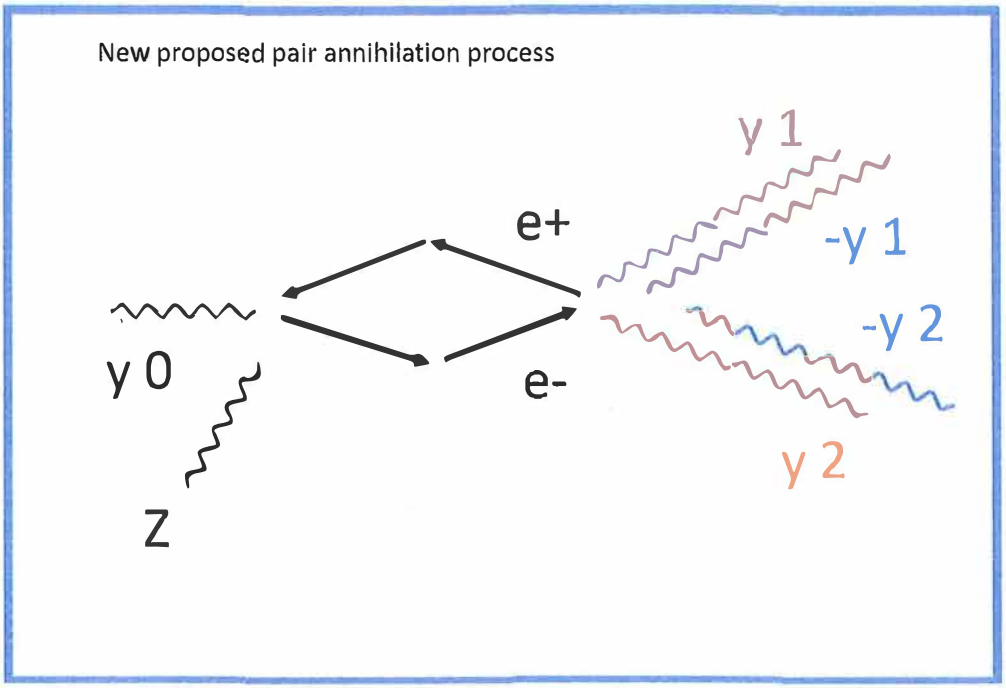

Image 7: New interpretation of the pair annihilation process with total generation of 4 photons

Whereas the annihilation process of one electron and one positron yields in fact the annihilation of 2 electrons and 2 positrons with net emission of 2 positive

energy gamma rays normally detected in experimental setups as well as 2 negative energy gamma rays.

To understand equation (6) we must also reference the theorical framework of hadron mechanic formulations, where not all strong interactions necessarily conserve mass and energy since excess energy can be provided by aetherinos [7]:

The excess mass of the neutron of 0.78 MeV when referred to a bound state of a proton and electron.

$$p^+ + a_n + e^- \rightarrow n \tag{7}$$

$$E_{a_n} = 0.782\ MeV \tag{8}$$

The excess mass of pions, kahons, etc when referred to bond states of electrons and positrons in a state of partial mutual penetration.

$$e^+ + a_{\pi_0} + e^- \rightarrow \pi_0 \tag{9}$$

$$E_{\pi_0} = 133.95\ MeV \tag{10}$$

In the case of equation (6), the strong interaction of electron and positron within their isoselfdual state seems to imply an aetheric interaction which namely doubles the number of effective particles at play in the annihilation process.

Moreover in equation (6) there are no new law of conservation of matter (and separately of anti-matter) because of the finite transition probability among these particles established by the Dirac's equation.

Nominally the mass of the positron, being negative as seen from our ISO state, would not violate mass conservation when its appearance out of the aetheric substrate is associated with an electron paired to said positron which fully balance the total mass of the system when accounting for positive masses (of electrons) and negative masses (of positrons).

4 Production of isodual light by means of laser beams

A first possibility to test the conjecture in (6) is to generate bunches of electron-positron pairs [8] by means of a powerful laser beam pointed toward a suitable metallic target.

The subsequent annihilation of electron positron should yield a great number of gamma rays along with "anti-gamma rays" (isodual photons).

The gamma rays can be focused toward a suitable target by means of standard concave lenses and is focused toward a metallic target (ie lead) capable of adsorbing said gamma rays thus causing the metal to warm up.

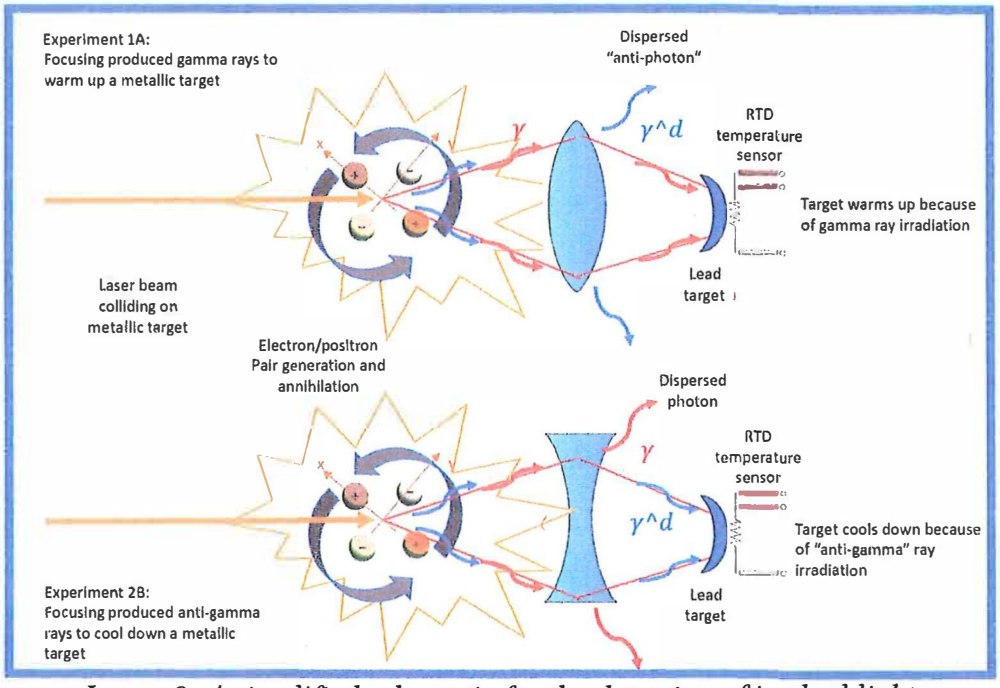

Image 8: A simplified schematic for the detection of isodual light

The anti-gamma ray (or isoselfdual photons) can only be focused by means of concave lenses similarly to what has been done in Santilli's telescopes.

The target should subsequently show a decrease in temperature because of the negative energy content of the isoselfdual photons.

The limits of said experimental method lie in the difficulty of delivering a sufficiently powerful laser capable of exciting pair production beyond the energy threshold of circa 1 MeV per pair.

In this case being 2 x m_e= 2 x 0.511 MeV = 1.022 MeV would require the use of Titan grade laser setup similar to the ones used in inertial nuclear fusion experiments.

5 Production of isodual light by means of positron cyclotron radiation

A possible simplification of the experimental setup depicted in image 8 would be to use a positron source and subsequently use magnetic fields to induce cyclotron or synchrotron radiation to generate a focused isodual light beam.

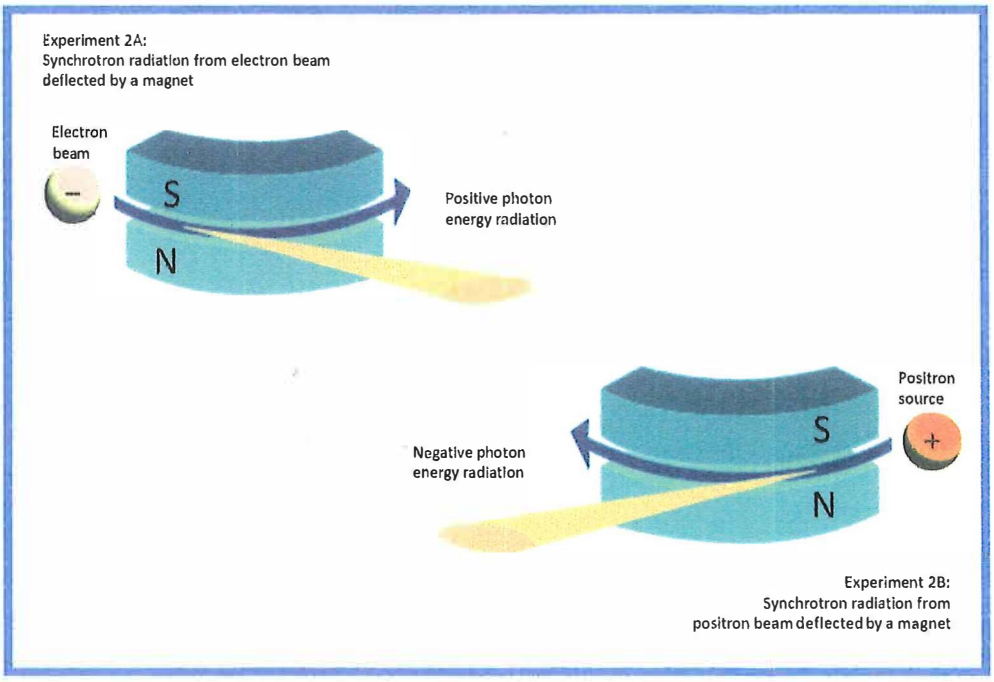

Image 9: Synchrotron radiation from electrons and positron beams should generate photons with positive and negative energy content respectively

Once again a suitable metallic target should be placed radially to intercept the radiation from the positron beam and a cool down effect should be measured.

In this experimental setup the challenge is to obtain a powerful, well focused positron source capable of delivering sufficient radiation power to the target and induce a measurable cooling.

A different approach for the detection and study of positron radiation is to use an undulator setup capable of more effectively converting the positron (negative!) kinetic energy into a well-focused isodual light beam per proposed experimental setup in image 10.

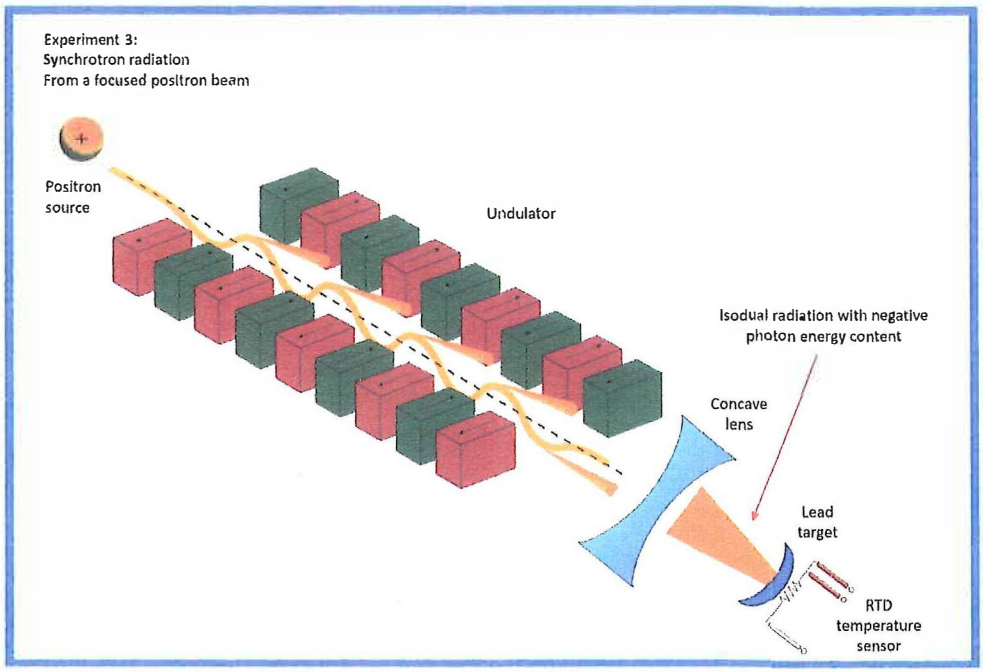

Image 10: Synchrotron radiation from a positron / undulator

In this setup we are once again attempting measuring a temperature drop on the radiation target, however a more precise detection could be achieved by means of a camera sensor and a suitable light source of the same frequency as the produced undulator light per image 11:

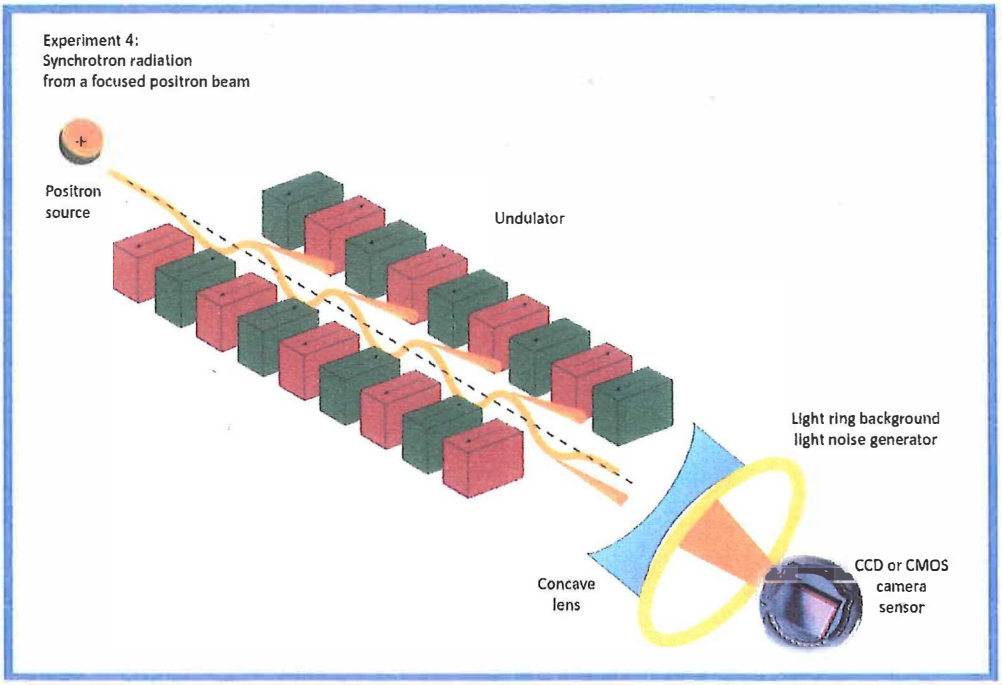

Image 11: Dimming of background radiation by means of a focused isodual light beam

In this final setup we have added a camera sensor similar to a Santilli telescope, as well as an artificial light source or light ring.

This normal light source is meant to provide an electromagnetic background noise toward the camera sensor of the same frequency of the cyclotron radiation produced by the undulator and with a comparable radiated power of the undulator radiation.

The goal of this setup is to measure a dimming of the background noise light from the light ring when positron beams are fed into the undulator in a similar way the detection of anti-matter galaxies leave "dark streaks" on camera sensors otherwise detecting mostly background noise radiation.

6 Possible interactions between isodual light and normal matter

The study of isodual light has been thus far confined to the detection of said radiation emitted by anti-matter galaxies leaving dark streaks on standard camera sensors [5].

This light is indeed very faint and with a fairly low energy content, thus inducing only but minor cooling on electrons or atoms adsorbing it.

The possibility of producing well focused and potentially high (negative!) energy isodual light beams per the methods hereby described can now open a number of applications in the domain of cryogenics and other setups using isodual light beams as the main cooling method as opposed to conventional mechanical cryogenic machines.

An intriguing albeit highly speculative hypothesis at this stage is the possibility to cool electrons or atoms down to temperatures below zero Kelvin.

This has already been achieved [9] on a handful of ions trapped in a lattice matrix at a temperature few billionths of a degree below absolute zero, for which an apparent reversal of gravity was observed as said ions tended to gather toward the top of the magnetic bottle setup as opposed to the bottom prior to sub kelvin cooling.

The apparent reversal of gravity on matter cooled below zero Kelvin could be explained either as a change of the particle mass from positive to negative OR it might have been caused by the reversal of the isodual unit of reference from 1 into -1 (see ref [2] as well as formula (1)), thus implying:

Prediction 5: Matter cooled below zero Kelvin experiences antigravity (repulsion) in the domain of matter and gravity (attraction) in the domain of anti-matter.

Likewise anti-matter heated above zero Kelvin experiences antigravity in the domain of anti-matter and gravity in the domain of matter.

Finally, we would like to propose one last possible interaction of matter with isodual light, when an anti-photon is energetic enough not just to cause an

intercepting electron to cool down to below zero Kelvin, but is powerful enough to reverse the mass of the electron from positive into negative, thus causing the electron to flip into a negative mass positron:

$$e^- + \gamma^d = e^{-d} = e^+ \tag{11}$$

Whereas the minimum energy of the anti-photon γ^d for this reaction to occur must be greater than 1.022 MeV in order to energetically offset the "un-creation" of a positive mass electron (0.511 MeV) as well as provide sufficient negative energy for the "creation" of a negative mass positron (-0.511 MeV), whilst the kinetic energy content of the original electron is hereby ignored from this mass balance because of its negligible value compared to the mass terms.

The experimental detection of said reaction should be pretty straightforward to achieve since the subsequent annihilation of the produced positron against common electrons would yield a very characteristic gamma ray signature in the range of 0.5 MeV.

References

[1] Does antimatter emit a new light?
https://www.santilli-foundation.org/docs/Santilli-28.pdf

[2] Problematic aspects of 20-th century antiparticles and their apparent resolution via isodual mathematics
https://www.santilli-foundation.org/docs/7-RM-SI-Vol-52-2024-fin.pdfp

[3] *Isodual Theory of Antimatter with Application to Antigravity, Grand Unification and the Spacetime Machine*
http://www.santilli-foundation.org/docs/santilli-79.pdf

[4] Apparent Detection of a New Antimatter Galaxy in the Capella Region of the Night Sky
https://www.santilli-foundation.org/docs/capella-antimatter-galaxy.pdf

[5] Apparent detection of antimatter galaxies via a refractive telescope with concave lenses
http://www.santilli-foundation.org/docs/Antimatter-telescope-2013-final.pdf

[6] Additional experimental confirmations of Santilli's IsoRedShift and the consequential expected absence of the universe expansion
https://www.santilli-foundation.org/docs/IRS-confirmations-212.pdf

[7] The Etherino and/or the Neutrino Hypothesis
https://santilli-foundation.org/docs/EtherinoFoundPhys.pdf

[8] Pair production
https://en.wikipedia.org/wiki/Pair_production

[9] A temperature below absolute zero
https://www.sciencedaily.com/releases/2013/01/130104143516.htm

[10] Scientific description of Santilli's comparative test of the gravity of electrons and positrons in a horizontal super-cooled vacuum tube
https://www.santilli-foundation.org/docs/Santilli-gravity-experiment.pdf

HADRONIC JOURNAL 48, 265 - 306 (2025)
DOI 10.29083/HJ.48.03.2025/SC265

VARIATIONAL FORMULATIONS FOR A HYDROGEN NUCLEAR FUSION CHEMICAL REACTION INCLUDING AN EULERIAN CONTEXT

Fabio Silva Botelho
Department of Mathematics
Federal University of Santa Catarina - UFSC
Florianópolis, SC, Brazil
fabio.botelho@ufsc.br

Received October 3, 2024
Revised June 17, 2025

Abstract

This article develops variational formulations for a chemical reaction corresponding to a hydrogen nuclear fusion. The results are obtained through standard tools of calculus of variations and optimization theory in function spaces.

In such a chemical reaction, at an appropriate high temperature, a Deuterium ion reacts with a Tritium one resulting a Helium ion and an energetic neutron.

We highlight such a reaction result of an energetic neutron field has a great variety of practical applications, including the possibility of clean electric energy production.

Finally, we also emphasize in the last sections the results have been developed in an Eulerian context.

AMS Classification 70G75, 76A02, 76N15
Keywords. Variational formulation, hydrogen nuclear fusion, high temperature scalar field.

Copyright © 2025 by Hadronic Press, Inc., Palm Harbor, FL 34684, USA

1 Introduction

In this article we obtain variational formulations for modeling a hydrogen nuclear fusion in a high temperature process.

Recalling that a deuterium hydrogen atom is comprised by one proton, one neutron and one electron, a tritium hydrogen atom is comprised by one proton, two neutrons and one electron, a helium atom is comprised by two protons, two neutrons and two electrons, we consider a gas comprised by deuterium and an amount of tritium, which at a high temperature are ionized resulting in a plasma which chemically reacts resulting in a helium field and an energetic neutron one.

Such a chemical reaction may be summarized by the following equation

$$\text{Deuterium}^{+} + \text{ Tritium}^{+} \rightarrow \text{ Helium}^{++} + \text{ Neutron (Energetic)}.$$

In terms of mass we shall represent this reaction as it follows:

$$1 = \alpha_D + \alpha_T = \alpha_{H_e} + \alpha_N,$$

that is, a unit mass fraction α_D of Deuterium reacts with a unit mass fraction α_T of tritium, resulting in a unit mass fraction α_{H_e} of Helium and a unit mass fraction α_N of neutrons.

We emphasize the results here presented have been obtained through standard tools of calculus of variations, basic constrained optimization and related Lagrange multipliers approach in infinite dimensional spaces.

Furthermore, as standard references in theoretical fluid mechanics we would cite [1, 2, 3, 4, 5, 6]. For related numerical methods we would mention [7, 8, 9]. Concerning similar models, we would cite [10, 11, 12, 13, 14].

Finally, details on the Sobolev and other function spaces involved may be found in [15].

2 The main variational formulation for a Lagrangian approach

Let $\Omega \subset \mathbb{R}^3$ be an open, bounded and connected set with a regular (Lipschitzian) boundary denoted by $\partial\Omega$.

Denoting time by t we consider such a nuclear fusion process develops in Ω on a time interval $[0, t_f]$, so that $t \in [0, t_f]$.

We define the following density fields:

For the Deuterium proton,

$$\rho_D^p(x,y,z,t) = |\hat{\phi}_D^p(x,y,z,t)|^2 |\phi_D^A(y,z,t)|^2 |\phi_D(z,t)|^2 \frac{m_p}{m_D^A} \equiv |\phi_D^p(x,y,z,t)|^2,$$

Here, ρ_D^p stands for the density of a proton field in (x, y, z, t), at an Deuterium atom with density at (y, z, t) and with a macroscopic Deuterium density in $(z, t) \in \Omega \times [0, t_f]$.

Similarly, for the Deuterium neutron density field, we define

$$\rho_D^N(x,y,z,t) = |\hat{\phi}_D^N(x,y,z,t)|^2 |\phi_D^A(y,z,t)|^2 |\phi_D(z,t)|^2 \frac{m_N}{m_D^A} \equiv |\phi_D^N(x,y,z,t)|^2.$$

For the Tritium proton field

$$\rho_T^p(x,y,z,t) = |\hat{\phi}_T^p(x,y,z,t)|^2 |\phi_T^A(y,z,t)|^2 |\phi_T(z,t)|^2 \frac{m_p}{m_T^A} \equiv |\phi_T^p(x,y,z,t)|^2.$$

and for the tritium neutron fields

$$\rho_T^{N_1}(x,y,z,t) = |\hat{\phi}_T^{N_1}(x,y,z,t)|^2 |\phi_T^A(y,z,t)|^2 |\phi_T(z,t)|^2 \frac{m_N}{m_T^A}| \equiv |\phi_T^{N_1}(x,y,z,t)|^2$$

and

$$\rho_T^{N_2}(x,y,z,t) = |\hat{\phi}_T^{N_2}(x,y,z,t)|^2 |\phi_T^A(y,z,t)|^2 |\phi_T(z,t)|^2 \frac{m_N}{m_T^A} \equiv |\phi_T^{N_2}(x,y,z,t)|^2.$$

For the Helium protons, we define

$$\rho_{H_e}^{p_1}(x,y,z,t) = |\hat{\phi}_{H_e}^{p_1}(x,y,z,t)|^2 |\phi_{H_e}^A(y,z,t)|^2 |\phi_{H_e}(z,t)|^2 \frac{m_p}{m_{H_e}^A} \equiv |\phi_{H_e}^{p_1}(x,y,z,t)|^2$$

and

$$\rho_{H_e}^{p_2}(x,y,z,t) = |\hat{\phi}_{H_e}^{p_2}(x,y,z,t)|^2 |\phi_{H_e}^A(y,z,t)|^2 |\phi_{H_e}(z,t)|^2 \frac{m_p}{m_{H_e}^A} \equiv |\phi_{H_e}^{p_2}(x,y,z,t)|^2.$$

For the Helium neutron fields

$$\rho_{H_e}^{N_1}(x,y,z,t) = |\hat{\phi}_{H_e}^{N_1}(x,y,z,t)|^2 |\phi_{H_e}^A(y,z,t)|^2 |\phi_{H_e}(z,t)|^2 \frac{m_N}{m_{H_e}^A} \equiv |\phi_{H_e}^{N_1}(x,y,z,t)|^2$$

and

$$\rho_{H_e}^{N_2}(x,y,z,t) = |\hat{\phi}_{H_e}^{N_2}(x,y,z,t)|^2 |\phi_{H_e}^A(y,z,t)|^2 |\phi_{H_e}(z,t)|^2 \frac{m_N}{m_{H_e}^A} \equiv |\phi_{H_e}^{N_2}(x,y,z,t)|^2.$$

For the single neutron field

$$\rho_N(y,z,t) = |\hat{\phi}_N(y,z,t)|^2 |\phi_N^M(z,t)|^2 \equiv |\phi_N(y,z,t)|^2$$

where ϕ_N^M denotes the macroscopic neutron density field.

Finally, for the electronic field resulting from the ionization of Deuterium and Tritium atoms,

$$\rho_e = |\hat{\phi}_e(y,z,t)|^2 |\phi_e^M(z,t)|^2 \equiv |\phi_e(y,z,t)|^2$$

where again ϕ_e^M denotes the macroscopic electronic density field.

The corresponding position fields stand for:

For the Deuterium proton

$$\mathbf{r}_D^p(x,y,z,t) = \mathbf{r}_D(z,t) + \mathbf{r}_D^A(y,z,t) + \hat{\mathbf{r}}_D^p(x,y,z,t),$$

where $\mathbf{r}_D(z,t)$ is the macroscopic Deuterium position field in (z,t), $\mathbf{r}_D^A(y,z,t)$ refers to the atom position field in (y,z,t) and $\hat{\mathbf{r}}_D^p(x,y,z,t)$ is the microscopic proton position field.

Similarly, for the Deuterium neutron position field we denote

$$\mathbf{r}_D^N(x,y,z,t) = \mathbf{r}_D(z,t) + \mathbf{r}_D^A(y,z,t) + \hat{\mathbf{r}}_D^N(x,y,z,t).$$

For the tritium proton

$$\mathbf{r}_T^p(x,y,z,t) = \mathbf{r}_T(z,t) + \mathbf{r}_T^A(y,z,t) + \hat{\mathbf{r}}_T^p(x,y,z,t),$$

and for the tritium neutron fields

$$\mathbf{r}_T^{N_1}(x,y,z,t) = \mathbf{r}_T(z,t) + \mathbf{r}_T^A(y,z,t) + \hat{\mathbf{r}}_T^{N_1}(x,y,z,t)$$

and

$$\mathbf{r}_T^{N_2}(x,y,z,t) = \mathbf{r}_T(z,t) + \mathbf{r}_T^A(y,z,t) + \hat{\mathbf{r}}_T^{N_2}(x,y,z,t).$$

For the Helium proton position fields, we denote

$$\mathbf{r}_{H_e}^{p_1}(x,y,z,t) = \mathbf{r}_{He}(z,t) + \mathbf{r}_{H_e}^A(y,z,t) + \hat{\mathbf{r}}_{H_e}^{p_1}(x,y,z,t)$$

and

$$\mathbf{r}_{H_e}^{p_2}(x,y,z,t) = \mathbf{r}_{H_e}(z,t) + \mathbf{r}_{H_e}^A(y,z,t) + \hat{\mathbf{r}}_{H_e}^{p_2}(x,y,z,t).$$

For the Helium neutron fields, we denote

$$\mathbf{r}_{H_e}^{N_1}(x,y,z,t) = \mathbf{r}_{He}(z,t) + \mathbf{r}_{H_e}^A(y,z,t) + \hat{\mathbf{r}}_{H_e}^{N_1}(x,y,z,t)$$

and

$$\mathbf{r}_{H_e}^{N_2}(x,y,z,t) = \mathbf{r}_{H_e}(z,t) + \mathbf{r}_{H_e}^A(y,z,t) + \hat{\mathbf{r}}_{H_e}^{N_2}(x,y,z,t).$$

For the neutron field

$$\mathbf{r}_N(y,z,t) = \mathbf{r}_N^M(z,t) + \hat{\mathbf{r}}_N(y,z,t)$$

Finally, for the electronic field resulting from ionization,

$$\mathbf{r}_e(y,z,t) = \mathbf{r}_e^M(z,t) + \hat{\mathbf{r}}_e(y,z,t)$$

The system is subject to the following constraints

$$\int_\Omega |\hat{\phi}_D^p(x,y,z,t)|^2\, dx = 1,$$

$$\int_\Omega |\hat{\phi}_D^N(x,y,z,t)|^2\, dx = 1,$$

$$\int_\Omega |\hat{\phi}_T^p(x,y,z,t)|^2\, dx = 1,$$

$$\int_\Omega |\hat{\phi}_T^{N_1}(x,y,z,t)|^2\, dx = 1,$$

$$\int_\Omega |\hat{\phi}_T^{N_2}(x,y,z,t)|^2\, dx = 1,$$

$$\int_\Omega |\hat{\phi}_{H_e}^{p_1}(x,y,z,t)|^2\, dx = 1,$$

$$\int_\Omega |\hat{\phi}_{H_e}^{p_2}(x,y,z,t)|^2\, dx = 1,$$

$$\int_\Omega |\hat{\phi}_{H_e}^{N_1}(x,y,z,t)|^2\, dx = 1,$$

$$\int_\Omega |\hat{\phi}_{H_e}^{N_2}(x,y,z,t)|^2\, dx = 1,$$

in $\Omega \times \Omega \times [0, t_f]$,

$$\int_\Omega |\hat{\phi}_N(y,z,t)|^2\, dy = 1,$$

$$\int_\Omega |\hat{\phi}_e(y,,z,t)|^2\, dy = 1,$$

$$\int_\Omega |\phi_D^A(y,z,t)|^2\, dy = 1,$$

$$\int_\Omega |\phi_T^A(y,z,t)|^2\, dy = 1,$$

and

$$\int_\Omega |\hat{\phi}_{H_e}^A(y,z,t)|^2\, dy = 1,$$

in $\Omega \times [0, t_f]$.

Defining

$$m_D(t) = \int_\Omega |\phi_D(z,t)|^2 \, dz,$$

$$m_T(t) = \int_\Omega |\phi_T(z,t)|^2 \, dz,$$

$$m_{H_e}(t) = \int_\Omega |\phi(z,t)_{H_e}|^2 \, dz,$$

$$m_N(t) = \int_\Omega |\phi_N^M(z,t)|^2 \, dz,$$

and

$$m_e(t) = \int_\Omega |\phi_e^M(z,t)|^2 \, dz,$$

and denoting

$$\rho_D(z,t) = |\phi_D(z,t)|^2,$$

$$\rho_T(z,t) = |\phi_T(z,t)|^2,$$

$$\rho_{H_e}(z,t) = |\phi_{H_e}(z,t)|^2,$$

$$\rho_N^M(z,t) = |\phi_N^M(z,t)|^2,$$

$$\rho_e^M(z,t) = |\phi_e^M(z,t)|^2,$$

and

$$\mathbf{v}_D = \frac{\partial \mathbf{r}_D(z,t)}{\partial t},$$

$$\mathbf{v}_T = \frac{\partial \mathbf{r}_T(z,t)}{\partial t},$$

$$\mathbf{v}_{H_e} = \frac{\partial \mathbf{r}_{H_e}(z,t)}{\partial t},$$

$$\mathbf{v}_N = \frac{\partial \mathbf{r}_N^M(z,t)}{\partial t},$$

and

$$\mathbf{v}_e = \frac{\partial \mathbf{r}_e^M(z,t)}{\partial t},$$

other constraints may be expressed by

$$\begin{aligned} m_D(t) &= (m_0)_D - \int_0^t \int_{\partial\Omega} \rho_D(z,\tau)\mathbf{v}_D(z,\tau)\cdot\mathbf{n}\, dSd\tau \\ &\quad -\alpha_D[m_{H_e}(t)+m_N(t)] - \alpha_D \int_0^t \int_{\partial\Omega} \rho_{H_e}(z,\tau)\mathbf{v}_{H_e}(z,\tau)\cdot\mathbf{n}\, dSd\tau \\ &\quad -\alpha_D \int_0^t \int_{\partial\Omega} \rho_N^M(z,\tau)\mathbf{v}_N(z,\tau)\cdot\mathbf{n}\, dSd\tau \end{aligned} \tag{1}$$

$$\begin{aligned} m_T(t) &= (m_0)_T - \int_0^t \int_{\partial\Omega} \rho_T(z,\tau)\mathbf{v}_T(z,\tau)\cdot\mathbf{n}\, dSd\tau \\ &\quad -\alpha_T[m_{H_e}(t)+m_N(t)] - \alpha_T \int_0^t \int_{\partial\Omega} \rho_{H_e}(z,\tau)\mathbf{v}_{H_e}(z,\tau)\cdot\mathbf{n}\, dSd\tau \\ &\quad -\alpha_T \int_0^t \int_{\partial\Omega} \rho_N^M(z,\tau)\mathbf{v}_N(z,\tau)\cdot\mathbf{n}\, dSd\tau \end{aligned} \tag{2}$$

$$\begin{aligned} &\alpha_N \left(m_{H_e}(t) + \int_0^t \int_{\partial\Omega} \rho_{H_e}(z,\tau)\mathbf{v}_{H_e}(z,\tau)\cdot\mathbf{n}\, dSd\tau \right) \\ = \;& \alpha_{H_e} \left(m_N(t) + \int_0^t \int_{\partial\Omega} \rho_N^M(z,\tau)\mathbf{v}_N(z,\tau)\cdot\mathbf{n}\, dSd\tau \right) \end{aligned} \tag{3}$$

$$m_e(t) = (m_0)_e - \int_0^t \int_{\partial\Omega} \rho_e^M(z,\tau)\mathbf{v}_e(z,\tau)\cdot\mathbf{n}\, dSd\tau, \tag{4}$$

where $\mathbf{n}$ denotes the outward normal field to $\partial\Omega = S$.

At this point, we define the kinetics energy functional E_C by

$$
\begin{aligned}
E_c \;=\; & \frac{1}{2}\int_0^{t_f}\int_\Omega\int_\Omega\int_\Omega \rho_D^p \frac{\partial \mathbf{r}_D^p}{\partial t}\cdot\frac{\partial \mathbf{r}_D^p}{\partial t}\,dxdydzdt \\
& +\frac{1}{2}\int_0^{t_f}\int_\Omega\int_\Omega\int_\Omega \rho_D^N \frac{\partial \mathbf{r}_D^N}{\partial t}\cdot\frac{\partial \mathbf{r}_D^N}{\partial t}\,dxdydzdt \\
& +\frac{1}{2}\int_0^{t_f}\int_\Omega\int_\Omega\int_\Omega \rho_T^p \frac{\partial \mathbf{r}_T^p}{\partial t}\cdot\frac{\partial \mathbf{r}_T^p}{\partial t}\,dxdydzdt \\
& +\frac{1}{2}\int_0^{t_f}\int_\Omega\int_\Omega\int_\Omega \rho_T^{N_1} \frac{\partial \mathbf{r}_T^{N_1}}{\partial t}\cdot\frac{\partial \mathbf{r}_T^{N_1}}{\partial t}\,dxdydzdt \\
& +\frac{1}{2}\int_0^{t_f}\int_\Omega\int_\Omega\int_\Omega \rho_T^{N_2} \frac{\partial \mathbf{r}_T^{N_2}}{\partial t}\cdot\frac{\partial \mathbf{r}_T^{N_2}}{\partial t}\,dxdydzdt \\
& +\frac{1}{2}\int_0^{t_f}\int_\Omega\int_\Omega\int_\Omega \rho_{He}^{p_1} \frac{\partial \mathbf{r}_{He}^{p_1}}{\partial t}\cdot\frac{\partial \mathbf{r}_{He}^{p_1}}{\partial t}\,dxdydzdt \\
& +\frac{1}{2}\int_0^{t_f}\int_\Omega\int_\Omega\int_\Omega \rho_{He}^{p_2} \frac{\partial \mathbf{r}_{He}^{p_2}}{\partial t}\cdot\frac{\partial \mathbf{r}_{He}^{p_2}}{\partial t}\,dxdydzdt \\
& +\frac{1}{2}\int_0^{t_f}\int_\Omega\int_\Omega\int_\Omega \rho_{He}^{N_1} \frac{\partial \mathbf{r}_{He}^{N_1}}{\partial t}\cdot\frac{\partial \mathbf{r}_{He}^{N_1}}{\partial t}\,dxdydzdt \\
& +\frac{1}{2}\int_0^{t_f}\int_\Omega\int_\Omega\int_\Omega \rho_{He}^{N_2} \frac{\partial \mathbf{r}_{He}^{N_2}}{\partial t}\cdot\frac{\partial \mathbf{r}_{He}^{N_2}}{\partial t}\,dxdydzdt \\
& +\frac{1}{2}\int_0^{t_f}\int_\Omega\int_\Omega \rho_N \frac{\partial \mathbf{r}_N}{\partial t}\cdot\frac{\partial \mathbf{r}_N}{\partial t}\,dydzdt \\
& +\frac{1}{2}\int_0^{t_f}\int_\Omega\int_\Omega \rho_e \frac{\partial \mathbf{r}_e}{\partial t}\cdot\frac{\partial \mathbf{r}_e}{\partial t}\,dydzdt, \qquad (5)
\end{aligned}
$$

Here we define the functional E_q where

$$
\begin{aligned}
E_q \;=\; & \frac{\gamma_D^p}{2}\int_0^{t_f}\int_\Omega\int_\Omega\int_\Omega \left|\nabla_x\phi_D^p - iw_D^p\mathbf{A}(z,t)\;\phi_D^p\right|^2\; dxdydzdt \\
& +\frac{\gamma_D^N}{2}\int_0^{t_f}\int_\Omega\int_\Omega\int_\Omega \left|\nabla_x\phi_D^N - iw_D^N\mathbf{A}(z,t)\;\phi_D^N\right|^2\; dxdydzdt \\
& +\frac{\gamma_T^p}{2}\int_0^{t_f}\int_\Omega\int_\Omega\int_\Omega \left|\nabla_x\phi_T^p - iw_T^p\mathbf{A}(z,t)\;\phi_T^p\right|^2\; dxdydzdt \\
& +\frac{\gamma_T^{N_1}}{2}\int_0^{t_f}\int_\Omega\int_\Omega\int_\Omega \left|\nabla_x\phi_T^{N_1} - iw_T^{N_1}\mathbf{A}(z,t)\;\phi_T^{N_1}\right|^2\; dxdydzdt \\
& +\frac{\gamma_T^{N_2}}{2}\int_0^{t_f}\int_\Omega\int_\Omega\int_\Omega \left|\nabla_x\phi_T^{N_2} - iw_T^{N_2}\mathbf{A}(z,t)\;\phi_T^{N_2}\right|^2\; dxdydzdt \\
& +\frac{\gamma_{H_e}^{p_1}}{2}\int_0^{t_f}\int_\Omega\int_\Omega\int_\Omega \left|\nabla_x\phi_{H_e}^{p_1} - iw_{H_e}^{p_1}\mathbf{A}(z,t)\;\phi_{H_e}^{p_1}\right|^2\; dxdydzdt \\
& +\frac{\gamma_{H_e}^{p_2}}{2}\int_0^{t_f}\int_\Omega\int_\Omega\int_\Omega \left|\nabla_x\phi_{H_e}^{p_2} - iw_{H_e}^{p_2}\mathbf{A}(z,t)\;\phi_{H_e}^{p_2}\right|^2\; dxdydzdt \\
& +\frac{\gamma_{H_e}^{N_1}}{2}\int_0^{t_f}\int_\Omega\int_\Omega\int_\Omega \left|\nabla_x\phi_{H_e}^{N_1} - iw_{H_e}^{N_1}\mathbf{A}(z,t)\;\phi_{H_e}^{N_1}\right|^2\; dxdydzdt \\
& +\frac{\gamma_{H_e}^{N_2}}{2}\int_0^{t_f}\int_\Omega\int_\Omega\int_\Omega \left|\nabla_x\phi_{H_e}^{N_2} - iw_{H_e}^{N_2}\mathbf{A}\;\phi_{H_e}^{N_2}\right|^2\; dxdydzdt \\
& +\frac{\gamma_N}{2}\int_0^{t_f}\int_\Omega\int_\Omega\int_\Omega |\nabla_y\phi_N - iw_N\mathbf{A}(z,t)\;\phi_N|^2\; dydzdt \\
& +\frac{\gamma_e}{2}\int_0^{t_f}\int_\Omega\int_\Omega\int_\Omega |\nabla_y\phi_e - iw_e\phi_e\mathbf{A}(z,t)\;\phi_e|^2\; dydzdt \\
& +\frac{\gamma_D^A}{2}\int_0^{t_f}\int_\Omega\int_\Omega |\nabla_y\phi_D^A - iw_D^A\mathbf{A}(z,t)\;\phi_D^A|^2\; dydzdt \\
& +\frac{\gamma_T^A}{2}\int_0^{t_f}\int_\Omega\int_\Omega |\nabla_y\phi_T^A - iw_T^A\mathbf{A}(z,t)\;\phi_T^A|^2\; dydzdt \\
& +\frac{\gamma_{H_e}^A}{2}\int_0^{t_f}\int_\Omega\int_\Omega |\nabla_y\phi_{H_e}^A - iw_{H_e}^A\mathbf{A}(z,t)\;\phi_{He}^A|^2\; dydzdt \\
& +\frac{\gamma_D}{2}\int_0^{t_f}\int_\Omega\int_\Omega |\nabla_z\phi_D - iw_D\mathbf{A}(z,t)\;\phi_D|^2\; dzdt \\
& +\frac{\gamma_T}{2}\int_0^{t_f}\int_\Omega\int_\Omega |\nabla_z\phi_T - iw_T\mathbf{A}(z,t)\;\phi_T|^2\; dzdt \\
& +\frac{\gamma_{H_e}}{2}\int_0^{t_f}\int_\Omega\int_\Omega |\nabla_z\phi_{H_e} - iw_{H_e}\mathbf{A}(z,t)\;\phi_{H_e}|^2\; dzdt \\
& +\frac{\gamma_N^M}{2}\int_0^{t_f}\int_\Omega\int_\Omega |\nabla_z\phi_N^M - \frac{}{9} iw_N^M\mathbf{A}(z,t)\;\phi_N^M|^2\; dzdt \\
& +\frac{\gamma_e^M}{2}\int_0^{t_f}\int_\Omega\int_\Omega |\nabla_z\phi_e^M - iw_N^M\mathbf{A}(z,t)\;\phi_e^M|^2\; dzdt. \qquad (6)
\end{aligned}
$$

We define also,

$$\begin{aligned} E_{q_1} &= \frac{\gamma_D^0}{2}\int_0^{t_f}\int_\Omega \frac{\partial\phi_D}{\partial t}\cdot\frac{\partial\phi_D}{\partial t}\,dzdt \\ &+\frac{\gamma_T^0}{2}\int_0^{t_f}\int_\Omega \frac{\partial\phi_T}{\partial t}\cdot\frac{\partial\phi_T}{\partial t}\,dzdt \\ &+\frac{\gamma_{H_e}^0}{2}\int_0^{t_f}\int_\Omega \frac{\partial\phi_{H_e}}{\partial t}\cdot\frac{\partial\phi_{H_e}}{\partial t}\,dzdt \\ &+\frac{\gamma_N^0}{2}\int_0^{t_f}\int_\Omega \frac{\partial\phi_N^M}{\partial t}\cdot\frac{\partial\phi_N^M}{\partial t}\,dxdt \\ &+\frac{\gamma_e^0}{2}\int_0^{t_f}\int_\Omega \frac{\partial\phi_e^M}{\partial t}\cdot\frac{\partial\phi_e^M}{\partial t}\,dzdt. \end{aligned} \tag{7}$$

For the interaction energy functional we consider only a simplified self interaction part, denoted by E_{int}, where

$$\begin{aligned} E_{int} &= \frac{\alpha_D}{2}\int_0^{t_f}\int_\Omega\int_\Omega\int_\Omega |\phi_D|^4\,dxdydzdt \\ &+\frac{\alpha_T}{2}\int_0^{t_f}\int_\Omega\int_\Omega\int_\Omega |\phi_T|^4\,dxdydzdt \\ &+\frac{\alpha_{H_e}}{2}\int_0^{t_f}\int_\Omega\int_\Omega\int_\Omega |\phi_{H_e}|^4\,dxdydzdt \\ &+\frac{\alpha_N}{2}\int_0^{t_f}\int_\Omega\int_\Omega |\phi_N|^4\,dydzdt \\ &+\frac{\alpha_e}{2}\int_0^{t_f}\int_\Omega\int_\Omega |\phi_e|^4\,dydzdt. \end{aligned} \tag{8}$$

Furthermore, concerning the scalar temperature field, we define

$$\begin{aligned} (C_v)_D\rho_D(z,t)T_D(z,t) &= \int_\Omega\int_\Omega \left(\frac{1}{2}|\phi_D^p|^2\frac{\partial\hat{\mathbf{r}}_D^p}{\partial t}\cdot\frac{\partial\hat{\mathbf{r}}_D^p}{\partial t}\right)dxdy \\ &+\int_\Omega\int_\Omega \left(\frac{1}{2}|\phi_D^N|^2\frac{\partial\hat{\mathbf{r}}_D^N}{\partial t}\cdot\frac{\partial\hat{\mathbf{r}}_D^N}{\partial t}\right)dxdy \end{aligned} \tag{9}$$

$$\begin{aligned} (C_v)_T\rho_T(z,t)T_T(z,t) &= \int_\Omega\int_\Omega \left(\frac{1}{2}|\phi_T^p|^2\frac{\partial\hat{\mathbf{r}}_T^p}{\partial t}\cdot\frac{\partial\hat{\mathbf{r}}_T^p}{\partial t}\right)dxdy \\ &+\int_\Omega\int_\Omega \left(\frac{1}{2}|\phi_T^{N_1}|^2\frac{\partial\hat{\mathbf{r}}_T^{N_1}}{\partial t}\cdot\frac{\partial\hat{\mathbf{r}}_T^{N_1}}{\partial t}\right)dxdy \\ &+\int_\Omega\int_\Omega \left(\frac{1}{2}|\phi_T^{N_2}|^2\frac{\partial\hat{\mathbf{r}}_T^{N_2}}{\partial t}\cdot\frac{\partial\hat{\mathbf{r}}_T^{N_2}}{\partial t}\right)dxdy \end{aligned} \tag{10}$$

$$
\begin{aligned}
(C_v)_{H_e}\rho_{H_e}(z,t)T_{H_e}(z,t) &= \int_\Omega\int_\Omega \left(\frac{1}{2}|\phi_{H_e}^{p_1}|^2\frac{\partial\hat{\mathbf{r}}_{H_e}^{p_1}}{\partial t}\cdot\frac{\partial\hat{\mathbf{r}}_{H_e}^{p_1}}{\partial t}\right)dxdy \\
&+ \int_\Omega\int_\Omega \left(\frac{1}{2}|\phi_{H_e}^{p_2}|^2\frac{\partial\hat{\mathbf{r}}_{H_e}^{p_2}}{\partial t}\cdot\frac{\partial\hat{\mathbf{r}}_{H_e}^{p_2}}{\partial t}\right)dxdy \\
&+ \int_\Omega\int_\Omega \left(\frac{1}{2}|\phi_{H_e}^{N_1}|^2\frac{\partial\hat{\mathbf{r}}_{H_e}^{N_1}}{\partial t}\cdot\frac{\partial\hat{\mathbf{r}}_{H_e}^{N_1}}{\partial t}\right)dxdy \\
&+ \int_\Omega\int_\Omega \left(\frac{1}{2}|\phi_{H_e}^{N_2}|^2\frac{\partial\hat{\mathbf{r}}_{H_e}^{N_2}}{\partial t}\cdot\frac{\partial\hat{\mathbf{r}}_{H_e}^{N_2}}{\partial t}\right)dxdy \qquad (11)
\end{aligned}
$$

$$
(C_v)_N\rho_N^M(z,t)T_N(z,t) = \int_\Omega \left(\frac{1}{2}|\phi_N|^2\frac{\partial\hat{\mathbf{r}}_N}{\partial t}\cdot\frac{\partial\hat{\mathbf{r}}_N}{\partial t}\right)dy \qquad (12)
$$

$$
(C_v)_e\rho_e^M(z,t)T_e = \int_\Omega \left(\frac{1}{2}|\phi_e|^2\frac{\partial\hat{\mathbf{r}}_e}{\partial t}\cdot\frac{\partial\hat{\mathbf{r}}_e}{\partial t}\right)dy \qquad (13)
$$

Moreover, we define

$$
T(z,t) = T_D + T_T + T_{H_e} + T_N + T_e
$$

and similarly as indicated in [16] for a non-viscous fluid, we also assume the following constraint

$$
\begin{aligned}
&|\phi_D|^2(C_v)_D\frac{\partial T_D}{\partial t} + |\phi_T|^2(C_v)_T\frac{\partial T_T}{\partial t} \\
&+|\phi_{H_e}|^2(C_v)_{H_e}\frac{\partial T_{H_e}}{\partial t} + |\phi_N|^2(C_v)_N\frac{\partial T_N}{\partial t} + |\phi_e|^2(C_v)_e\frac{\partial T_e}{\partial t} \\
&-K_D\nabla^2T_D - K_T\nabla^2T_T - K_{H_e}\nabla^2T_{H_e} - K_N\nabla^2T_N - K_e\nabla^2T_e \\
&+P_D\ \mathrm{div}\ \mathbf{v}_D + P_T\ \mathrm{div}\ \mathbf{v}_T + P_{H_e}\ \mathrm{div}\ \mathbf{v}_{H_e} \\
&+P_N\ \mathrm{div}\ \mathbf{v}_N + P_e\ \mathrm{div}\ \mathbf{v}_e - \frac{\partial Q}{\partial t} = 0,\ \text{in } \Omega\times[0,t_f], \qquad (14)
\end{aligned}
$$

where Q is a heat function and

$$
P_D = \frac{d(\hat{P}\rho_D)}{dt},
$$

$$
P_T = \frac{d(\hat{P}\rho_T)}{dt},
$$

$$
P_{H_e} = \frac{d(\hat{P}\rho_{H_e})}{dt},
$$

$$P_N = \frac{d(\hat{P}\rho_N)}{dt},$$

and

$$P_e = \frac{d(\hat{P}\rho_e)}{dt}.$$

Finally, we assume the following mass conservation equation as a constraint

$$\begin{aligned} &\frac{d\rho}{dt} + \rho_D \text{ div } (\mathbf{v}_D) + \rho_T \text{ div } (\mathbf{v}_T) \\ &+\rho_{H_e} \text{ div } (\mathbf{v}_{H_e}) + \rho_N \text{ div } (\mathbf{v}_N) \\ &+\rho_e \text{ div } (\mathbf{v}_e) = 0, \text{ in } \Omega \times [0, t_f], \end{aligned} \tag{15}$$

where we have denoted for not relabeled functions

$$\rho = \rho_D + \rho_T + \rho_{H_e} + \rho_N + \rho_e$$

and

$$\begin{aligned} \rho_D &= \rho_D(\mathbf{r}_D(z,t),t), \\ \rho_T &= \rho_T(\mathbf{r}_T(z,t),t), \\ \rho_{H_e} &= \rho_{H_e}(\mathbf{r}_{H_e}(z,t),t), \\ \rho_N &= \rho_N(\mathbf{r}_N^M(z,t),t), \end{aligned}$$

and

$$\rho_e = \rho_e(\mathbf{r}_e^M(z,t),t).$$

In order to model such a chemical reaction, we define the following functional J, which corresponds to a variational formulation for the model in question, where

$$\begin{aligned} J \;=\; & E_C + E_q + E_{q_1} + E_{int} \\ & - \int_0^{t_f} \int_\Omega \hat{P} \left(\frac{d\rho}{dt} + \rho_D \text{ div } (\mathbf{v}_D) + \rho_T \text{ div } (\mathbf{v}_T) \right. \\ & +\rho_{H_e} \text{ div } (\mathbf{v}_{H_e}) + \rho_N \text{ div } (\mathbf{v}_N) \\ & \left. +\rho_e \text{ div } (\mathbf{v}_e) \right) \, dzdt \\ & +J_{Aux_1} + J_{Aux_2} + J_{Aux_3} + J_{Aux_4} + J_{Aux_5} + J_{Aux_6}, \end{aligned} \tag{16}$$

where

$$
\begin{aligned}
J_{Aux_1} \;=\; & \int_0^{t_f}\int_\Omega \lambda_D \left((C_v)_D \rho_D(z,t) T_D(z,t) - \int_\Omega\int_\Omega \left(\frac{1}{2}|\phi_D^p|^2 \frac{\partial \hat{\mathbf{r}}_D^p}{\partial t} \cdot \frac{\partial \hat{\mathbf{r}}_D^p}{\partial t} \right) dxdy \right. \\
& \left. - \int_\Omega\int_\Omega \left(\frac{1}{2}|\phi_D^N|^2 \frac{\partial \hat{\mathbf{r}}_D^N}{\partial t} \cdot \frac{\partial \hat{\mathbf{r}}_D^N}{\partial t} \right) dxdy \right) dzdt \\
& - \int_0^{t_f}\int_\Omega \lambda_T \left((C_v)_T \rho_T(z,t) T_T(z,t) - \int_\Omega\int_\Omega \left(\frac{1}{2}|\phi_T^p|^2 \frac{\partial \hat{\mathbf{r}}_T^p}{\partial t} \cdot \frac{\partial \hat{\mathbf{r}}_T^p}{\partial t} \right) dxdy \right. \\
& - \int_\Omega\int_\Omega \left(\frac{1}{2}|\phi_T^{N_1}|^2 \frac{\partial \hat{\mathbf{r}}_T^{N_1}}{\partial t} \cdot \frac{\partial \hat{\mathbf{r}}_T^{N_1}}{\partial t} \right) dxdy \\
& \left. - \int_\Omega\int_\Omega \left(\frac{1}{2}|\phi_T^{N_2}|^2 \frac{\partial \hat{\mathbf{r}}_T^{N_2}}{\partial t} \cdot \frac{\partial \hat{\mathbf{r}}_T^{N_2}}{\partial t} \right) dxdy \right) dzdt \\
& + \int_0^{t_f}\int_\Omega \lambda_{H_e} \left((C_v)_{H_e} \rho_{H_e}(z,t) T_{H_e}(z,t) - \int_\Omega\int_\Omega \left(\frac{1}{2}|\phi_{H_e}^{p_1}|^2 \frac{\partial \hat{\mathbf{r}}_{H_e}^{p_1}}{\partial t} \cdot \frac{\partial \hat{\mathbf{r}}_{H_e}^{p_1}}{\partial t} \right) dxdy \right. \\
& - \int_\Omega\int_\Omega \left(\frac{1}{2}|\phi_{H_e}^{p_2}|^2 \frac{\partial \hat{\mathbf{r}}_{H_e}^{p_2}}{\partial t} \cdot \frac{\partial \hat{\mathbf{r}}_{H_e}^{p_2}}{\partial t} \right) dxdy \\
& - \int_\Omega\int_\Omega \left(\frac{1}{2}|\phi_{H_e}^{N_1}|^2 \frac{\partial \hat{\mathbf{r}}_{H_e}^{N_1}}{\partial t} \cdot \frac{\partial \hat{\mathbf{r}}_{H_e}^{N_1}}{\partial t} \right) dxdy \\
& \left. - \int_\Omega\int_\Omega \left(\frac{1}{2}|\phi_{H_e}^{N_2}|^2 \frac{\partial \hat{\mathbf{r}}_{H_e}^{N_2}}{\partial t} \cdot \frac{\partial \hat{\mathbf{r}}_{H_e}^{N_2}}{\partial t} \right) dxdy \right) dzdt \\
& + \int_0^{t_f}\int_\Omega \lambda_N \left((C_v)_N \rho_N^M(z,t) T_N(z,t) - \int_\Omega \left(\frac{1}{2}|\phi_N|^2 \frac{\partial \hat{\mathbf{r}}_N}{\partial t} \cdot \frac{\partial \hat{\mathbf{r}}_N}{\partial t} \right) dy \right) dzdt \\
& + \int_0^{t_f}\int_\Omega \lambda_e \left((C_v)_e \rho_e^M(z,t) T_e - \int_\Omega \left(\frac{1}{2}|\phi_e|^2 \frac{\partial \hat{\mathbf{r}}_e}{\partial t} \cdot \frac{\partial \hat{\mathbf{r}}_e}{\partial t} \right) dy \right) dzdt \\
& + \int_0^{t_f}\int_\Omega \lambda_1 \left(|\phi_D|^2 (C_v)_D \frac{\partial T_D}{\partial t} + |\phi_T|^2 (C_v)_T \frac{\partial T_T}{\partial t} \right. \\
& + |\phi_{H_e}|^2 (C_v)_{H_e} \frac{\partial T_{H_e}}{\partial t} + |\phi_N|^2 (C_v)_N \frac{\partial T_N}{\partial t} + |\phi_e|^2 (C_v)_e \frac{\partial T_e}{\partial t} \\
& - K_D \nabla^2 T_D - K_T \nabla^2 T_T - K_{H_e} \nabla^2 T_{H_e} - K_N \nabla^2 T_N - K_e \nabla^2 T_e \\
& + P_D \text{ div } \mathbf{v}_D + P_T \text{ div } \mathbf{v}_T + P_{H_e} \text{ div } \mathbf{v}_{H_e} \\
& \left. + P_N \text{ div } \mathbf{v}_N + P_e \text{ div } \mathbf{v}_e - \frac{\partial Q}{\partial t} \right) dzdt, \qquad (17)
\end{aligned}
$$

Moreover,

$$
\begin{aligned}
J_{Aux_2} \;=\; & \int_0^{t_f}\int_\Omega\int_\Omega E_D^p(y,z,t)\left(\int_\Omega |\hat{\phi}_D^p(x,y,z,t)|^2\,dx-1\right)\,dydzdt \\
& +\int_0^{t_f}\int_\Omega\int_\Omega E_D^p(y,z,t)\left(\int_\Omega |\hat{\phi}_D^N(x,y,z,t)|^2\,dx-1\right)\,dydzdt \\
& +\int_0^{t_f}\int_\Omega\int_\Omega E_T^p(y,z,t)\left(\int_\Omega |\hat{\phi}_T^p(x,y,z,t)|^2\,dx-1\right)\,dydzdt \\
& +\int_0^{t_f}\int_\Omega\int_\Omega E_T^{N_1}(y,z,t)\left(\int_\Omega |\hat{\phi}_T^{N_1}(x,y,z,t)|^2\,dx-1\right)\,dydzdt \\
& +\int_0^{t_f}\int_\Omega\int_\Omega E_T^{N_2}(y,z,t)\left(\int_\Omega |\hat{\phi}_T^{N_2}(x,y,z,t)|^2\,dx-1\right)\,dydzdt \\
& +\int_0^{t_f}\int_\Omega\int_\Omega E_{H_e}^{p_1}(y,z,t)\left(\int_\Omega |\hat{\phi}_{H_e}^{p_1}(x,y,z,t)|^2\,dx-1\right)\,dydzdt \\
& +\int_0^{t_f}\int_\Omega\int_\Omega E_{H_e}^{p_2}(y,z,t)\left(\int_\Omega |\hat{\phi}_{H_e}^{p_2}(x,y,z,t)|^2\,dx-1\right)\,dydzdt \\
& +\int_0^{t_f}\int_\Omega\int_\Omega E_{H_e}^{N_1}(y,z,t)\left(\int_\Omega |\hat{\phi}_{H_e}^{N_1}(x,y,z,t)|^2\,dx-1\right)\,dydzdt \\
& +\int_0^{t_f}\int_\Omega\int_\Omega E_{H_e}^{N_2}(y,z,t)\left(\int_\Omega |\hat{\phi}_{H_e}^{N_2}(x,y,z,t)|^2\,dx-1\right)\,dydzdt \qquad (18)
\end{aligned}
$$

$$
\begin{aligned}
J_{Aux_3} \;=\; & \int_0^{t_f}\int_\Omega E_N(z,t)\left(\int_\Omega\int_\Omega |\hat{\phi}_N(y,z,t)|^2\,dy-1\right)\,dzdt, \\
& +\int_0^{t_f}\int_\Omega E_e(z,t)\left(\int_\Omega |\hat{\phi}_e(y,,z,t)|^2\,dy-1\right)\,dzdt, \\
& +\int_0^{t_f}\int_\Omega E_D^A(z,t)\left(\int_\Omega |\phi_D^A(y,z,t)|^2\,dy-1\right)\,dzdt \\
& +\int_0^{t_f}\int_\Omega E_T^A(z,t)\left(\int_\Omega |\phi_T^A(y,z,t)|^2\,dy-1\right)\,dzdt \\
& +\int_0^{t_f}\int_\Omega E_{H_e}^A(z,t)\left(\int_\Omega |\phi_{H_e}^A(y,z,t)|^2\,dy-1\right)\,dzdt \qquad (19)
\end{aligned}
$$

and denoting

$$
\begin{aligned}
& J_{Aux_4} \\
= & \int_0^{t_f} \mu_D(t) \left(m_D(t) - (m_0)_D + \int_0^t \int_{\partial\Omega} \rho_D(z,\tau) \mathbf{v}_D(z,\tau) \cdot \mathbf{n} \, dS d\tau \right. \\
& + \alpha_D [m_{H_e}(t) + m_N(t)] - \alpha_D \int_0^t \int_{\partial\Omega} \rho_{H_e}(z,\tau) \mathbf{v}_{H_e}(z,\tau) \cdot \mathbf{n} \, dS d\tau \\
& \left. + \alpha_D \int_0^t \int_{\partial\Omega} \rho_N(z,\tau) \mathbf{v}_N(z,\tau) \cdot \mathbf{n} \, dS d\tau \right) \, dt \\
& + \int_0^{t_f} \mu_T(t) \left(m_T(t) - (m_0)_T + \int_0^t \int_{\partial\Omega} \rho_T(z,\tau) \mathbf{v}_T(z,\tau) \cdot \mathbf{n} \, dS d\tau \right. \\
& + \alpha_T [m_{H_e}(t) + m_N(t)] + \alpha_T \int_0^t \int_{\partial\Omega} \rho_{H_e}(z,\tau) \mathbf{v}_{H_e}(z,\tau) \cdot \mathbf{n} \, dS d\tau \\
& \left. + \alpha_T \int_0^t \int_{\partial\Omega} \rho_N(z,\tau) \mathbf{v}_N(z,\tau) \cdot \mathbf{n} \, dS d\tau \right) \, dt \\
& + \int_0^{t_f} \mu_3(t) \left(\alpha_N \left(m_{H_e}(t) + \int_0^t \int_{\partial\Omega} \rho_{H_e}(z,\tau) \mathbf{v}_{H_e}(z,\tau) \cdot \mathbf{n} \, dS d\tau \right) \right. \\
& \left. - \alpha_{H_e} \left(m_N(t) + \int_0^t \int_{\partial\Omega} \rho_N(z,\tau) \mathbf{v}_N(z,\tau) \cdot \mathbf{n} \, dS d\tau \right) \right) \, dt \\
& + \int_0^{t_f} \mu_4(t) \left(m_e(t) - (m_0)_e + \int_0^t \int_{\partial\Omega} \rho_e^M(z,\tau) \mathbf{v}_e(z,\tau) \cdot \mathbf{n} \, dS d\tau \right) \, dt. \quad (20)
\end{aligned}
$$

Furthermore,

$$
\begin{aligned}
& J_{Aux_5} \\
= \; & -K_1 \int_0^{t_f} \int_\Omega \int_\Omega \int_\Omega V(\mathbf{r}_D^p, \mathbf{r}_T^p, \mathbf{r}_{H_e}^{p_1}, \mathbf{r}_{H_e}^{p_2}, \mathbf{r}_e) \\
& \times (|\phi_D^p|^2 + |\phi_T^p|^2 + |\phi_{H_e}^{p_1}|^2 + |\phi_{H_e}^{p_2}|^2 + |\phi_e|^2)\, dxdydzdt \\
& -K_1 \int_0^{t_f} \int_\Omega \int_\Omega \int_\Omega |\phi_D^p|^2 \mathbf{B} \times \frac{\partial \mathbf{r}_D^p}{\partial t} \cdot \left(\mathbf{r}_D^p(z, \varepsilon t) - (\mathbf{r}_0)_D^p\right)\, dxdydzdt \\
& -K_1 \int_0^{t_f} \int_\Omega \int_\Omega \int_\Omega |\phi_T^p|^2 \mathbf{B} \times \frac{\partial \mathbf{r}_T^p}{\partial t} \cdot \left(\mathbf{r}_T^p(z, \varepsilon t) - (\mathbf{r}_0)_T^p\right)\, dxdydzdt \\
& -K_1 \int_0^{t_f} \int_\Omega \int_\Omega \int_\Omega |\phi_{H_e}^{p_1}|^2 \mathbf{B} \times \frac{\partial \mathbf{r}_{H_e}^{p_1}}{\partial t} \cdot \left(\mathbf{r}_{H_e}^{p_1}(z, \varepsilon t) - (\mathbf{r}_0)_{H_e}^{p_1}\right)\, dxdydzdt \\
& -K_1 \int_0^{t_f} \int_\Omega \int_\Omega \int_\Omega |\phi_{H_e}^{p_2}|^2 \mathbf{B} \times \frac{\partial \mathbf{r}_{H_e}^{p_2}}{\partial t} \cdot \left(\mathbf{r}_{H_e}^{p_2}(z, \varepsilon t) - (\mathbf{r}_0)_{H_e}^{p_2}\right)\, dxdydzdt \\
& -K_1 \int_0^{t_f} \int_\Omega \int_\Omega \int_\Omega |\phi_e|^2 \mathbf{B} \times \frac{\partial \mathbf{r}_e}{\partial t} \cdot (\mathbf{r}_e(z, \varepsilon t) - (\mathbf{r}_0)_e)\, dxdydzdt \\
& + \frac{1}{8\pi} \int_0^{t_f} \int_\Omega |\operatorname{curl} \mathbf{A}(z,t) - \mathbf{B}_0(z,t)|^2\, dzdt \\
& + \frac{1}{8\pi} \int_0^{t_f} \int_\Omega \left| \int_\Omega \int_\Omega \nabla_z V(\mathbf{r}_D^p, \mathbf{r}_T^p, \mathbf{r}_{H_e}^{p_1}, \mathbf{r}_{H_e}^{p_2}, \mathbf{r}_e)\, dxdy + \frac{1}{c} \frac{\partial \mathbf{A}}{\partial t} \right|^2 dzdt, \quad (21)
\end{aligned}
$$

where

$$\mathbf{B}(z,t) = \operatorname{curl} \mathbf{A}(z,t) - \mathbf{B}_0(z,t)$$

is the total magnetic field,

$$\mathbf{A} = (A_1, A_2, A_3) \in W^{1,2}(\Omega \times [0, t_f]; \mathbb{R}^3)$$

denotes the magnetic potential and

$$\mathbf{E} = -\int_\Omega \int_\Omega \nabla_z V(\mathbf{r}_D^p, \mathbf{r}_T^p, \mathbf{r}_{H_e}^{p_1}, \mathbf{r}_{H_e}^{p_2}, \mathbf{r}_e)\, dxdy - \frac{1}{c} \frac{\partial \mathbf{A}}{\partial t},$$

denotes the electric field.

Finally,

$$\begin{aligned} J_{Aux_6} &= -K_1 \int_0^{t_f} \int_\Omega \int_\Omega \int_\Omega |\phi_D^p|^2 \mathbf{A} \cdot \frac{\partial \mathbf{r}_D^p}{\partial t}\, dxdydzdt \\ &\quad -K_1 \int_0^{t_f} \int_\Omega \int_\Omega \int_\Omega |\phi_T^p|^2 \mathbf{A} \cdot \frac{\partial \mathbf{r}_T^p}{\partial t}\, dxdydzdt \\ &\quad -K_1 \int_0^{t_f} \int_\Omega \int_\Omega \int_\Omega |\phi_{H_e}^{p_1}|^2 \mathbf{A} \cdot \frac{\partial \mathbf{r}_{H_e}^{p_1}}{\partial t}\, dxdydzdt \\ &\quad -K_1 \int_0^{t_f} \int_\Omega \int_\Omega \int_\Omega |\phi_{H_e}^{p_2}|^2 \mathbf{A} \cdot \frac{\partial \mathbf{r}_{H_e}^{p_2}}{\partial t}\, dxdydzdt \\ &\quad -K_2 \int_0^{t_f} \int_\Omega \int_\Omega |\phi_e|^2 \mathbf{A} \cdot \frac{\partial \mathbf{r}_e}{\partial t}\, dydzdt. \end{aligned} \tag{22}$$

Remark 2.1. *About the domain of the functional J, we generically define it as sets of smooth C^2 functions, specifying only the following boundary and initial conditions*

$$\mathbf{r} = (\mathbf{r}_D, \mathbf{r}_T, \mathbf{r}_{H_e}, \mathbf{r}_N^M, \mathbf{r}_e^M) = \mathbf{0}, \ \textit{on } \partial\Omega \times [0, t_f],$$

$$\mathbf{r}|_{t=0} = z, \ \textit{in } \Omega,$$

$$\mathbf{v} = (\mathbf{v}_D, \mathbf{v}_T, \mathbf{v}_{H_e}, \mathbf{v}_N^M, \mathbf{v}_e^M) = \mathbf{0}, \ \textit{on } \partial\Omega \times [0, t_f],$$

$$\mathbf{v}_{t=0} = \mathbf{v}_0 \ \textit{in } \Omega,$$

$$T = T_0(z,t) \ \textit{on } \partial\Omega \times [0, t_f]$$

$$T|_{t=0} = T_1(z), \ \textit{in } \Omega$$

and

$$\rho|_{t=0} = (\rho_D, \rho_T, \rho_{H_e}, \rho_N, \rho_e)|_{t=0} = ((\rho_D)_0, (\rho_T)_0, 0, 0, (\rho_e)_0) \ \textit{in } \Omega.$$

Remark 2.2. *Concerning the variation of J in $\mathbf{r}$, we consider variations in the context*

$$(\mathbf{r} + h\varphi) \ \textit{and} \ (\mathbf{r}(\cdot, \varepsilon t) + h\varphi),$$

that is, the same variable variation φ and real constant h for both $\mathbf{r}$ and $\mathbf{r}(\cdot, \varepsilon t)$ for obtaining an approximate Euler-Lagrange equation. Finally, letting $\varepsilon \to 0$ we obtain the correct Euler-Lagrange equation.

Remark 2.3. *With the boundary conditions we have set, surface integrals I_n similar as that below indicated equal zero, that is,*

$$I_n = \int_0^t \int_{\partial\Omega} \rho_D(z,\tau) \mathbf{v}_D(z,\tau) \cdot \mathbf{n}\, dSd\tau = 0.$$

Anyway, we keep such more general expressions in the main functionals considering that, in the next sections, we address a more general approach with a concerning control volume and fields in an Eulerian context.

3 The main variational formulation for an Eulerian approach

Let $\Omega \subset \mathbb{R}^3$ be an open, bounded and connected set with a regular (Lipschitzian) boundary denoted by $\partial\Omega$.

Denoting time by t we consider such a nuclear fusion process develops in Ω on a time interval $[0, t_f]$, so that $t \in [0, t_f]$.

We define the following density fields:

For the Deuterium proton,

$$\rho_D^p(x,y,z,t) = |\hat{\phi}_D^p(x,y,z,t)|^2 |\phi_D^A(y,z,t)|^2 |\phi_D(z,t)|^2 \frac{m_p}{m_D^A} \equiv |\phi_D^p(x,y,z,t)|^2,$$

Here, ρ_D^p stands for the density of a proton field in (x,y,z,t), at an Deuterium atom with density at (y,z,t) and with a macroscopic Deuterium density in $(z,t) \in \Omega \times [0,t_f]$.

Similarly, for the Deuterium neutron density field, we define

$$\rho_D^N(x,y,z,t) = |\hat{\phi}_D^N(x,y,z,t)|^2 |\phi_D^A(y,z,t)|^2 |\phi_D(z,t)|^2 \frac{m_N}{m_D^A} \equiv |\phi_D^N(x,y,z,t)|^2.$$

For the Tritium proton field

$$\rho_T^p(x,y,z,t) = |\hat{\phi}_T^p(x,y,z,t)|^2 |\phi_T^A(y,z,t)|^2 |\phi_T(z,t)|^2 \frac{m_p}{m_T^A} \equiv |\phi_T^p(x,y,z,t)|^2.$$

and for the tritium neutron fields

$$\rho_T^{N_1}(x,y,z,t) = |\hat{\phi}_T^{N_1}(x,y,z,t)|^2 |\phi_T^A(y,z,t)|^2 |\phi_T(z,t)|^2 \frac{m_N}{m_T^A}| \equiv |\phi_T^{N_1}(x,y,z,t)|^2$$

and

$$\rho_T^{N_2}(x,y,z,t) = |\hat{\phi}_T^{N_2}(x,y,z,t)|^2 |\phi_T^A(y,z,t)|^2 |\phi_T(z,t)|^2 \frac{m_N}{m_T^A} \equiv |\phi_T^{N_2}(x,y,z,t)|^2.$$

For the Helium protons, we define

$$\rho_{H_e}^{p_1}(x,y,z,t) = |\hat{\phi}_{H_e}^{p_1}(x,y,z,t)|^2 |\phi_{H_e}^A(y,z,t)|^2 |\phi_{H_e}(z,t)|^2 \frac{m_p}{m_{H_e}^A} \equiv |\phi_{H_e}^{p_1}(x,y,z,t)|^2$$

and

$$\rho^{p_2}_{H_e}(x,y,z,t) = |\hat{\phi}^{p_2}_{H_e}(x,y,z,t)|^2 |\phi^A_{H_e}(y,z,t)|^2 |\phi_{H_e}(z,t)|^2 \frac{m_p}{m^A_{H_e}} \cong |\phi^{p_2}_{H_e}(x,y,z,t)|^2.$$

For the Helium neutron fields

$$\rho^{N_1}_{H_e}(x,y,z,t) = |\hat{\phi}^{N_1}_{H_e}(x,y,z,t)|^2 |\phi^A_{H_e}(y,z,t)|^2 |\phi_{H_e}(z,t)|^2 \frac{m_N}{m^A_{H_e}} \cong |\phi^{N_1}_{H_e}(x,y,z,t)|^2$$

and

$$\rho^{N_2}_{H_e}(x,y,z,t) = |\hat{\phi}^{N_2}_{H_e}(x,y,z,t)|^2 |\phi^A_{H_e}(y,z,t)|^2 |\phi_{H_e}(z,t)|^2 \frac{m_N}{m^A_{H_e}} \cong |\phi^{N_2}_{H_e}(x,y,z,t)|^2.$$

For the single neutron field

$$\rho_N(y,z,t) = |\hat{\phi}_N(y,z,t)|^2 |\phi^M_N(z,t)|^2 \equiv |\phi_N(y,z,t)|^2$$

where ϕ^M_N denotes the macroscopic neutron density field.

Finally, for the electronic field resulting from the ionization of Deuterium and Tritium atoms,

$$\rho_e = |\hat{\phi}_e(y,z,t)|^2 |\phi^M_e(z,t)|^2 \equiv |\phi_e(y,z,t)|^2$$

where again ϕ^M_e denotes the macroscopic electronic density field.

The corresponding position fields stand for:

For the Deuterium proton

$$\begin{aligned} \mathbf{r}^p_D(x,y,z,t) &= \mathbf{r}_D(z,t) + \mathbf{r}^A_D(y,\mathbf{r}_D(z,t),t) \\ &\quad + \tilde{\mathbf{r}}^p_D(x,\mathbf{r}^A_D(y,\mathbf{r}_D(z,t),t),\mathbf{r}_D(z,t),t) \\ &= \mathbf{r}_D(z,t) + \hat{\mathbf{r}}^p_D(x,y,\mathbf{r}_D(z,t),t), \end{aligned} \tag{23}$$

where

$$\hat{\mathbf{r}}^p_D(x,y,\mathbf{r}_D(z,t),t) = \mathbf{r}^A_D(y,\mathbf{r}_D(z,t),t) + \tilde{\mathbf{r}}^p_D(x,\mathbf{r}^A_D(y,\mathbf{r}_D(z,t),t),\mathbf{r}_D(z,t),t).$$

Here $\mathbf{r}_D(z,t)$ is the macroscopic Deuterium position field in (z,t),

$$\mathbf{r}^A_D(y,\mathbf{r}(z,t),t)$$

refers to the atom position field in (y,z,t) and

$$\tilde{\mathbf{r}}^p_D(x,\mathbf{r}^A_D(y,\mathbf{r}_D(z,t),t),\mathbf{r}_D(z,t),t)$$

is the microscopic proton position field.

Similarly, for the Deuterium neutron position field we denote

$$\begin{aligned}\mathbf{r}_D^N(x,y,z,t) &= \mathbf{r}_D(z,t)+\mathbf{r}_D^A(y,\mathbf{r}_D(z,t),t)\\ &\quad+\tilde{\mathbf{r}}_D^N(x,\mathbf{r}_D^A(y,\mathbf{r}_D(z,t),t),\mathbf{r}_D(z,t),t)\\ &= \mathbf{r}_D(z,t)+\hat{\mathbf{r}}_D^N(x,y,\mathbf{r}_D(z,t),t),\end{aligned} \tag{24}$$

where

$$\hat{\mathbf{r}}_D^N(x,y,\mathbf{r}_D(z,t),t)=\mathbf{r}_D^A(y,\mathbf{r}_D(z,t),t)+\tilde{\mathbf{r}}_D^N(x,\mathbf{r}_D^A(y,\mathbf{r}_D(z,t),t),\mathbf{r}_D(z,t),t).$$

For the tritium proton

$$\begin{aligned}\mathbf{r}_T^p(x,y,z,t) &= \mathbf{r}_T(z,t)+\mathbf{r}_T^A(y,\mathbf{r}_T(z,t),t)\\ &\quad+\tilde{\mathbf{r}}_T^p(x,\mathbf{r}_T^A(y,\mathbf{r}_T(z,t),t),\mathbf{r}_T(z,t),t)\\ &= \mathbf{r}_T(z,t)+\hat{\mathbf{r}}_T^p(x,y,\mathbf{r}_D(z,t),t),\end{aligned} \tag{25}$$

where

$$\hat{\mathbf{r}}_T^p(x,y,\mathbf{r}_T(z,t),t)=\mathbf{r}_T^A(y,\mathbf{r}_T(z,t),t)+\tilde{\mathbf{r}}_T^p(x,\mathbf{r}_T^A(y,\mathbf{r}_T(z,t),t),\mathbf{r}_T(z,t),t).$$

and for the tritium neutron fields

$$\begin{aligned}\mathbf{r}_T^{N_1}(x,y,z,t) &= \mathbf{r}_T(z,t)+\mathbf{r}_T^A(y,\mathbf{r}_T(z,t),t)\\ &\quad+\tilde{\mathbf{r}}_T^{N_1}(x,\mathbf{r}_T^A(y,\mathbf{r}_T(z,t),t),\mathbf{r}_T(z,t),t)\\ &= \mathbf{r}_T(z,t)+\hat{\mathbf{r}}_T^{N_1}(x,y,\mathbf{r}_T(z,t),t),\end{aligned} \tag{26}$$

where

$$\hat{\mathbf{r}}_T^{N_1}(x,y,\mathbf{r}_D(z,t),t)=\mathbf{r}_T^A(y,\mathbf{r}_T(z,t),t)+\tilde{\mathbf{r}}_T^{N_1}(x,\mathbf{r}_T^A(y,\mathbf{r}_T(z,t),t),\mathbf{r}_T(z,t),t).$$

and

$$\begin{aligned}\mathbf{r}_T^{N_2}(x,y,z,t) &= \mathbf{r}_T(z,t)+\mathbf{r}_T^A(y,\mathbf{r}_T(z,t),t)\\ &\quad+\tilde{\mathbf{r}}_T^{N_2}(x,\mathbf{r}_T^A(y,\mathbf{r}_T(z,t),t),\mathbf{r}_T(z,t),t)\\ &= \mathbf{r}_T(z,t)+\hat{\mathbf{r}}_T^{N_2}(x,y,\mathbf{r}_T(z,t),t),\end{aligned} \tag{27}$$

where

$$\hat{\mathbf{r}}_T^{N_2}(x,y,\mathbf{r}_D(z,t),t)=\mathbf{r}_T^A(y,\mathbf{r}_T(z,t),t)+\tilde{\mathbf{r}}_T^{N_2}(x,\mathbf{r}_T^A(y,\mathbf{r}_T(z,t),t),\mathbf{r}_T(z,t),t).$$

For the Helium proton position fields, we denote

$$\begin{aligned}\mathbf{r}_{H_e}^{p_1}(x,y,z,t) &= \mathbf{r}_{H_e}(z,t)+\mathbf{r}_{H_e}^A(y,\mathbf{r}_{H_e}(z,t),t)\\ &\quad+\tilde{\mathbf{r}}_{H_e}^{p_1}(x,\mathbf{r}_{H_e}^A(y,\mathbf{r}_{H_e}(z,t),t),\mathbf{r}_{H_e}(z,t),t)\\ &= \mathbf{r}_{H_e}(z,t)+\hat{\mathbf{r}}_{H_e}^{p_1}(x,y,\mathbf{r}_{H_e}(z,t),t),\end{aligned} \tag{28}$$

where

$$\hat{\mathbf{r}}^{p_1}_{H_e}(x,y,\mathbf{r}_{H_e}(z,t),t) = \mathbf{r}^{A}_{H_e}(y,\mathbf{r}_{H_e}(z,t),t) + \tilde{\mathbf{r}}^{p_1}_{H_e}(x,\mathbf{r}^{A}_{H_e}(y,\mathbf{r}_{H_e}(z,t),t),\mathbf{r}_{H_e}(z,t),t).$$

and

$$\begin{aligned}\mathbf{r}^{p_2}_{H_e}(x,y,z,t) &= \mathbf{r}_{H_e}(z,t) + \mathbf{r}^{A}_{H_e}(y,\mathbf{r}_{H_e}(z,t),t) \\ &\quad + \tilde{\mathbf{r}}^{p_2}_{H_e}(x,\mathbf{r}^{A}_{H_e}(y,\mathbf{r}_{H_e}(z,t),t),\mathbf{r}_{H_e}(z,t),t) \\ &= \mathbf{r}_{H_e}(z,t) + \hat{\mathbf{r}}^{p_2}_{H_e}(x,y,\mathbf{r}_{H_e}(z,t),t), \qquad (29)\end{aligned}$$

where

$$\hat{\mathbf{r}}^{p_2}_{H_e}(x,y,\mathbf{r}_{H_e}(z,t),t) = \mathbf{r}^{A}_{H_e}(y,\mathbf{r}_{H_e}(z,t),t) + \tilde{\mathbf{r}}^{p_2}_{H_e}(x,\mathbf{r}^{A}_{H_e}(y,\mathbf{r}_{H_e}(z,t),t),\mathbf{r}_{H_e}(z,t),t).$$

For the Helium neutron fields, we denote

$$\begin{aligned}\mathbf{r}^{N_1}_{H_e}(x,y,z,t) &= \mathbf{r}_{H_e}(z,t) + \mathbf{r}^{A}_{H_e}(y,\mathbf{r}_{H_e}(z,t),t) \\ &\quad + \tilde{\mathbf{r}}^{N_1}_{H_e}(x,\mathbf{r}^{A}_{H_e}(y,\mathbf{r}_{H_e}(z,t),t),\mathbf{r}_{H_e}(z,t),t) \\ &= \mathbf{r}_{h_e}(z,t) + \hat{\mathbf{r}}^{N_1}_{H_e}(x,y,\mathbf{r}_{H_e}(z,t),t), \qquad (30)\end{aligned}$$

where

$$\hat{\mathbf{r}}^{N_1}_{H_e}(x,y,\mathbf{r}_{H_e}(z,t),t) = \mathbf{r}^{A}_{H_e}(y,\mathbf{r}_{H_e}(z,t),t) + \tilde{\mathbf{r}}^{N_1}_{H_e}(x,\mathbf{r}^{A}_{H_e}(y,\mathbf{r}_{H_e}(z,t),t),\mathbf{r}_{H_e}(z,t),t).$$

and

$$\begin{aligned}\mathbf{r}^{N_2}_{H_e}(x,y,z,t) &= \mathbf{r}_{H_e}(z,t) + \mathbf{r}^{A}_{H_e}(y,\mathbf{r}_{H_e}(z,t),t) \\ &\quad + \tilde{\mathbf{r}}^{N_2}_{H_e}(x,\mathbf{r}^{A}_{H_e}(y,\mathbf{r}_{H_e}(z,t),t),\mathbf{r}_{H_e}(z,t),t) \\ &= \mathbf{r}_{H_e}(z,t) + \hat{\mathbf{r}}^{N_2}_{H_e}(x,y,\mathbf{r}_{H_e}(z,t),t), \qquad (31)\end{aligned}$$

where

$$\hat{\mathbf{r}}^{N_2}_{H_e}(x,y,\mathbf{r}_{H_e}(z,t),t) = \mathbf{r}^{A}_{H_e}(y,\mathbf{r}_{H_e}(z,t),t) + \tilde{\mathbf{r}}^{N_2}_{H_e}(x,\mathbf{r}^{A}_{H_e}(y,\mathbf{r}_{H_e}(z,t),t),\mathbf{r}_{H_e}(z,t),t).$$

For the neutron field

$$\mathbf{r}_N(y,z,t) = \mathbf{r}^{M}_{N}(z,t) + \hat{\mathbf{r}}_N(y,\mathbf{r}^{M}_{N}(z,t),t)$$

Finally, for the electronic field resulting from ionization,

$$\mathbf{r}_e(y,z,t) = \mathbf{r}^{M}_{e}(z,t) + \hat{\mathbf{r}}_e(y,\mathbf{r}^{M}_{e}(z,t),t)$$

The system is subject to the following constraints

$$\int_\Omega |\hat{\phi}_D^p(x,y,z,t)|^2\,dx = 1,$$

$$\int_\Omega |\hat{\phi}_D^N(x,y,z,t)|^2\,dx = 1,$$

$$\int_\Omega |\hat{\phi}_T^p(x,y,z,t)|^2\,dx = 1,$$

$$\int_\Omega |\hat{\phi}_T^{N_1}(x,y,z,t)|^2\,dx = 1,$$

$$\int_\Omega |\hat{\phi}_T^{N_2}(x,y,z,t)|^2\,dx = 1,$$

$$\int_\Omega |\hat{\phi}_{H_e}^{p_1}(x,y,z,t)|^2\,dx = 1,$$

$$\int_\Omega |\hat{\phi}_{H_e}^{p_2}(x,y,z,t)|^2\,dx = 1,$$

$$\int_\Omega |\hat{\phi}_{H_e}^{N_1}(x,y,z,t)|^2\,dx = 1,$$

$$\int_\Omega |\hat{\phi}_{H_e}^{N_2}(x,y,z,t)|^2\,dx = 1,$$

in $\Omega \times \Omega \times [0, t_f]$,

$$\int_\Omega |\hat{\phi}_N(y,z,t)|^2\,dy = 1,$$

$$\int_\Omega |\hat{\phi}_e(y,,z,t)|^2\,dy = 1,$$

$$\int_\Omega |\phi_D^A(y,z,t)|^2\,dy = 1,$$

$$\int_\Omega |\phi_T^A(y,z,t)|^2\,dy = 1,$$

and

$$\int_\Omega |\hat{\phi}_{He}^A(y,z,t)|^2\,dy = 1,$$

in $\Omega \times [0, t_f]$.

Defining

$$m_D(t) = \int_\Omega |\phi_D(z,t)|^2\,dz,$$

$$m_T(t) = \int_\Omega |\phi_T(z,t)|^2\, dz,$$

$$m_{H_e}(t) = \int_\Omega |\phi(z,t)_{H_e}|^2\, dz,$$

$$m_N(t) = \int_\Omega |\phi_N^M(z,t)|^2\, dz,$$

and

$$m_e(t) = \int_\Omega |\phi_e^M(z,t)|^2\, dz,$$

and also defining

$$\rho_D(\mathbf{r}_D(z,t),t) = |\phi_D(z,t)|^2,$$

$$\rho_T(\mathbf{r}_T(z,t),t) = |\phi_T(z,t)|^2,$$

$$\rho_{H_e}(\mathbf{r}_{H_e}(z,t),t) = |\phi_{H_e}(z,t)|^2,$$

$$\rho_N^M(\mathbf{r}_N^M(z,t),t) = |\phi_N^M(z,t)|^2,$$

$$\rho_e^M(\mathbf{r}_e^M(z,t),t) = |\phi_e^M(z,t)|^2,$$

and

$$\mathbf{v}_D(\mathbf{r}_D(z,t),t) = \frac{\partial \mathbf{r}_D(z,t)}{\partial t},$$

$$\mathbf{v}_T(\mathbf{r}_T(z,t),t) = \frac{\partial \mathbf{r}_T(z,t)}{\partial t},$$

$$\mathbf{v}_{H_e}(\mathbf{r}_{H_e}(z,t),t) = \frac{\partial \mathbf{r}_{H_e}(z,t)}{\partial t},$$

$$\mathbf{v}_N(\mathbf{r}_N^M(z,t),t) = \frac{\partial \mathbf{r}_N^M(z,t)}{\partial t},$$

and

$$\mathbf{v}_e(\mathbf{r}_e^M(z,t),t) = \frac{\partial \mathbf{r}_e^M(z,t)}{\partial t},$$

other constraints may be expressed by

$$\begin{aligned} m_D(t) \;=\; & (m_0)_D - \int_0^t \int_{\partial\Omega} \rho_D(\mathbf{r}_D(z,\tau),\tau)\mathbf{v}_D(\mathbf{r}_D(z,\tau),\tau)\cdot\mathbf{n}\, dS d\tau \\ & -\alpha_D[m_{H_e}(t) + m_N(t)] \\ & -\alpha_D \int_0^t \int_{\partial\Omega} \rho_{H_e}(\mathbf{r}_{H_e}(z,\tau),\tau)\mathbf{v}_{H_e}(\mathbf{r}_{H_e}(z,\tau),\tau)\cdot\mathbf{n}\, dS d\tau \\ & -\alpha_D \int_0^t \int_{\partial\Omega} \rho_N^M(\mathbf{r}_N^M(z,\tau),\tau)\mathbf{v}_N(\mathbf{r}_N^M(z,\tau),\tau)\cdot\mathbf{n}\, dS d\tau \end{aligned} \qquad (32)$$

$$
\begin{aligned}
m_T(t) &= (m_0)_T - \int_0^t \int_{\partial\Omega} \rho_T(\mathbf{r}_T(z,\tau),\tau)\mathbf{v}_T(\mathbf{r}(z,\tau),\tau)\cdot\mathbf{n}\, dSd\tau \\
&\quad -\alpha_T[m_{H_e}(t)+m_N(t)] \\
&\quad -\alpha_T \int_0^t \int_{\partial\Omega} \rho_{H_e}(\mathbf{r}_{H_e}(z,tau),\tau)\mathbf{v}_{H_e}(\mathbf{r}_{H_e}(z,\tau),\tau)\cdot\mathbf{n}\, dSd\tau \\
&\quad -\alpha_T \int_0^t \int_{\partial\Omega} \rho_N^M(\mathbf{r}_N^M(z,\tau),\tau)\mathbf{v}_N(\mathbf{r}_N^M(z,\tau),\tau)\cdot\mathbf{n}\, dSd\tau \qquad (33)
\end{aligned}
$$

$$
\begin{aligned}
&\alpha_N\left(m_{H_e}(t)+\int_0^t\int_{\partial\Omega}\rho_{H_e}(\mathbf{r}_{H_e}(z,\tau),\tau)\mathbf{v}_{H_e}(\mathbf{r}_{H_e}(z,\tau),\tau)\cdot\mathbf{n}\, dSd\tau\right) \\
= \;& \alpha_{H_e}\left(m_N(t)+\int_0^t\int_{\partial\Omega}\rho_N^M(\mathbf{r}_N^M(z,\tau),\tau)\mathbf{v}_N(\mathbf{r}_N^M(z,\tau),\tau)\cdot\mathbf{n}\, dSd\tau\right) \qquad (34)
\end{aligned}
$$

$$
m_e(t) = (m_0)_e - \int_0^t \int_{\partial\Omega} \rho_e^M(\mathbf{r}_e^M(z,\tau),\tau)\mathbf{v}_e(\mathbf{r}_e^M(z,\tau),\tau)\cdot\mathbf{n}\, dSd\tau, \qquad (35)
$$

where $\mathbf{n}$ denotes the outward normal field to $\partial\Omega = S$.

At this point, we define the kinetics energy functional E_C by

$$
\begin{aligned}
E_C \;=\; & \frac{1}{2}\int_0^{t_f}\int_\Omega\int_\Omega\int_\Omega \rho_D^p \frac{\partial \mathbf{r}_D^p}{\partial t}\cdot\frac{\partial \mathbf{r}_D^p}{\partial t}\,dxdydzdt \\
& +\frac{1}{2}\int_0^{t_f}\int_\Omega\int_\Omega\int_\Omega \rho_D^N \frac{\partial \mathbf{r}_D^N}{\partial t}\cdot\frac{\partial \mathbf{r}_D^N}{\partial t}\,dxdydzdt \\
& +\frac{1}{2}\int_0^{t_f}\int_\Omega\int_\Omega\int_\Omega \rho_T^p \frac{\partial \mathbf{r}_T^p}{\partial t}\cdot\frac{\partial \mathbf{r}_T^p}{\partial t}\,dxdydzdt \\
& +\frac{1}{2}\int_0^{t_f}\int_\Omega\int_\Omega\int_\Omega \rho_T^{N_1} \frac{\partial \mathbf{r}_T^{N_1}}{\partial t}\cdot\frac{\partial \mathbf{r}_T^{N_1}}{\partial t}\,dxdydzdt \\
& +\frac{1}{2}\int_0^{t_f}\int_\Omega\int_\Omega\int_\Omega \rho_T^{N_2} \frac{\partial \mathbf{r}_T^{N_2}}{\partial t}\cdot\frac{\partial \mathbf{r}_T^{N_2}}{\partial t}\,dxdydzdt \\
& +\frac{1}{2}\int_0^{t_f}\int_\Omega\int_\Omega\int_\Omega \rho_{He}^{p_1} \frac{\partial \mathbf{r}_{He}^{p_1}}{\partial t}\cdot\frac{\partial \mathbf{r}_{He}^{p_1}}{\partial t}\,dxdydzdt \\
& +\frac{1}{2}\int_0^{t_f}\int_\Omega\int_\Omega\int_\Omega \rho_{He}^{p_2} \frac{\partial \mathbf{r}_{He}^{p_2}}{\partial t}\cdot\frac{\partial \mathbf{r}_{He}^{p_2}}{\partial t}\,dxdydzdt \\
& +\frac{1}{2}\int_0^{t_f}\int_\Omega\int_\Omega\int_\Omega \rho_{He}^{N_1} \frac{\partial \mathbf{r}_{He}^{N_1}}{\partial t}\cdot\frac{\partial \mathbf{r}_{He}^{N_1}}{\partial t}\,dxdydzdt \\
& +\frac{1}{2}\int_0^{t_f}\int_\Omega\int_\Omega\int_\Omega \rho_{He}^{N_2} \frac{\partial \mathbf{r}_{He}^{N_2}}{\partial t}\cdot\frac{\partial \mathbf{r}_{He}^{N_2}}{\partial t}\,dxdydzdt \\
& +\frac{1}{2}\int_0^{t_f}\int_\Omega\int_\Omega \rho_N \frac{\partial \mathbf{r}_N}{\partial t}\cdot\frac{\partial \mathbf{r}_N}{\partial t}\,dydzdt \\
& +\frac{1}{2}\int_0^{t_f}\int_\Omega\int_\Omega \rho_e \frac{\partial \mathbf{r}_e}{\partial t}\cdot\frac{\partial \mathbf{r}_e}{\partial t}\,dydzdt, \qquad (36)
\end{aligned}
$$

We may expand such an expression obtaining

$$E_C = E_{C_1} + E_{C_2} + E_{C_3}$$

where

$$
\begin{aligned}
E_{C_1} \;=\; & \frac{1}{2}\int_0^{t_f}\int_\Omega\int_\Omega \rho_D \frac{\partial \mathbf{r}_D}{\partial t}\cdot\frac{\partial \mathbf{r}_D}{\partial t}\,dzdt \\
& +\frac{1}{2}\int_0^{t_f}\int_\Omega \rho_T \frac{\partial \mathbf{r}_T}{\partial t}\cdot\frac{\partial \mathbf{r}_T}{\partial t}\,dzdt \\
& +\frac{1}{2}\int_0^{t_f}\int_\Omega \rho_{H_e} \frac{\partial \mathbf{r}_{H_e}}{\partial t}\cdot\frac{\partial \mathbf{r}_{H_e}}{\partial t}\,dzdt \\
& +\frac{1}{2}\int_0^{t_f}\int_\Omega \rho_N \frac{\partial \mathbf{r}_N^M}{\partial t}\cdot\frac{\partial \mathbf{r}_N^M}{\partial t}\,dzdt \\
& +\frac{1}{2}\int_0^{t_f}\int_\Omega \rho_e \frac{\partial \mathbf{r}_e^M}{\partial t}\cdot\frac{\partial \mathbf{r}_e^M}{\partial t}\,dzdt, \qquad (37)
\end{aligned}
$$

$$
\begin{aligned}
E_{C_2} \;=\; & \frac{1}{2}\int_0^{t_f}\int_\Omega\int_\Omega\int_\Omega \rho_D^p \frac{\partial \hat{\mathbf{r}}_D^p}{\partial t}\cdot\frac{\partial \hat{\mathbf{r}}_D^p}{\partial t}\,dxdydzdt \\
& +\frac{1}{2}\int_0^{t_f}\int_\Omega\int_\Omega\int_\Omega \rho_D^N \frac{\partial \hat{\mathbf{r}}_D^N}{\partial t}\cdot\frac{\partial \hat{\mathbf{r}}_D^N}{\partial t}\,dxdydzdt \\
& +\frac{1}{2}\int_0^{t_f}\int_\Omega\int_\Omega\int_\Omega \rho_T^p \frac{\partial \hat{\mathbf{r}}_T^p}{\partial t}\cdot\frac{\partial \hat{\mathbf{r}}_T^p}{\partial t}\,dxdydzdt \\
& +\frac{1}{2}\int_0^{t_f}\int_\Omega\int_\Omega\int_\Omega \rho_T^{N_1} \frac{\partial \hat{\mathbf{r}}_T^{N_1}}{\partial t}\cdot\frac{\partial \hat{\mathbf{r}}_T^{N_1}}{\partial t}\,dxdydzdt \\
& +\frac{1}{2}\int_0^{t_f}\int_\Omega\int_\Omega\int_\Omega \rho_T^{N_2} \frac{\partial \hat{\mathbf{r}}_T^{N_2}}{\partial t}\cdot\frac{\partial \hat{\mathbf{r}}_T^{N_2}}{\partial t}\,dxdydzdt \\
& +\frac{1}{2}\int_0^{t_f}\int_\Omega\int_\Omega\int_\Omega \hat{\rho}_{H_e}^{p_1} \frac{\partial \hat{\mathbf{r}}_{H_e}^{p_1}}{\partial t}\cdot\frac{\partial \hat{\mathbf{r}}_{H_e}^{p_1}}{\partial t}\,dxdydzdt \\
& +\frac{1}{2}\int_0^{t_f}\int_\Omega\int_\Omega\int_\Omega \rho_{H_e}^{p_2} \frac{\partial \hat{\mathbf{r}}_{H_e}^{p_2}}{\partial t}\cdot\frac{\partial \hat{\mathbf{r}}_{H_e}^{p_2}}{\partial t}\,dxdydzdt \\
& +\frac{1}{2}\int_0^{t_f}\int_\Omega\int_\Omega\int_\Omega \rho_{H_e}^{N_1} \frac{\partial \hat{\mathbf{r}}_{H_e}^{N_1}}{\partial t}\cdot\frac{\partial \hat{\mathbf{r}}_{H_e}^{N_1}}{\partial t}\,dxdydzdt \\
& +\frac{1}{2}\int_0^{t_f}\int_\Omega\int_\Omega\int_\Omega \rho_{H_e}^{N_2} \frac{\partial \hat{\mathbf{r}}_{H_e}^{N_2}}{\partial t}\cdot\frac{\partial \hat{\mathbf{r}}_{H_e}^{N_2}}{\partial t}\,dxdydzdt \\
& +\frac{1}{2}\int_0^{t_f}\int_\Omega\int_\Omega \rho_N \frac{\partial \hat{\mathbf{r}}_N}{\partial t}\cdot\frac{\partial \hat{\mathbf{r}}_N}{\partial t}\,dydzdt \\
& +\frac{1}{2}\int_0^{t_f}\int_\Omega\int_\Omega \rho_e \frac{\partial \hat{\mathbf{r}}_e}{\partial t}\cdot\frac{\partial \hat{\mathbf{r}}_e}{\partial t}\,dydzdt, \qquad (38)
\end{aligned}
$$

and

$$
\begin{aligned}
E_{C_3} \;=\; & \int_0^{t_f}\int_\Omega\int_\Omega\int_\Omega \rho_D^p \frac{\partial \hat{\mathbf{r}}_D^p}{\partial t}\cdot\frac{\partial \mathbf{r}_D}{\partial t}\,dxdydzdt \\
& + \int_0^{t_f}\int_\Omega\int_\Omega\int_\Omega \rho_D^N \frac{\partial \hat{\mathbf{r}}_D^N}{\partial t}\cdot\frac{\partial \mathbf{r}_D}{\partial t}\,dxdydzdt \\
& + \int_0^{t_f}\int_\Omega\int_\Omega\int_\Omega \rho_T^p \frac{\partial \hat{\mathbf{r}}_T^p}{\partial t}\cdot\frac{\partial \mathbf{r}_T}{\partial t}\,dxdydzdt \\
& + \int_0^{t_f}\int_\Omega\int_\Omega\int_\Omega \rho_T^{N_1} \frac{\partial \hat{\mathbf{r}}_T^{N_1}}{\partial t}\cdot\frac{\partial \mathbf{r}_T}{\partial t}\,dxdydzdt \\
& + \int_0^{t_f}\int_\Omega\int_\Omega\int_\Omega \rho_T^{N_2} \frac{\partial \hat{\mathbf{r}}_T^{N_2}}{\partial t}\cdot\frac{\partial \mathbf{r}_T}{\partial t}\,dxdydzdt \\
& + \int_0^{t_f}\int_\Omega\int_\Omega\int_\Omega \hat{\rho}_{H_e}^{p_1} \frac{\partial \hat{\mathbf{r}}_{H_e}^{p_1}}{\partial t}\cdot\frac{\partial \mathbf{r}_{H_e}}{\partial t}\,dxdydzdt \\
& + \int_0^{t_f}\int_\Omega\int_\Omega\int_\Omega \rho_{H_e}^{p_2} \frac{\partial \hat{\mathbf{r}}_{H_e}^{p_2}}{\partial t}\cdot\frac{\partial \mathbf{r}_{H_e}}{\partial t}\,dxdydzdt \\
& + \int_0^{t_f}\int_\Omega\int_\Omega\int_\Omega \rho_{H_e}^{N_1} \frac{\partial \hat{\mathbf{r}}_{H_e}^{N_1}}{\partial t}\cdot\frac{\partial \mathbf{r}_{H_e}}{\partial t}\,dxdydzdt \\
& + \int_0^{t_f}\int_\Omega\int_\Omega\int_\Omega \rho_{H_e}^{N_2} \frac{\partial \hat{\mathbf{r}}_{H_e}^{N_2}}{\partial t}\cdot\frac{\partial \mathbf{r}_{H_e}}{\partial t}\,dxdydzdt \\
& + \int_0^{t_f}\int_\Omega\int_\Omega \rho_N \frac{\partial \hat{\mathbf{r}}_N}{\partial t}\cdot\frac{\partial \mathbf{r}_N^M}{\partial t}\,dydzdt \\
& + \int_0^{t_f}\int_\Omega\int_\Omega \rho_e \frac{\partial \hat{\mathbf{r}}_e}{\partial t}\cdot\frac{\partial \mathbf{r}_e^M}{\partial t}\,dydzdt, \qquad (39)
\end{aligned}
$$

Here we define the functional E_q where

$$
\begin{aligned}
E_q \;=\; & \frac{\gamma_D^p}{2}\int_0^{t_f}\int_\Omega\int_\Omega\int_\Omega \left|\nabla_x\phi_D^p - iw_D^p\mathbf{A}(z,t)\;\phi_D^p\right|^2\,dxdydzdt \\
& +\frac{\gamma_D^N}{2}\int_0^{t_f}\int_\Omega\int_\Omega\int_\Omega \left|\nabla_x\phi_D^N - iw_D^N\mathbf{A}(z,t)\;\phi_D^N\right|^2\,dxdydzdt \\
& +\frac{\gamma_T^p}{2}\int_0^{t_f}\int_\Omega\int_\Omega\int_\Omega \left|\nabla_x\phi_T^p - iw_T^p\mathbf{A}(z,t)\;\phi_T^p\right|^2\,dxdydzdt \\
& +\frac{\gamma_T^{N_1}}{2}\int_0^{t_f}\int_\Omega\int_\Omega\int_\Omega \left|\nabla_x\phi_T^{N_1} - iw_T^{N_1}\mathbf{A}(z,t)\;\phi_T^{N_1}\right|^2\,dxdydzdt \\
& +\frac{\gamma_T^{N_2}}{2}\int_0^{t_f}\int_\Omega\int_\Omega\int_\Omega \left|\nabla_x\phi_T^{N_2} - iw_T^{N_2}\mathbf{A}(z,t)\;\phi_T^{N_2}\right|^2\,dxdydzdt \\
& +\frac{\gamma_{H_e}^{p_1}}{2}\int_0^{t_f}\int_\Omega\int_\Omega\int_\Omega \left|\nabla_x\phi_{H_e}^{p_1} - iw_{H_e}^{p_1}\mathbf{A}(z,t)\;\phi_{H_e}^{p_1}\right|^2\,dxdydzdt \\
& +\frac{\gamma_{H_e}^{p_2}}{2}\int_0^{t_f}\int_\Omega\int_\Omega\int_\Omega \left|\nabla_x\phi_{H_e}^{p_2} - iw_{H_e}^{p_2}\mathbf{A}(z,t)\;\phi_{H_e}^{p_2}\right|^2\,dxdydzdt \\
& +\frac{\gamma_{H_e}^{N_1}}{2}\int_0^{t_f}\int_\Omega\int_\Omega\int_\Omega \left|\nabla_x\phi_{H_e}^{N_1} - iw_{H_e}^{N_1}\mathbf{A}(z,t)\;\phi_{H_e}^{N_1}\right|^2\,dxdydzdt \\
& +\frac{\gamma_{H_e}^{N_2}}{2}\int_0^{t_f}\int_\Omega\int_\Omega\int_\Omega \left|\nabla_x\phi_{H_e}^{N_2} - iw_{H_e}^{N_2}\mathbf{A}\;\phi_{H_e}^{N_2}\right|^2\,dxdydzdt \\
& +\frac{\gamma_N}{2}\int_0^{t_f}\int_\Omega\int_\Omega\int_\Omega |\nabla_y\phi_N - iw_N\mathbf{A}(z,t)\;\phi_N|^2\,dydzdt \\
& +\frac{\gamma_e}{2}\int_0^{t_f}\int_\Omega\int_\Omega\int_\Omega |\nabla_y\phi_e - iw_e\phi_e\mathbf{A}(z,t)\;\phi_e|^2\,dydzdt \\
& +\frac{\gamma_D^A}{2}\int_0^{t_f}\int_\Omega\int_\Omega |\nabla_y\phi_D^A - iw_D^A\mathbf{A}(z,t)\;\phi_D^A|^2\,dydzdt \\
& +\frac{\gamma_T^A}{2}\int_0^{t_f}\int_\Omega\int_\Omega |\nabla_y\phi_T^A - iw_T^A\mathbf{A}(z,t)\;\phi_T^A|^2\,dydzdt \\
& +\frac{\gamma_{H_e}^A}{2}\int_0^{t_f}\int_\Omega\int_\Omega |\nabla_y\phi_{H_e}^A - iw_{H_e}^A\mathbf{A}(z,t)\;\phi_{He}^A|^2\,dydzdt \\
& +\frac{\gamma_D}{2}\int_0^{t_f}\int_\Omega\int_\Omega |\nabla_z\phi_D - iw_D\mathbf{A}(z,t)\;\phi_D|^2\,dzdt \\
& +\frac{\gamma_T}{2}\int_0^{t_f}\int_\Omega\int_\Omega |\nabla_z\phi_T - iw_T\mathbf{A}(z,t)\;\phi_T|^2\,dzdt \\
& +\frac{\gamma_{H_e}}{2}\int_0^{t_f}\int_\Omega\int_\Omega |\nabla_z\phi_{H_e} - iw_{H_e}\mathbf{A}(z,t)\;\phi_{H_e}|^2\,dzdt \\
& +\frac{\gamma_N^M}{2}\int_0^{t_f}\int_\Omega\int_\Omega |\nabla_z\phi_N^M - iw_N^M\mathbf{A}(z,t)\;\phi_N^M|^2\,dzdt \\
& +\frac{\gamma_e^M}{2}\int_0^{t_f}\int_\Omega\int_\Omega |\nabla_z\phi_e^M - iw_N^M\mathbf{A}(z,t)\;\phi_e^M|^2\,dzdt. \qquad (40)
\end{aligned}
$$

We define also,

$$\begin{aligned} E_{q_1} &= \frac{\gamma_D^0}{2}\int_0^{t_f}\int_\Omega \frac{\partial\phi_D}{\partial t}\cdot\frac{\partial\phi_D}{\partial t}\,dzdt \\ &+\frac{\gamma_T^0}{2}\int_0^{t_f}\int_\Omega \frac{\partial\phi_T}{\partial t}\cdot\frac{\partial\phi_T}{\partial t}\,dzdt \\ &+\frac{\gamma_{H_e}^0}{2}\int_0^{t_f}\int_\Omega \frac{\partial\phi_{H_e}}{\partial t}\cdot\frac{\partial\phi_{H_e}}{\partial t}\,dzdt \\ &+\frac{\gamma_N^0}{2}\int_0^{t_f}\int_\Omega \frac{\partial\phi_N^M}{\partial t}\cdot\frac{\partial\phi_N^M}{\partial t}\,dxdt \\ &+\frac{\gamma_e^0}{2}\int_0^{t_f}\int_\Omega \frac{\partial\phi_e^M}{\partial t}\cdot\frac{\partial\phi_e^M}{\partial t}\,dzdt. \end{aligned} \tag{41}$$

For the interaction energy functional we consider only a simplified self interaction part, denoted by E_{int}, where

$$\begin{aligned} E_{int} &= \frac{\alpha_D}{2}\int_0^{t_f}\int_\Omega\int_\Omega\int_\Omega |\phi_D|^4\,dxdydzdt \\ &+\frac{\alpha_T}{2}\int_0^{t_f}\int_\Omega\int_\Omega\int_\Omega |\phi_T|^4\,dxdydzdt \\ &+\frac{\alpha_{H_e}}{2}\int_0^{t_f}\int_\Omega\int_\Omega\int_\Omega |\phi_{H_e}|^4\,dxdydzdt \\ &+\frac{\alpha_N}{2}\int_0^{t_f}\int_\Omega\int_\Omega |\phi_N|^4\,dydzdt \\ &+\frac{\alpha_e}{2}\int_0^{t_f}\int_\Omega\int_\Omega |\phi_e|^4\,dydzdt. \end{aligned} \tag{42}$$

Furthermore, concerning the scalar temperature field, we define

$$\begin{aligned} (C_v)_D\rho_D(z,t)T_D(z,t) &= \int_\Omega\int_\Omega \left(\frac{1}{2}|\phi_D^p|^2\frac{\partial\hat{\mathbf{r}}_D^p}{\partial t}\cdot\frac{\partial\hat{\mathbf{r}}_D^p}{\partial t}\right)dxdy \\ &+\int_\Omega\int_\Omega \left(\frac{1}{2}|\phi_D^N|^2\frac{\partial\hat{\mathbf{r}}_D^N}{\partial t}\cdot\frac{\partial\hat{\mathbf{r}}_D^N}{\partial t}\right)dxdy \end{aligned} \tag{43}$$

$$\begin{aligned} (C_v)_T\rho_T(z,t)T_T(z,t) &= \int_\Omega\int_\Omega \left(\frac{1}{2}|\phi_T^p|^2\frac{\partial\hat{\mathbf{r}}_T^p}{\partial t}\cdot\frac{\partial\hat{\mathbf{r}}_T^p}{\partial t}\right)dxdy \\ &+\int_\Omega\int_\Omega \left(\frac{1}{2}|\phi_T^{N_1}|^2\frac{\partial\hat{\mathbf{r}}_T^{N_1}}{\partial t}\cdot\frac{\partial\hat{\mathbf{r}}_T^{N_1}}{\partial t}\right)dxdy \\ &+\int_\Omega\int_\Omega \left(\frac{1}{2}|\phi_T^{N_2}|^2\frac{\partial\hat{\mathbf{r}}_T^{N_2}}{\partial t}\cdot\frac{\partial\hat{\mathbf{r}}_T^{N_2}}{\partial t}\right)dxdy \end{aligned} \tag{44}$$

$$
\begin{aligned}
(C_v)_{H_e}\rho_{H_e}(z,t)T_{H_e}(z,t) &= \int_\Omega\int_\Omega \left(\frac{1}{2}|\phi_{H_e}^{p_1}|^2\frac{\partial\hat{\mathbf{r}}_{H_e}^{p_1}}{\partial t}\cdot\frac{\partial\hat{\mathbf{r}}_{H_e}^{p_1}}{\partial t}\right)dxdy \\
&+ \int_\Omega\int_\Omega \left(\frac{1}{2}|\phi_{H_e}^{p_2}|^2\frac{\partial\hat{\mathbf{r}}_{H_e}^{p_2}}{\partial t}\cdot\frac{\partial\hat{\mathbf{r}}_{H_e}^{p_2}}{\partial t}\right)dxdy \\
&+ \int_\Omega\int_\Omega \left(\frac{1}{2}|\phi_{H_e}^{N_1}|^2\frac{\partial\hat{\mathbf{r}}_{H_e}^{N_1}}{\partial t}\cdot\frac{\partial\hat{\mathbf{r}}_{H_e}^{N_1}}{\partial t}\right)dxdy \\
&+ \int_\Omega\int_\Omega \left(\frac{1}{2}|\phi_{H_e}^{N_2}|^2\frac{\partial\hat{\mathbf{r}}_{H_e}^{N_2}}{\partial t}\cdot\frac{\partial\hat{\mathbf{r}}_{H_e}^{N_2}}{\partial t}\right)dxdy \qquad (45)
\end{aligned}
$$

$$
(C_v)_N\rho_N^M(z,t)T_N(z,t) = \int_\Omega \left(\frac{1}{2}|\phi_N|^2\frac{\partial\hat{\mathbf{r}}_N}{\partial t}\cdot\frac{\partial\hat{\mathbf{r}}_N}{\partial t}\right)dy \qquad (46)
$$

$$
(C_v)_e\rho_e^M(z,t)T_e = \int_\Omega \left(\frac{1}{2}|\phi_e|^2\frac{\partial\hat{\mathbf{r}}_e}{\partial t}\cdot\frac{\partial\hat{\mathbf{r}}_e}{\partial t}\right)dy \qquad (47)
$$

Moreover, we define

$$
T(z,t) = T_D + T_T + T_{H_e} + T_N + T_e
$$

and similarly as indicated in [16] for a non-viscous fluid, we also assume the following constraint

$$
\begin{aligned}
&|\phi_D|^2(C_v)_D\frac{\partial T_D}{\partial t} + |\phi_T|^2(C_v)_T\frac{\partial T_T}{\partial t} \\
&+|\phi_{He}|^2(C_v)_{H_e}\frac{\partial T_{H_e}}{\partial t} + |\phi_N|^2(C_v)_N\frac{\partial T_N}{\partial t} + |\phi_e|^2(C_v)_e\frac{\partial T_e}{\partial t} \\
&-K_D\nabla^2T_D - K_T\nabla^2T_T - K_{H_e}\nabla^2T_{H_e} - K_N\nabla^2T_N - K_e\nabla^2T_e \\
&+P_D\ \text{div}\ \mathbf{v}_D + P_T\ \text{div}\ \mathbf{v}_T + P_{H_e}\ \text{div}\ \mathbf{v}_{H_e} \\
&+P_N\ \text{div}\ \mathbf{v}_N + P_e\ \text{div}\ \mathbf{v}_e - \frac{\partial Q}{\partial t} = 0,\ \text{in}\ \Omega\times[0,t_f], \qquad (48)
\end{aligned}
$$

where Q is a heat function and

$$
P_D = \frac{d(\hat{P}\rho_D)}{dt},
$$

$$
P_T = \frac{d(\hat{P}\rho_T)}{dt},
$$

$$
P_{H_e} = \frac{d(\hat{P}\rho_{H_e})}{dt},
$$

$$P_N = \frac{d(\hat{P}\rho_N)}{dt},$$

and

$$P_e = \frac{d(\hat{P}\rho_e)}{dt}.$$

Finally, we assume the following mass conservation equation as a constraint

$$\begin{aligned} &\frac{d\rho}{dt} + \rho_D \text{ div } (\mathbf{v}_D) + \rho_T \text{ div } (\mathbf{v}_T) \\ &+\rho_{H_e} \text{ div } (\mathbf{v}_{H_e}) + \rho_N \text{ div } (\mathbf{v}_N) \\ &+\rho_e \text{ div } (\mathbf{v}_e) = 0, \text{ in } \Omega \times [0, t_f], \end{aligned} \tag{49}$$

where we recall to have denoted

$$\rho = \rho_D + \rho_T + \rho_{H_e} + \rho_N + \rho_e$$

and

$$\rho_D = \rho_D(\mathbf{r}_D(z,t),t),$$

$$\rho_T = \rho_T(\mathbf{r}_T(z,t),t),$$

$$\rho_{H_e} = \rho_{H_e}(\mathbf{r}_{H_e}(z,t),t),$$

$$\rho_N = \rho_N(\mathbf{r}_N^M(z,t),t),$$

and

$$\rho_e = \rho_e(\mathbf{r}_e^M(z,t),t).$$

In order to model such a chemical reaction, we define the following functional J, which corresponds to a variational formulation for the model in question, where

$$
\begin{aligned}
J \;=\; & E_{C_1} + E_{C_2} + E_{C_3} + E_q + E_{q_1} + E_{int} \\
& - \int_0^{t_f} \int_\Omega \hat{P} \left(\frac{d\rho}{dt} + \rho_D \text{ div } (\mathbf{v}_D) + \rho_T \text{ div } (\mathbf{v}_T) \right. \\
& + \rho_{H_e} \text{ div } (\mathbf{v}_{H_e}) + \rho_N \text{ div } (\mathbf{v}_N) \\
& \left. + \rho_e \text{ div } (\mathbf{v}_e) \right) \, dzdt \\
& - \int_0^{t_f} \int_\Omega \mathbf{g} \cdot (\rho_D \mathbf{r}_D + \rho_T \mathbf{r}_T + \rho_{H_e} \mathbf{r}_{H_e} + \rho_N \mathbf{r}_N^M + \rho_e \mathbf{r}_e^M) \, dzdt \\
& + \int_0^{t_f} \int_\Omega \hat{\lambda}_1 \left(\mathbf{v}_D(\mathbf{r}_D(z,t),t) - \frac{\partial \mathbf{r}_D(z,t)}{\partial t} \right) \, dzdt \\
& + \int_0^{t_f} \int_\Omega \hat{\lambda}_2 \left(\mathbf{v}_T(\mathbf{r}_T(z,t),t) - \frac{\partial \mathbf{r}_T(z,t)}{\partial t} \right) \, dzdt \\
& + \int_0^{t_f} \int_\Omega \hat{\lambda}_3 \left(\mathbf{v}_{H_e}(\mathbf{r}_{H_e}(z,t),t) - \frac{\partial \mathbf{r}_{H_e}(z,t)}{\partial t} \right) \, dzdt \\
& + \int_0^{t_f} \int_\Omega \hat{\lambda}_4 \left(\mathbf{v}_N(\mathbf{r}_N^M(z,t),t) - \frac{\partial \mathbf{r}_N^M(z,t)}{\partial t} \right) \, dzdt \\
& + \int_0^{t_f} \int_\Omega \hat{\lambda}_5 \left(\mathbf{v}_e(\mathbf{r}_e^M(z,t),t) - \frac{\partial \mathbf{r}_e^M(z,t)}{\partial t} \right) \, dzdt \\
& + \int_0^{t_f} \int_\Omega \hat{\lambda}_6 (\rho_D(\mathbf{r}_D(z,t),t) - |\phi_D(z,t)|^2) \, dzdt \\
& + \int_0^{t_f} \int_\Omega \hat{\lambda}_7 (\rho_T(\mathbf{r}_T(z,t),t) - |\phi_T(z,t)|^2) \, dzdt \\
& + \int_0^{t_f} \int_\Omega \hat{\lambda}_8 (\rho_{H_e}(\mathbf{r}_{H_e}(z,t),t) - |\phi_{H_e}(z,t)|^2) \, dzdt \\
& + \int_0^{t_f} \int_\Omega \hat{\lambda}_9 (\rho_N(\mathbf{r}_N^M(z,t),t) - |\phi_N^M(z,t)|^2) \, dzdt \\
& + \int_0^{t_f} \int_\Omega \hat{\lambda}_{10} (\rho_e(\mathbf{r}_e^M(z,t),t) - |\phi_e^M(z,t)|^2) \, dzdt \\
& + J_{Aux_1} + J_{Aux_2} + J_{Aux_3} + J_{Aux_4} + J_{Aux_5} + J_{Aux_6}, \qquad (50)
\end{aligned}
$$

where

$$
\begin{aligned}
& J_{Aux_1} \\
= & \int_0^{t_f} \int_\Omega \lambda_D \left((C_v)_D \rho_D(z,t) T_D(z,t) - \int_\Omega \int_\Omega \left(\frac{1}{2} |\phi_D^p|^2 \frac{\partial \hat{\mathbf{r}}_D^p}{\partial t} \cdot \frac{\partial \hat{\mathbf{r}}_D^p}{\partial t} \right) dxdy \right. \\
& \left. - \int_\Omega \int_\Omega \left(\frac{1}{2} |\phi_D^N|^2 \frac{\partial \hat{\mathbf{r}}_D^N}{\partial t} \cdot \frac{\partial \hat{\mathbf{r}}_D^N}{\partial t} \right) dxdy \right) dzdt \\
& - \int_0^{t_f} \int_\Omega \lambda_T \left((C_v)_T \rho_T(z,t) T_T(z,t) - \int_\Omega \int_\Omega \left(\frac{1}{2} |\phi_T^p|^2 \frac{\partial \hat{\mathbf{r}}_T^p}{\partial t} \cdot \frac{\partial \hat{\mathbf{r}}_T^p}{\partial t} \right) dxdy \right. \\
& - \int_\Omega \int_\Omega \left(\frac{1}{2} |\phi_T^{N_1}|^2 \frac{\partial \hat{\mathbf{r}}_T^{N_1}}{\partial t} \cdot \frac{\partial \hat{\mathbf{r}}_T^{N_1}}{\partial t} \right) dxdy \\
& \left. - \int_\Omega \int_\Omega \left(\frac{1}{2} |\phi_T^{N_2}|^2 \frac{\partial \hat{\mathbf{r}}_T^{N_2}}{\partial t} \cdot \frac{\partial \hat{\mathbf{r}}_T^{N_2}}{\partial t} \right) dxdy \right) dzdt \\
& + \int_0^{t_f} \int_\Omega \lambda_{H_e} \left((C_v)_{H_e} \rho_{H_e}(z,t) T_{H_e}(z,t) - \int_\Omega \int_\Omega \left(\frac{1}{2} |\phi_{H_e}^{p_1}|^2 \frac{\partial \hat{\mathbf{r}}_{H_e}^{p_1}}{\partial t} \cdot \frac{\partial \hat{\mathbf{r}}_{H_e}^{p_1}}{\partial t} \right) dxdy \right. \\
& - \int_\Omega \int_\Omega \left(\frac{1}{2} |\phi_{H_e}^{p_2}|^2 \frac{\partial \hat{\mathbf{r}}_{H_e}^{p_2}}{\partial t} \cdot \frac{\partial \hat{\mathbf{r}}_{H_e}^{p_2}}{\partial t} \right) dxdy \\
& - \int_\Omega \int_\Omega \left(\frac{1}{2} |\phi_{H_e}^{N_1}|^2 \frac{\partial \hat{\mathbf{r}}_{H_e}^{N_1}}{\partial t} \cdot \frac{\partial \hat{\mathbf{r}}_{H_e}^{N_1}}{\partial t} \right) dxdy \\
& \left. - \int_\Omega \int_\Omega \left(\frac{1}{2} |\phi_{H_e}^{N_2}|^2 \frac{\partial \hat{\mathbf{r}}_{H_e}^{N_2}}{\partial t} \cdot \frac{\partial \hat{\mathbf{r}}_{H_e}^{N_2}}{\partial t} \right) dxdy \right) dzdt \\
& + \int_0^{t_f} \int_\Omega \lambda_N \left((C_v)_N \rho_N^M(z,t) T_N(z,t) - \int_\Omega \left(\frac{1}{2} |\phi_N|^2 \frac{\partial \hat{\mathbf{r}}_N}{\partial t} \cdot \frac{\partial \hat{\mathbf{r}}_N}{\partial t} \right) dy \right) dzdt \\
& + \int_0^{t_f} \int_\Omega \lambda_e \left((C_v)_e \rho_e^M(z,t) T_e - \int_\Omega \left(\frac{1}{2} |\phi_e|^2 \frac{\partial \hat{\mathbf{r}}_e}{\partial t} \cdot \frac{\partial \hat{\mathbf{r}}_e}{\partial t} \right) dy \right) dzdt \\
& + \int_0^{t_f} \int_\Omega \lambda_1 \left(|\phi_D|^2 (C_v)_D \frac{\partial T_D}{\partial t} + |\phi_T|^2 (C_v)_T \frac{\partial T_T}{\partial t} \right. \\
& + |\phi_{H_e}|^2 (C_v)_{H_e} \frac{\partial T_{H_e}}{\partial t} + |\phi_N|^2 (C_v)_N \frac{\partial T_N}{\partial t} + |\phi_e|^2 (C_v)_e \frac{\partial T_e}{\partial t} \\
& - K_D \nabla^2 T_D - K_T \nabla^2 T_T - K_{H_e} \nabla^2 T_{H_e} - K_N \nabla^2 T_N - K_e \nabla^2 T_e \\
& + P_D \text{ div } \mathbf{v}_D + P_T \text{ div } \mathbf{v}_T + P_{H_e} \text{ div } \mathbf{v}_{H_e} \\
& \left. + P_N \text{ div } \mathbf{v}_N + P_e \text{ div } \mathbf{v}_e - \frac{\partial Q}{\partial t} \right) dzdt, \qquad (51)
\end{aligned}
$$

Moreover,

$$
\begin{aligned}
& J_{Aux_2} \\
= & \int_0^{t_f} \int_\Omega \int_\Omega E_D^p(y,z,t) \left(\int_\Omega |\hat{\phi}_D^p(x,y,z,t)|^2 \, dx - 1 \right) dydzdt \\
& + \int_0^{t_f} \int_\Omega \int_\Omega E_D^p(y,z,t) \left(\int_\Omega |\hat{\phi}_D^N(x,y,z,t)|^2 \, dx - 1 \right) dydzdt \\
& + \int_0^{t_f} \int_\Omega \int_\Omega E_T^p(y,z,t) \left(\int_\Omega |\hat{\phi}_T^p(x,y,z,t)|^2 \, dx - 1 \right) dydzdt \\
& + \int_0^{t_f} \int_\Omega \int_\Omega E_T^{N_1}(y,z,t) \left(\int_\Omega |\hat{\phi}_T^{N_1}(x,y,z,t)|^2 \, dx - 1 \right) dydzdt \\
& + \int_0^{t_f} \int_\Omega \int_\Omega E_T^{N_2}(y,z,t) \left(\int_\Omega |\hat{\phi}_T^{N_2}(x,y,z,t)|^2 \, dx - 1 \right) dydzdt \\
& + \int_0^{t_f} \int_\Omega \int_\Omega E_{H_e}^{p_1}(y,z,t) \left(\int_\Omega |\hat{\phi}_{H_e}^{p_1}(x,y,z,t)|^2 \, dx - 1 \right) dydzdt \\
& + \int_0^{t_f} \int_\Omega \int_\Omega E_{H_e}^{p_2}(y,z,t) \left(\int_\Omega |\hat{\phi}_{H_e}^{p_2}(x,y,z,t)|^2 \, dx - 1 \right) dydzdt \\
& + \int_0^{t_f} \int_\Omega \int_\Omega E_{H_e}^{N_1}(y,z,t) \left(\int_\Omega |\hat{\phi}_{H_e}^{N_1}(x,y,z,t)|^2 \, dx - 1 \right) dydzdt \\
& + \int_0^{t_f} \int_\Omega \int_\Omega E_{H_e}^{N_2}(y,z,t) \left(\int_\Omega |\hat{\phi}_{H_e}^{N_2}(x,y,z,t)|^2 \, dx - 1 \right) dydzdt \qquad (52)
\end{aligned}
$$

$$
\begin{aligned}
& J_{Aux_3} \\
= & \int_0^{t_f} \int_\Omega E_N(z,t) \left(\int_\Omega \int_\Omega |\hat{\phi}_N(y,z,t)|^2 \, dy - 1 \right) dzdt, \\
& + \int_0^{t_f} \int_\Omega E_e(z,t) \left(\int_\Omega |\hat{\phi}_e(y,,z,t)|^2 \, dy - 1 \right) dzdt, \\
& + \int_0^{t_f} \int_\Omega E_D^A(z,t) \left(\int_\Omega |\phi_D^A(y,z,t)|^2 \, dy - 1 \right) dzdt \\
& + \int_0^{t_f} \int_\Omega E_T^A(z,t) \left(\int_\Omega |\phi_T^A(y,z,t)|^2 \, dy - 1 \right) dzdt \\
& + \int_0^{t_f} \int_\Omega E_{H_e}^A(z,t) \left(\int_\Omega |\phi_{H_e}^A(y,z,t)|^2 \, dy - 1 \right) dzdt \qquad (53)
\end{aligned}
$$

and denoting

$$
\begin{aligned}
&J_{Aux_4} = \\
&\int_0^{t_f} \mu_D(t) \left(m_D(t) - (m_0)_D + \int_0^t \int_{\partial\Omega} \rho_D(\mathbf{r}_D(z,t),\tau),\tau)\mathbf{v}_D(\mathbf{r}_D(z,\tau),\tau) \cdot \mathbf{n}\, dSd\tau \right. \\
&+\alpha_D[m_{H_e}(t) + m_N(t)] - \alpha_D \int_0^t \int_{\partial\Omega} \rho_{H_e}(\mathbf{r}_{H_e}(z,\tau),\tau)\mathbf{v}_{H_e}(\mathbf{r}_{He}(z,\tau),\tau) \cdot \mathbf{n}\, dSd\tau \\
&\left. +\alpha_D \int_0^t \int_{\partial\Omega} \rho_N(\mathbf{r}_N^M(z,\tau),\tau)\mathbf{v}_N(\mathbf{r}_N^M(z,\tau),\tau) \cdot \mathbf{n}\, dSd\tau \right)\, dt \\
&+ \int_0^{t_f} \mu_T(t) \left(m_T(t) - (m_0)_T + \int_0^t \int_{\partial\Omega} \rho_T(\mathbf{r}_T(z,\tau),\tau)\mathbf{v}_T(\mathbf{r}_T(z,\tau),\tau) \cdot \mathbf{n}\, dSd\tau \right. \\
&+\alpha_T[m_{H_e}(t) + m_N(t)] + \alpha_T \int_0^t \int_{\partial\Omega} \rho_{H_e}(\mathbf{r}_{H_e}(z,\tau),\tau)\mathbf{v}_{H_e}(z,\tau) \cdot \mathbf{n}\, dSd\tau \\
&\left. +\alpha_T \int_0^t \int_{\partial\Omega} \rho_N(\mathbf{r}_N^M(z,\tau),\tau)\mathbf{v}_N(\mathbf{r}_N^M(z,\tau),\tau) \cdot \mathbf{n}\, dSd\tau \right)\, dt \\
&+ \int_0^{t_f} \mu_3(t) \left(\alpha_N \left(m_{H_e}(t) + \int_0^t \int_{\partial\Omega} \rho_{H_e}(\mathbf{r}_{H_e}(z,\tau),\tau)\mathbf{v}_{H_e}(\mathbf{r}_{H_e}(z,\tau),\tau) \cdot \mathbf{n}\, dSd\tau \right) \right. \\
&\left. -\alpha_{H_e} \left(m_N(t) + \int_0^t \int_{\partial\Omega} \rho_N(\mathbf{r}_N^M(z,\tau),\tau)\mathbf{v}_N(\mathbf{r}_N^M(z,\tau),\tau) \cdot \mathbf{n}\, dSd\tau \right) \right)\, dt \\
&+ \int_0^{t_f} \mu_4(t) \left(m_e(t) - (m_0)_e \right. \\
&\left. + \int_0^t \int_{\partial\Omega} \rho_e^M(\mathbf{r}_e^M(z,\tau),\tau)\mathbf{v}_e(\mathbf{r}_e^M(z,\tau),\tau) \cdot \mathbf{n}\, dSd\tau \right)\, dt. \qquad (54)
\end{aligned}
$$

Furthermore,

$$
\begin{aligned}
& J_{Aux_5} \\
= \; & -K_1 \int_0^{t_f} \int_\Omega \int_\Omega \int_\Omega V(\mathbf{r}_D^p, \mathbf{r}_T^p, \mathbf{r}_{H_e}^{p_1}, \mathbf{r}_{H_e}^{p_2}, \mathbf{r}_e) \\
& \times (|\phi_D^p|^2 + |\phi_T^p|^2 + |\phi_{H_e}^{p_1}|^2 + |\phi_{H_e}^{p_2}|^2 + |\phi_e|^2)\, dxdydzdt \\
& -K_1 \int_0^{t_f} \int_\Omega \int_\Omega \int_\Omega |\phi_D^p|^2 \mathbf{B} \times \frac{\partial \mathbf{r}_D^p}{\partial t} \cdot \left(\mathbf{r}_D^p(z, \varepsilon t) - (\mathbf{r}_0)_D^p\right)\, dxdydzdt \\
& -K_1 \int_0^{t_f} \int_\Omega \int_\Omega \int_\Omega |\phi_T^p|^2 \mathbf{B} \times \frac{\partial \mathbf{r}_T^p}{\partial t} \cdot \left(\mathbf{r}_T^p(z, \varepsilon t) - (\mathbf{r}_0)_T^p\right)\, dxdydzdt \\
& -K_1 \int_0^{t_f} \int_\Omega \int_\Omega \int_\Omega |\phi_{H_e}^{p_1}|^2 \mathbf{B} \times \frac{\partial \mathbf{r}_{H_e}^{p_1}}{\partial t} \cdot \left(\mathbf{r}_{H_e}^{p_1}(z, \varepsilon t) - (\mathbf{r}_0)_{H_e}^{p_1}\right)\, dxdydzdt \\
& -K_1 \int_0^{t_f} \int_\Omega \int_\Omega \int_\Omega |\phi_{H_e}^{p_2}|^2 \mathbf{B} \times \frac{\partial \mathbf{r}_{H_e}^{p_2}}{\partial t} \cdot \left(\mathbf{r}_{H_e}^{p_2}(z, \varepsilon t) - (\mathbf{r}_0)_{H_e}^{p_2}\right)\, dxdydzdt \\
& -K_1 \int_0^{t_f} \int_\Omega \int_\Omega \int_\Omega |\phi_e|^2 \mathbf{B} \times \frac{\partial \mathbf{r}_e}{\partial t} \cdot (\mathbf{r}_e(z, \varepsilon t) - (\mathbf{r}_0)_e)\, dxdydzdt \\
& + \frac{1}{8\pi} \int_0^{t_f} \int_\Omega |\operatorname{curl} \mathbf{A}(z,t) - \mathbf{B}_0(z,t)|^2\, dzdt \\
& + \frac{1}{8\pi} \int_0^{t_f} \int_\Omega \left| \int_\Omega \int_\Omega \nabla_z V(\mathbf{r}_D^p, \mathbf{r}_T^p, \mathbf{r}_{H_e}^{p_1}, \mathbf{r}_{H_e}^{p_2}, \mathbf{r}_e)\, dxdy + \frac{1}{c} \frac{\partial \mathbf{A}}{\partial t} \right|^2 dzdt, \quad (55)
\end{aligned}
$$

where

$$\mathbf{B}(z,t) = \operatorname{curl} \mathbf{A}(z,t) - \mathbf{B}_0(z,t)$$

is the total magnetic field,

$$\mathbf{A} = (A_1, A_2, A_3) \in W^{1,2}(\Omega \times [0, t_f]; \mathbb{R}^3)$$

denotes the magnetic potential and

$$\mathbf{E} = -\int_\Omega \int_\Omega \nabla_z V(\mathbf{r}_D^p, \mathbf{r}_T^p, \mathbf{r}_{H_e}^{p_1}, \mathbf{r}_{H_e}^{p_2}, \mathbf{r}_e)\, dxdy - \frac{1}{c} \frac{\partial \mathbf{A}}{\partial t},$$

denotes the electric field.

Finally,

$$
\begin{aligned}
J_{Aux_6} \;=\; & -K_1 \int_0^{t_f} \int_\Omega \int_\Omega \int_\Omega |\phi_D^p|^2 \mathbf{A} \cdot \frac{\partial \mathbf{r}_D^p}{\partial t}\, dxdydzdt \\
& -K_1 \int_0^{t_f} \int_\Omega \int_\Omega \int_\Omega |\phi_T^p|^2 \mathbf{A} \cdot \frac{\partial \mathbf{r}_T^p}{\partial t}\, dxdydzdt \\
& -K_1 \int_0^{t_f} \int_\Omega \int_\Omega \int_\Omega |\phi_{H_e}^{p_1}|^2 \mathbf{A} \cdot \frac{\partial \mathbf{r}_{H_e}^{p_1}}{\partial t}\, dxdydzdt \\
& -K_1 \int_0^{t_f} \int_\Omega \int_\Omega \int_\Omega |\phi_{H_e}^{p_2}|^2 \mathbf{A} \cdot \frac{\partial \mathbf{r}_{H_e}^{p_2}}{\partial t}\, dxdydzdt \\
& -K_2 \int_0^{t_f} \int_\Omega \int_\Omega |\phi_e|^2 \mathbf{A} \cdot \frac{\partial \mathbf{r}_e}{\partial t}\, dydzdt. \qquad (56)
\end{aligned}
$$

Remark 3.1. *About the domain of the functional J, we generically define it as sets of smooth C^2 functions, specifying only the following boundary and initial conditions*

$$\mathbf{r} = (\mathbf{r}_D, \mathbf{r}_T, \mathbf{r}_{H_e}, \mathbf{r}_N^M, \mathbf{r}_e^M) = \mathbf{0}, \;\; on\ \partial\Omega \times [0, t_f],$$

$$\mathbf{r}|_{t=0} = z, \;\; in\ \Omega,$$

$$\mathbf{v} = (\mathbf{v}_D, \mathbf{v}_T, \mathbf{v}_{H_e}, \mathbf{v}_N^M, \mathbf{v}_e^M) = \mathbf{0}, \;\; on\ \partial\Omega_1 \times [0, t_f],$$

where

$$S = \partial\Omega = \partial\Omega_1 \cup \partial\Omega_2,$$

$$\mathbf{v}_{t=0} = \mathbf{v}_0 \;\; in\ \Omega,$$

$$T = T_0(z,t) \;\; on\ \partial\Omega \times [0, t_f]$$

$$T|_{t=0} = T_1(z), \;\; in\ \Omega$$

and

$$\rho|_{t=0} = (\rho_D, \rho_T, \rho_{H_e}, \rho_N, \rho_e)|_{t=0} = ((\rho_D)_0, (\rho_T)_0, 0, 0, (\rho_e)_0) \;\; in\ \Omega.$$

Remark 3.2. *Concerning the variation of J in $\mathbf{r}$, we consider variations in the context*

$$(\mathbf{r} + h\varphi) \;\; and \;\; (\mathbf{r}(\cdot, \varepsilon t) + h\varphi),$$

that is, the same variable variation φ and real constant h for both $\mathbf{r}$ and $\mathbf{r}(\cdot, \varepsilon t)$ for obtaining an approximate Euler-Lagrange equation. Finally, letting $\varepsilon \to 0$ we obtain the correct Euler-Lagrange equation.

3.1 About some of the Euler-Lagrange equations

The variation of J in $\mathbf{v}_D$ stands for

$$\rho_D \mathbf{v}_D + \hat{\lambda}_1 + \nabla(\rho_D \hat{P}) - \nabla(\lambda_1 P_D) = \mathbf{0},$$

in $\Omega \times [0, t_f]$.

Symbolically, the variation of J in $\mathbf{r}_D$ stands for

$$\begin{aligned} \frac{dJ}{d\mathbf{r}_D} &= \frac{\partial J}{\partial \mathbf{v}} \frac{\partial \mathbf{v}}{\partial \mathbf{r}_D} + \frac{\partial J}{\partial \rho} \frac{\partial \rho}{\partial \mathbf{r}_D} + \frac{\partial J}{\partial \mathbf{r}_D} \\ &= \frac{\partial J}{\partial \mathbf{r}_D} \\ &= \mathbf{0}, \end{aligned} \tag{57}$$

that is,

$$\begin{aligned} &\frac{\partial \hat{\lambda}_1}{\partial t} - \int_\Omega \int_\Omega \frac{d}{dt} \left(\rho_D^p \frac{d\hat{\mathbf{r}}_D^p}{dt} \right) dxdy \\ &- \int_\Omega \int_\Omega \frac{d}{dt} \left(\rho_D^N \frac{d\hat{\mathbf{r}}_D^N}{dt} \right) dxdy \\ &- K_1 \int_\Omega \int_\Omega \left(|\phi_D|^2 \mathbf{B} \times \frac{\partial \mathbf{r}_D^p}{\partial t} \right) dxdy \\ &- \int_\Omega \int_\Omega \left(K_1 \frac{\partial V}{\partial \mathbf{r}_D} (|\phi_D^p|^2 + |\phi_T^p|^2 + |\phi_{H_e}^{p_1}|^2 + |\phi_{H_e}^{p_2}|^2 + |\phi_e|^2) \right. \\ &\left. + \frac{1}{4\pi} \operatorname{div}(\mathbf{E}) \frac{\partial V}{\partial \mathbf{r}_D} \right) dxdy \\ &+ K_1 \frac{\partial}{\partial t} \left(|\phi_D|^2 \mathbf{A} \right) + \mathcal{O}(\varepsilon) - \rho_D \mathbf{g} \\ = \; &\mathbf{0} \end{aligned} \tag{58}$$

Letting $\varepsilon \to 0$ and considering a Maxwell equation in question, we obtain

$$\begin{aligned} &\frac{\partial \hat{\lambda}_1}{\partial t} - \int_\Omega \int_\Omega \frac{d}{dt} \left(\rho_D^p \frac{d\hat{\mathbf{r}}_D^p}{dt} \right) dxdy \\ &- \int_\Omega \int_\Omega \frac{d}{dt} \left(\rho_D^N \frac{d\hat{\mathbf{r}}_D^N}{dt} \right) dxdy - K_1 \int_\Omega \int_\Omega \left(|\phi_D|^2 \mathbf{B} \times \frac{\partial \mathbf{r}_D^p}{\partial t} \right) dxdy \\ &+ K_1 \frac{\partial}{\partial t} \left(|\phi_D|^2 \mathbf{A} \right) - \rho_D \mathbf{g} = \mathbf{0}, \text{ in } \Omega \times [0, t_f]. \end{aligned} \tag{59}$$

Combining these two last Euler-Lagrange equations we obtain

$$
\begin{aligned}
&-\frac{d(\rho_D \mathbf{v}_D)}{dt} - \frac{d(\nabla(\rho_D \hat{P}))}{dt} + \frac{d(\nabla(\lambda_1 P_D))}{dt} \\
&- \int_\Omega \int_\Omega \frac{d}{dt}\left(\rho_D^p \frac{d\hat{\mathbf{r}}_D^p}{dt}\right) dxdy \\
&- \int_\Omega \int_\Omega \frac{d}{dt}\left(\rho_D^N \frac{d\hat{\mathbf{r}}_D^N}{dt}\right) dxdy - K_1 \int_\Omega \int_\Omega \left(|\phi_D|^2 \mathbf{B} \times \frac{\partial \mathbf{r}_D^p}{\partial t}\right) dxdy \\
&+K_1 \frac{\partial}{\partial t}\left(|\phi_D|^2 \mathbf{A}\right) - \rho_D \mathbf{g} = \mathbf{0}, \text{ in } \Omega \times [0, t_f].
\end{aligned} \tag{60}
$$

Thus,

$$
\begin{aligned}
&-\frac{\partial(\rho_D \mathbf{v}_D)}{\partial t} - \frac{\partial(\rho_D \mathbf{v}_D)}{\partial (X_D)_k}(v_D)_k \\
&-\frac{d(\nabla(\rho_D \hat{P}))}{dt} + \frac{d(\nabla(\lambda_1 P_D))}{dt} \\
&- \int_\Omega \int_\Omega \frac{d}{dt}\left(\rho_D^p \frac{d(\hat{\mathbf{r}}_D^p)}{dt}\right) dxdy \\
&- \int_\Omega \int_\Omega \frac{d}{dt}\left(\rho_D^N \frac{d(\hat{\mathbf{r}}_D^N)}{dt}\right) dxdy \\
&-K_1 \int_\Omega \int_\Omega \left(|\phi_D|^2 \mathbf{B} \times \frac{\partial \mathbf{r}_D^p}{\partial t}\right) dxdy \\
&+K_1 \frac{\partial}{\partial t}\left(|\phi_D|^2 \mathbf{A}\right) - \rho_D \mathbf{g} = \mathbf{0}, \text{ in } \Omega \times [0, t_f].
\end{aligned} \tag{61}
$$

From such a result, considering an Eulerian identification

$$
\mathbf{r}_D(z,t) = (X_D(z,t), Y_D(z,t), Z_D(z,t)) \approx z,
$$

we finally obtain the Eulerian equation

$$
\begin{aligned}
&-\frac{\partial(\rho_D \mathbf{v}_D)}{\partial t} - \frac{\partial(\rho_D \mathbf{v}_D)}{\partial z_k}(v_D)_k \\
&-\nabla P_D + \frac{d(\nabla(\lambda_1 P_D))}{dt} \\
&-\int_\Omega \int_\Omega \left(\frac{\partial(\rho_D^p \hat{\mathbf{v}}_D^p)}{\partial t} + \frac{\partial(\rho_D^p \hat{\mathbf{v}}_D^p)}{\partial z_k}(v_D)_k \right) dxdy \\
&-\int_\Omega \int_\Omega \left(\frac{\partial(\rho_D^N \hat{\mathbf{v}}_D^N)}{\partial t} + \frac{\partial(\rho_D^N \hat{\mathbf{v}}_D^N)}{\partial z_k}(v_D)_k \right) dxdy \\
&-K_1 \int_\Omega \int_\Omega \left(|\phi_D|^2 \mathbf{B} \times \mathbf{v}_D^p \right) dxdy \\
&+K_1 \frac{\partial}{\partial t}\left(|\phi_D|^2 \mathbf{A} \right) - \rho_D \mathbf{g} = \mathbf{0}, \text{ in } \Omega \times [0, t_f].
\end{aligned} \tag{62}
$$

Moreover, from the variation of J in ρ_D, we obtain

$$
\frac{\mathbf{v}_D \cdot \mathbf{v}_D}{2} + \frac{d\hat{P}}{\partial t} - \hat{P} \text{ div } (\mathbf{v}_D) - \mathbf{g} \cdot \mathbf{r}_D + \lambda_6 = 0, \tag{63}
$$

in $\Omega \times [0, t_f]$.

Here we recall that

$$
P_D = \frac{d(\hat{P}\rho_D)}{dt}.
$$

Therefore

$$
P_D = \frac{d\hat{P}}{dt}\rho_D + \hat{P}\frac{d\rho_D}{dt},
$$

so that

$$
\frac{d\hat{P}}{dt} = \frac{P_D}{\rho_D} - \frac{\hat{P}}{\rho_D}\frac{d\rho_D}{dt}.
$$

From this and the last Euler-Lagrange equation, we have

$$
\frac{\mathbf{v}_D \cdot \mathbf{v}_D}{2} + \frac{P_D}{\rho_D} - \frac{\hat{P}}{\rho_D}\frac{d\rho_D}{dt} - \hat{P} \text{ div } (\mathbf{v}_D) + gZ_D(z,t) + \lambda_6 = 0, \tag{64}
$$

in $\Omega \times [0, t_f]$.

From such a result and the previously indicated Eulerian identification we finally obtain

$$
\frac{\mathbf{v}_D \cdot \mathbf{v}_D}{2} + \frac{P_D}{\rho_D} - \frac{\hat{P}}{\rho_D}\left(\frac{d\rho_D}{dt} + \rho_D \text{ div } (\mathbf{v}_D) \right) + g\, z + \lambda_6 = 0, \tag{65}
$$

in $\Omega \times [0, t_f]$.

This last equation is a kind of a generalization of the Bernoulli one concerning the present context.

Similar results may be obtained for the remaining Euler-Lagrange equations for J.

4 Conclusion

In this article we have developed variational formulations for modeling a hydrogen nuclear fusion through a high temperature process. In the last sections, our approach here presented has been non-relativistic and in an Eulerian context.

In a near future research we intend to develop similar results in a relativistic context.

Acknowledgments. The author is deeply grateful to the referee for careful reading of the manuscript.

References

[1] P. CONSTANTIN , C. FOIAS, *Navier-Stokes equations,* University of Chicago Press, Chicago, 1989.

[2] C. De Lellis, E. Brué, D. Albritton, M. Colombo, V. Giri, M. Janisch and H. Kwon, *Instability and Non-uniqueness for the 2D Euler Equations,* after M. Vishik (AMS-219) Volume 219 in the series Annals of Mathematics Studies, Princeton University Press, New Jersey, 2024. https://doi.org/10.1515/9780691257846

[3] F. Botelho, *Variational Formulations for the Euler System in Fluid Mechanics and Related Models.* Authorea. July 31, 2024. DOI: 10.22541/au.172243894.42056083/v1

[4] M. Hamouda, D. Han, C-Y. Jung, R. Temam, *Boundary layers for the 3D primitive equations in a cube: the zero-mode,* Journal of Applied Analysis and Computation. 2018; 8, No. 3, (873-889), DOI:10.11948/2018.873.

[5] A. Giorgini, A. Miranville, R. Temam, *Uniqueness and regularity for the Navier-Stokes-Cahn-Hilliard system,* SIAM J. of Mathematical Analysis (SIMA).2019; 51, 3, (2535-2574), https://doi.org/10.1137/18M1223459.

[6] C. Foias, R.M. Rosa, R. Temam R, *Properties of stationary statistical solutions of the three-dimensional Navier-Stokes equations,* J. of Dynamics and Differential Equations, Special issue in memory of George Sell. 2019; 31, 3, 1689-1741, https://doi.org/10.1007/s10884-018-9719-2.

[7] R. Temam, *Navier-Stokes Equations,* AMS Chelsea, reprint (2001).

[8] J.C. Strikwerda, *finite difference cchemes and partial differential equations*, second edition Philadelphia, SIAM, 2004.

[9] F.S. Botelho, *Approximate numerical procedures for the Navier-Stokes system through the generalized method of lines,* Nonlinear Engineering, vol. 13, no. 1, 2024, pp. 20220376. https://doi.org/10.1515/nleng-2022-0376

[10] F. Botelho, *Existence of solution for the Ginzburg-Landau system, a related optimal control problem and its computation by the generalized method of lines*, Applied Mathematics and Computation, 2012; 218 (11976-11989).

[11] F.S. Botelho, *An approximate proximal numerical procedure concerning the generalized method of lines.* Mathematics 2022, 10(16), 2950; https://doi.org/10.3390/math10162950.

[12] F. Botelho, *Functional Analysis and Applied Optimization in Banach Spaces*, (Springer Switzerland, 2014).

[13] F.S. Botelho, *Functional Analysis, Calculus of Variations and Numerical Methods for Models in Physics and Engineering,* CRC Taylor and Francis, Florida, 2020.

[14] F.S. Botelho, *Advanced Calculus and its Applications in Variational Quantum Mechanics and Relativity Theory,* CRC Taylor and Francis, Florida, 2021.

[15] R.A. Adams RA and J.F. Fournier, *Sobolev Spaces*, 2nd edn. (Elsevier, New York, 2003).

[16] J.C. Tannehill, D.A. Anderson, R.H. Pletcher, *Computational Fluid Mechanics and Heat Transfer,* 2nd edn., Taylor and Francis, Philadelphia, PA, 1997.

HADRONIC JOURNAL 48, 307 - 339 (2025)
DOI 10.29083/HJ.48.03.2025/SC307

DIRECT OBSERVATION OF UNUSUAL PROPERTIES OF STRONG INTERACTIONS INACCESSIBLE BY ACCELERATOR

V.G. Plekhanov
Fonoriton Sci. Lab.
Garon Ltd, Tallinn 11413, Estonia
vgplekhanov@proton.me

Received August 6, 2025
Revised August 13, 2025

Abstract

This brief review is devoted to the manifestation in the mass isotope effect of the nonlinear dependence of the strong interaction on the neutron - binding energy which may indicated the manifestation of the new unknown force. A striking new manifestation of the strong interaction is the acquisition of mass by massless fermions (leptons) of Dirac in graphene. We emphasize that the study of the isotope effect remains at the forefront of nuclear and high energy physics.

Keywords: strong interaction, hadrons, quarks, gluons, excitons, phonons, quantum electrodynamics, quantum chromodynamics

Copyright © 2025 by Hadronic Press, Inc., Palm Harbor, FL 34684, USA

I. **Introduction.**

Modern physics distinguishes three fundamental properties of atomic nuclei: mass , spin (and related magnetic moment), volume (surrounding field strength), which are the source of isotope effect. The stable elementary particles (electrons, protons and neutrons) have intrinsic properties. Some of these properties such as mass and electrical charge are the same for macroscopic objects. Some are purely quantum mechanical and have no macroscopic analog. Spin is an intrinsic angular momentum associated with elementary particles. The spin angular moment of an electron, measure along any particular direction, can only take on the values $\hbar/2$ or $-\hbar/2$. The nuclear magnetic moment associates with nuclear spin and produces the magnetic interaction with its environment. The ability to manipulate and control electron and/or nucleus spin in semiconductor devices provides a new route to expand the capabilities of inorganic semiconductor - based electronics and to design innovative devices with potential application in quantum computing.

Among the prime premises of quantum physics is the principle of indistinguishability of elementary particles. All electrons are by definition 'the same' and hence, after two (or more) electrons interact, it is possible to say 'who is who'. The same applies to other elementary particles and even identical atoms (e.g., two ^{70}Ge atoms are indistinguishable). Not so for isotopes. Due to their mass difference, various isotopes of the same chemical element (e.g., ^{70}Ge and ^{76}Ge) are classical distinguishable particles. Within the framework of statistical thermodynamics, this classical distinguishability of isotopes renders isotopic mixtures a prime illustrative tool for a discussion of the Gibbs paradox. The latter refers to the (alleged) discontinuity of entropy upon the mixture of two slightly different species.

The discovery of the neutron by Chadwick in 1932 may be viewed as the birth of the strong interaction: it indicated that nuclei consists of protons and neutrons and hence the presence of a force that holds them together, strong enough to counteract the electromagnetic repulsion. It is well - known that most of the mass of an atom is concentrated in the tiny nucleus surrounded by a cloud of electrons. The nucleus in turn is formed of protons and neutrons, but these are not elementary either (see, e.g. Fig. 1 in Chapter 2 of [1]). They are actually composed of even smaller particles, called quarks. Gradually over the last century physicists built up what we now call the Standard Model (SM) of particle physics [2], which describes the particles we now believe to be fundamental and their interaction. The SM includes Quantum

Chromodynamics (QCD), the theory of the strong nuclear interactions. According to this model, all matter is built from a small number of fundamental spin 1/2 particles, or fermions; six quarks and six leptons (see below Table 1). The leptons carry integral electric charge. The electron e with unit negative charge is familiar to everyone, and the charged leptons are the muon μ and tauon τ. These are heavy versions of the electron. The neutral leptons are called neutrinos, denoted by the generic symbol ν. A different 'flavor' of neutrino is paired with each 'flavor' of charged lepton, a indicated by the subscript. For example, in nuclear β - decay, an electron e is emitted together with an electron - type neutrino, ν_e. The charged muon and tauon are both unstable, and decay spontaneously to electrons, neutrinos and other particles (see, e.g. [3]). The mean lifetime of the muon is 2.2×10^{-6}s, that of the tauon only 2.9×10^{-13}s. In the theory of strong interquark forces, QCD, there are six types of strong charge, called color charges; color is just a name for an internal degree of freedom. A quark can carry one of three primary colors (say red, blue and green), and its antiquark then carries the corresponding anticolor. The quark combinations called hadrons have no color. A baryon (proton or neutron) of one red, one blue and one green quark, the combination being white (i.e. colorless) Similarly, a meson consisting of a quark of a particular color and antiquark of that anticolor, is also colorless. Gluons, unlike photons, carry a color charge, consisting of one color and one anticolor.

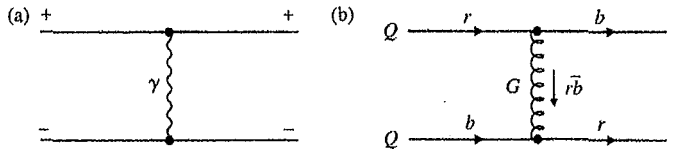

Fig. 1. Comparison of the Feynman diagrams of electromagnetic (a) and strong (b) interactions. The electromagnetic interaction in (a) involves two types of electric charge, (+) and (-) is mediated by an uncharged photon. In (b) the strong interquark force involves six types of color charge. The diagram depicts the interaction of a red quark with a blue quark via the exchange of a red - antiblue gluon.

As an example , Fig. 1^{b}shows a red quark r interacting with a blue quark b via

exchange of $r\bar{b}$ gluon. Note that the gluon carrier itself is endowed with a color charge ($r\bar{b}$ in our case). On this account, gluons have self - interaction, with triple (and quadrupole) gluon vertices [4]. This marks a crucial difference from Quantum Electrodynamics (QED), where the photon uncharged and there is no first - order photon - photon interaction [4]. In the jargon, QED is said to be an Abelian, and QCD is a non - Abelian theory [5]. Since the gluons carry one color and one anticolor, there should be $3^2 = 9$ possible color combinations. However, one of these turns out to be a colorless singlet (in the form $r\bar{r} + b\bar{b} + g\bar{g}$ [3]), leaving eight active gluon states: so - called eight - fold way [6j].

The diagram of Fig. 1 is drawn for the case of single – gluon exchange, but taking into account that strong constant coupling $\alpha_s \sim 1$, multiple exchanges, involving terms α_s^2, α_s^3, ... must also be very probable. However, it turns out that for violent 'close' collisions at very high q^2, $\alpha_s \ll 1$ and single - gluon exchange is a good approximation, while at low q^2 or, equivalently, larger distances, the coupling becomes very large and the theory is incalculable. This large - distance behavior is presumably linked with of confinement of quarks and gluons inside hadrons. Since gluons are massless, one might expect the static QCD potential to have a similar: 1/r, form to that in QED. In fact the quark - antiquark potential is often taken to be of the form

$$V_s = -\frac{4}{3}\frac{\alpha_s}{r} + kr \qquad (1)$$

where the first term, dominating at small r, arises from single - gluon exchange. It is similar to the Coulomb potential between two unit charges of

$$V_{em} = = -\frac{\alpha}{r} \qquad (2)$$

The factor 4/3 in (1) is plausible in view of the fact that there eight color gluon states, to be averaged over three quark colors, giving factor 8/3 as compared with QED (one 'color' of photon and one fermion charge). This has to divided by 2 because, for historical reasons [4], a factor 2 enters into definition of α_s in terms of the square of the strong color charge. However, at larger distances the second term in (1) is dominant and is responsible for quark confinement. The value of k is about o.85 $GeVfm^{-1}$. In equation (1) the attractive force at large r is $dV/dr = k = 085\ Gevfm^{-1}$

[4]. The estimation of the k equals k = 13.9 tonnes weight - a great deal for those tiny quarks, each weighting less than 10^{-24} gm because gluons carry a color charge (unlike photons which are uncharged) there is a strong gluon - gluon interaction. If one tries to pull apart the two quarks, the energy required to do so grows linearly with the string (distance) as in (1), and eventually it requires less energy to produce another quark - antiquark pair, thus involving two short string instead one long one. Thus even the most violent efforts to separate quarks just result in production of lot of quark - antiquark pairs (mesons) [3]. Since the protons and neutrons which make up the nucleus are themselves considered to be up of quarks are considered to be held together by the color force [3], the strong force between nucleons may be considered to be residual color force (see e.g.[1]).

In modern physics, particles are classified into two groups based on their properties. There are known as fermions and bosons. In the SM fermions are the fundamental particles of matter. Elementary fermions are leptons (see Table 1).

Table 1. Quarks and leptons

	Family			Electric charge (e)
	1	2	3	
Leptons	e^-	μ^-	τ^-	- 1
	ν_e	ν_μ	ν_t	0
Quarks	u	c	t	2/3
	d	s	b	- 1/3

Fermions are the half - integer spin particles and described by the Fermi - Dirac statistics. The quarks and leptons are building block of matter and antimatter [1 - 3]. In the SM, the base exchange is the gluon which mediates the forces between quarks. Bosons are identical particles having zero of integer spin. Behaviors of bosons are described by the Bose - Einstein statistics. The SM [2 - 4] only consists of five elementary bosons and twelve of leptons and quarks. Besides that there are gluons and Higgs boson (Fig. 2).

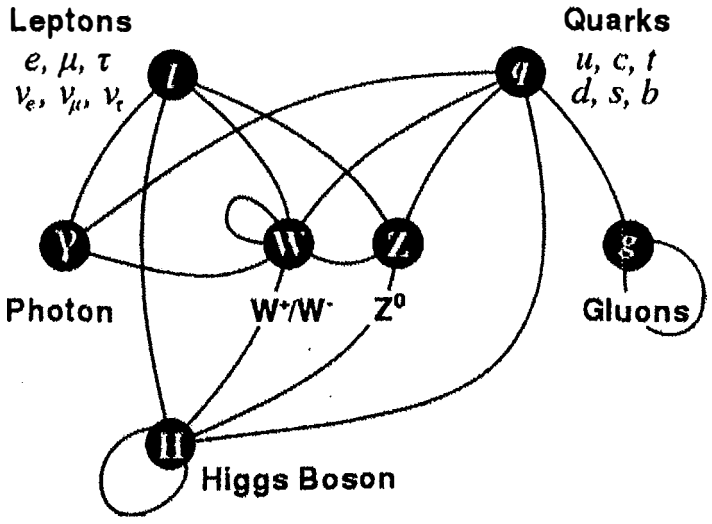

Fig. 2. Summary of interactions between particles described by the Standard Model.

According to contemporary physics the strong force does not act on lepton (electrons, positrons, muons and neutrinos), but only on protons and neutrons (more generally, on baryons and mesons - this is the reason for the collective name hadrons) (see, however below). It should be add that the forces between the quarks must be long range, because the gluons (as photons) have zero mass. This does not imply that the forces between hadrons are also long - range, because hadrons have zero color charges overall. The forces between the colorless hadrons are the residues of the for as between their quark constituents, and cancel when the hadrons are far apart [2 - 4]. In 1935, Yukawa [7] pointed out that the nuclear force could be generated by the exchange of a hypothetical spinless particle, provided its mass intermediate between the masses of proton and electron - a meson. Yukawa predicted the pion [1 - 4].The macroscopic manifestations of the strong interaction are restricted up to now to radioactivity and the release of nuclear energy. Yutaka's potential has the form[4, 5]

$$V = g\frac{e^{-kr}}{r^n}, \qquad (3)$$

for some n. Here the strength of the force is measured by the constant k (see, also [5]). The most important feature Yukawa's forces is that they have a small range (~ 10^{-15} m). The central dogma of atomic physics after Yukawa's paper that proton -

electron attraction could be explained in terms of classical electrostatic theory, while the strong force effects were essentially new and inexplicable. So, far the best theoretical guess is the Yukawa potential, but it is a static potential not dependent on velocities of the nucleons. A static force is not a complete one because it can not explain the propagation of the nuclear interaction. Moreover, as was indicated above, a phenomenological Yukawa potential can not be directly verified experimentally. We should note that nowadays in text books and elsewhere the separation of electromagnetic and strong interaction tacitly assumed. It is very strange up to present time we do not even know the strong force very well. And what is more we have some contradiction taking into account that the forces between quarks must be long - range, because the gluons have zero mass. But as was mentioned above the force between colorless hadrons is short - range, when the distance between hadrons is more than nuclear size [1, 7].

Table 2. The four fundamental forces.

Interaction	FQ	Mass	Range (m)	RS	Spin	TC-S (m^2)	TTS(s)
Str	Gluon	0	10^{-15}	1	1	10^{-30}	10^{-23}
We	W , Z	81, 93 GeV/c2	10^{-18}	10^{-5}	1, 1	10^{-44}	10^{-8}
Elec	Photon	0	∞	1/137	1	10^{-33}	10^{-20}
Gra	Graviton	0	∞	10^{-38}	2	-	-

Here - FQ field quant, RS relative strength, TC - S Typical cross - section, TTS - Typical time scale.

The Table 2 (see also [2, 4]) given for the strength and range of the forces come from a comparison of the effects they produce on two protons. In some respect these resemble an ordinary Newtonian force between the protons, varying with the distance between them as if the force was derived from a potential function (1): for some n. This is an inverse - power force which is diminished by an exponential factor at distances larger than a certain distance R, the range of the force. The strength of the force is measured by the constant k. The unit of strength is $hc/2\pi$ where h is Planck's

constant and c the speed of light. Thus nuclear physics was essentially the paradigmatic example of understanding particle physics. The modern quantummechanical view of the three fundamental forces (all except gravity) is that particles of matter (fermions neutrons, protons, electrons) do not directly interact with each other, but rather carry a charge, and exchange virtual particles (gauge bosons photons, gluons, gravitons) which are the interaction carriers or force mediators. As can be seen from Table 2, photons are the mediators of the interaction of electric charges (protons, electrons, positrons); and gluons are the mediators of the interaction of color charges (quarks). In our days, the accepted view is that all matter is made of quarks and leptons . As can be seen, of the three pairs of quarks and leptons, one pair of each - the quark u and d and the leptons e^- and ν_e (electrons neutrino) - are necessary to make up the every day world, and a world which contained only these would seem to be quite possible.

As we can see above the method of the scattering particles allows to determine only length of scattering as well as the size and depth (highest) of the neutron's potential. In the present paper we attempt to measure the energy of the neutron - electron interaction via spectroscopic study of the optical characteristics of solids with isotope effect at low temperature. Therefore, it is purpose of our paper to advance a description of the manifestation of strong nuclear interaction in solids, using partly published and new non - accelerator experimental results. Our spectroscopic measurement of the low temperature optical characteristics of LiH_xD_{1-x} crystals is permitted to quantitative study of the dependence of strong coupling constant, α_s, on the proton - neutron distance in the deuteron nuclei. Carbon, being the second element after silicon on Earth, has unusually wide range of allotropic compounds with completely different physical properties [8]. The use of our object allows the investigation of not only the isotope effects in lattice dynamics (vibrational, elastic and thermal properties), but also the influence of such effects on the electronic excitations (for example, the renormalization of the band - to - band transition energy E_g). We emphasize that the study of the isotope effect remains at the forefront not only in materials science, but also nuclear and high energy physics. In connection with of our analysis, we must emphasize that outstanding works on strong interaction in hadrons mechanics deserve separate and fundamental study [9]. A detailed comparison with the theory of hadron mechanics [9] and interpretation will be given in the forthcoming paper (see also [10] and referencies therein).

II.Experimental.

Below we briefly describe the results of the low - temperature optical spectroscopy of isotope - mixed solids. The apparatus used in our experiments has been described in several previous publication [10 - 12]. For clarity, we should mentioned here that immersion home - made helium cryostat and two identical double - prism monochromators were used. one monochromator was used for the excitation and the other, which was placed at right - angle to the first for analyzing the luminescence and scattering of light. In our experiments we investigated two kinds of crystals (LiH and LiD) which are differ by a term of one neutron. Lithium hydride and lithium deuteride are ionic insulating crystals with simple electronic structure, four electrons per unit cell, both fairly well – described structurally (neutron diffraction) and dynamically (second – order Raman spectroscopy) and through ab initio electronic structure simulation. Among other arguments, LiH and LiD are very interesting systems due to their extremely simple electronic and energy structure and to the large isotopic effects when the hydrogen ions are replaced by the deuterium ones. On the other hand, the light mass of the ions, specially H and D, makes that these solids have to be considered like quantum crystals, and consequently, described theoretically by quantum theory. In a solid one deals with a large number of interacting particles, and consequently the problem of calculating the electronic wave functions and energy levels is extremely complicated. It is necessary to introduce a number of simplifying assumptions. In the first place we shall assume that nuclei in the crystalline solid are at rest. In an actual crystal this is of course never the case, but the influence of nuclear motion on the behavior of electrons may be treated as a perturbation for the case in which they are assumed to be at rest. Even with above assumption, however, we are still with a many – electron problem which can be solved only be approximative methods. In the case of solids, the most important approximative method which has been applied extensively is the so – called one – electron approximation. In this approximation the total wave function for the system is given by a combination of wave functions, each of which involves the coordinates of only one electron. In other words, the field seen by a given electron is assumed to be that of the fixed nuclei plus some average field produced by the charge distribution of all other electrons [13].

The difference between a good conductor and a good insulator is striking. The electrical resistivity of a pure metal may be as low as 10^{-10} ohm-cm at a temperature of 1 K, apart from the possibility of superconductivity. The resistivity of good

insulator may as high as 10^{22} ohm-cm. The understand the difference between insulators and conductors, we shall use the band – gap picture (Fig. 3 below). Since atom are located in space strictly periodically in the crystal, the full potential $V(\vec{r}) = \tilde{U}_i(\vec{r}\ ) + U(\vec{r})$ must have a three - dimensional periodicity (here $U_i(\vec{r}$ and $U(\vec{r})$ are potential energy if i - electron and all others). Although the exact species $V(\vec{r})$ is unknown, it is important to know that this potential is a periodic function whose period coincides with the period of the crystal lattice of the object under study. This periodicity leads to the formation of a band energy structure (Fig. 3). An electron from the valence band (see Fig. 3) is excited into the conduction band. The possibility of band gap is the most important property of solids.

The single crystals of LiH and LiD were grown from the melt by the modified method of Bridgeman - Stockbarger (see [14, 15] and references quoted therein). The crystals were synthesized from ^{7}Li metal and hydrogen of 99.7% purity and deuterium of 99.5% purity. Virgin crystals had a slightly blue - grew color, which can be attributed to nonstoichiometric excess of lithium present during the grown cycle. On annealing for several days (up to 20) at 500^0C under ~ 3 atm of hydrogen or deuterium, this color could be almost completely eliminated. Because of the high reactivity and high hygroscope of investigated crystals an efficient protection against the atmosphere was necessing. Taking into account this circumstance, we have developed special equipment which is allowed to prepare samples with a clean surface cleaving their in the bath of helium cryostat with normal or superfluid liquid helium [10]. The samples with such surface allow to perform measurements during 15 hours. An improved of LiH (LiD) as well as mixed crystals were used in the present study. In spite of the identical structure of all free - exciton luminescence spectra, it is necessary to note a rather big variation of the luminescence intensity of the crystals from the different batches observed in experiment.

We should remind very briefly about the electronic excitations in solids. According to modern concept, the excitons can be considered [13] as the excited of the N - particles system: An electron from the valence band (see Fig. 3) is excited into the conduction band.

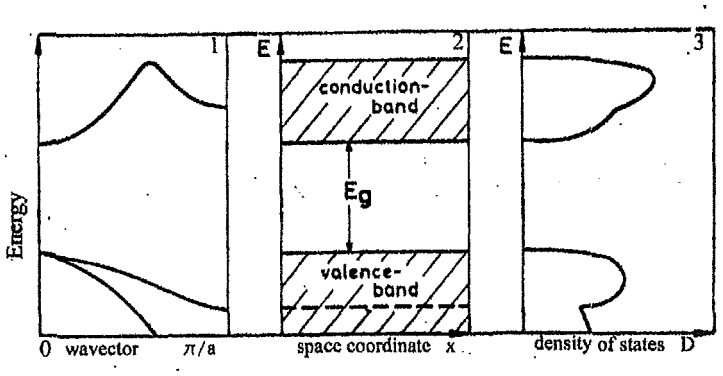

Fig. 3. Various possibilities to present the band - structure of homogeneous, undoped insulator (semiconductor). 1 - the dispersion relation, i.e. the energy E as a function of the wave vector $\vec{k}$, 2 - the energy regions of allowed and forbidden states as function of a space coordinate x and , 3 - the density of states (all curves are schematic ones).

The attractive Coulomb potential between the missing electron in the valence band, which can be regarded as a positively charged hole, and the electron in the conduction band gives a hydrogen - like spectrum with an infinitive number of bound state and ionization continuum (Fig. 4).

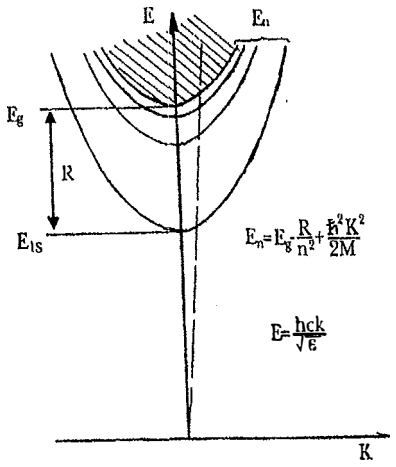

Fig. 4. Discrete and continuos (hatched area) Wannier - Mott exciton energy spectrum taking into account its kinetic energy. The broken line connects to the dispersion of light in the medium. R - is the exciton binding energy, n = 1, 2, 3, ...

In our short review we call the bound states of electron - hole (e - h) pairs exciton states (exc), while we refer to ionized e - h pairs as free carriers. however, the expression free carriers does not imply that the effect of the strong Coulomb forces between electronic excitation could be neglected. Thus, an exc - state can be built by appropriate superposition of e - h pairs, which in a simple two - band model for cubic crystal symmetry is given (more details see [10]). In our experiments we have investigated the low - temperature optical spectra (reflection, photoluminescence and scattering of light) of LiH_xD_{1-x} crystals ($0 \leq x \leq 1$) which are differ by term of one neutron from each other.

Spectra were excited by various lines of a 400 W deuterium lamp and a 120 W mercury arc lamp (see Fig. 5). The excitation light was felt on the entrance slit of the first monochromator and after leaving it passed through quartz windows of the immersion helium cryostat and irradiated of the crystals. The luminescence and scattering light from the samples was dispersed in another double prism (grating) monochromator and photoelectrically detected. A photoelectric registration of the optical signal was realized by a cooled photopmultiplier for ultraviolet (UV) range of the spectrum and the subsequent high - sensitivity photon - counting system with a

storage facilities (computer). The signal - to - noise ratio was approximately $n \cdot 10^2$ where $n = 2 \div 5$ for different batches of crystals. The light scattering experiments were performed in the usual backscattering geomentry, at temperatures of 2 to 300 K. To allow for the $\approx \omega^4$ law, a freshly cleaved of LiF crystal was used, whose dispersion of the refractive index in the spectral region 4 to 6 eV is small. The experiments were carried out in the same way for two (LiH and LiD) compounds, which differ by a term of one neutron.

An improved of LiH (LiD) crystals were used in the present study. In spite of the identical structure of all free - exciton luminescence spectra, it is necessary to note a rather big variation of the luminescence intensity of the crystals from the different batches observed in experiment.

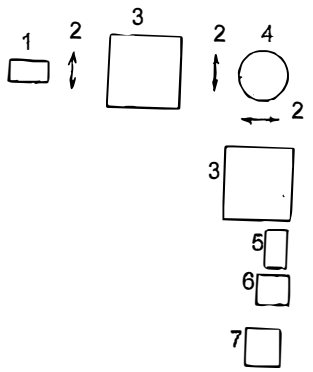

Fig. 5. Scheme of experimental setup: 1 - lamp, 2 - lens, 3 - monochromator, 4 - He cryostat, 5 - photomultiplier, 6 - photon counter, 7 - personal computer.

III. Results.

The usual way to determine the optical properties of a solid is to shine monochromatic light onto an appropriate sample and then to measure the reflectance or transmittance of the sample as a function of photon energy. In the spectral region of greatest interest is generally quite high, so that often a negligible small fraction of the incident light is transmitted. It is the main reason, that the most experiments are

measurements of the reflectivity. The mirror reflection spectra of mixed and pure LiH and LiD crystals, cleaved in superfluid helium are presented on Fig. 6. All spectra have been measured with the same apparatus under the same conditions. As can clearly seen in Fig. 6 all spectra exhibit a similar long – wave structure. As the deuterium concentration increases, the long – wave maximum (n = 1S excitons [10, 13]) broadens and shifts towards the shorter wavelengths. The energy values of exciton maxima for pure and mixed crystals at 2 K are presented in Table 2.

Table 3. Values of the energy of maxima (E_1 and E_2) (in meV) in exciton reflection spectra of pure and mixed crystals at 2 K, and energies of exciton binding energy E_b, band - to - band transitions E_g.

	LiH	$LiH_{0.82}D_{0.18}$	$LiH_{0.40}D_{0.60}$	LiD	Li^6H (78 K)
E_1	4950	4967	5003	5043	4939
E_2	4982	5001	5039	5082	4970
E_b	42	45	48	52	41
E_g	4992	5012	5051	5095	4980

As demonstrated early (see, e.g. book [15) most low - energy electron excitation in LiH crystals are the large - radius excitons [13].

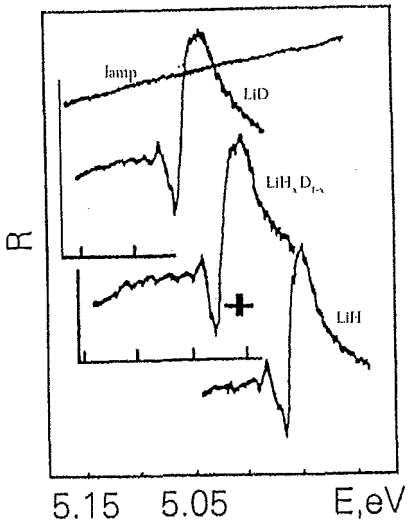

Fig. 6. Mirror reflection spectra in indicated crystals at 2 K cleaved in superfluid helium. Light source without crystals, curve lamp.

Going back to Fig. 6, it is hard to miss the growth of Δ_{12}, which in hydrogen - like model [13] causes an increase in exciton Rydberg (E_b) with the replacement of isotopes (for details see [15]). The single - mode nature of exciton reflection spectra of mixed crystals LiH_xD_{1-x} agrees qualitatively with the results obtained with the virtual crystal model [16]. All of these results are documented in Table 2, where the variation of E_g, E_b are shown at the isotope effect. We should highlight here that the most prominent isotope effect is observed in LiH crystals, where the dependence of $E_g = F(C_D)$ is also observed and investigated (see below Fig. 9).

Photoluminescence is the optical radiation emitted by a physical system (in excess of the thermal equilibrium blackbody radiation) resulting from excitation to a nonequilibrium state by irradiation with light. Photoluminescence is also rapidly evolving into major basic research tool comparable to absorption (reflection) measurements in importance. Two reason for this stand out as significant. First is the sensitivity of the luminescence technique. It often happens that features which are just discernible in absorption will completely dominate the luminescence spectra. The converse is also sometimes true, making luminescence and absorption (reflection) complementary techniques. Second is the simplicity of data collection. In last half-century the luminescence method has become one of the most common techniques for studying excitons in dielectrics and semiconductors. While the structure of spectra of fundamental reflection (absorption) depends on the internal degrees of freedom of Wannier – Mott exciton, the structure and shape of the luminescence spectrum are determined primarily by its external degrees of freedom. The latter are associated with the translation motion of large – radius exciton as a whole, with the translation mass $M = m_e + m_h$, where m_e and m_h – effective masses of electron and hole, respectively.

Free exciton luminescence is observed when LiH (LiD) crystals are excited in the midst of the fundamental absorption. The spectrum of free exciton photoluminescence of LiH crystals cleaved in superfluid helium consists of a narrow (in the best crystals, its half - width is $\Delta E \leq 10$ meV) phononless emission line and its broader phonon repetitions, which arise due to radiated annihilation of excitons with the production of one to five longitudinal optical (LO) phonons (see Fig. 7).

The phononless emission line coincides in an almost resonant way with the reflection line of the exciton ground state which is indication of the direct electron transition $X_1 - X_4'$ of the first Brillouin zone [17].The lines of phonon replicas form

an equidistant series biased toward lower energies from the resonance emission line of excitons. The energy difference between these lines in LiH crystals is about 140 meV, which is very close to the calculated energy of the LO phonon in the middle of the Brillouin zone [18] and which was measured early (see, e.g. [15] and references quoted therein). The isotopic shift of the zero - phonon emission line of LiH crystals equals 103 meV. As we can see from Fig. 7 the photoluminescence spectrum of LiD crystals is largely similar to the spectrum of intrinsic luminescence of LiH crystals. There are, however, some distinctions one is related. Firstly the zero - phonon emission line of free excitons in LiD crystals shifts to the short - wavelength side on 103 meV. These results directly show the violation of the strong conclusion (see, e.g. [1, 2, 4]) that the strong force does not act on leptons. The second difference concludes in less value of the LO phonon energy, which is equal to 104 meV. The simplest approximation, in which crystals of mixed isotopic composition are treated as crystals of identical atoms having the average isotopic mass, is referred to as virtual crystal approximation (VCA) [15].

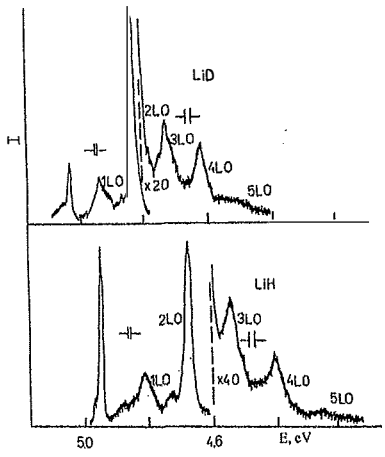

Fig. 7. Photoluminescence spectra of free excitons at 2 K in LiH and LiD crystals cleaved in superfluid helium.

When light is excited by photons in a region of fundamental absorption in mixed LiH_xD_{1-x} crystals at low temperature, line luminescence is observed (Fig. 8), like in the pure LiH and LiD crystals. As before [15], the luminescence spectrum of crystals

cleaved in superfluid liquid helium consists of the relatively zero - phonon line and its wide LO replicas. For the sake of convenience, and without scarfing generality, Fig. 8 shows the lines of two replicas. Usually up to five LO repetitions are observed in the luminescence spectrum as described in detail in [18, 14]. In Fig. 8 we see immediately that the structure of all three spectra is the same. The difference is in the distance between the observed lines, as well as in the energy at which the luminescence spectrum begins, and in the half - width of the lines (see, also Table 3).

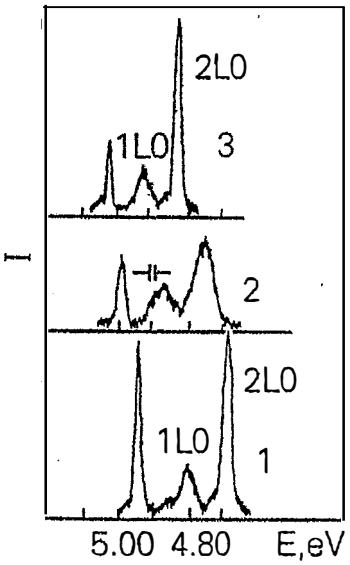

Fig. 8. Photoluminiscence spectra of free excitons in LiH (1), LiH_xD_{1-x} (2) and LiD (3) crystals cleaved in superfluid helium at 2 K. Spectrometer resolution is shown.

At the excitation below the intrinsic absorption edge ($E_{n=1s}$ = 5.043 eV for LiD [19]) we have succeeded in observing the multiphonon resonance Raman scattering (RRS) with the creation of up four phonons (Fig. 9). Indeed, the energy difference between peaks in the RRS spectrum is equal the energy of the LO phonons in the center of the Brillouin zone [18, 14].

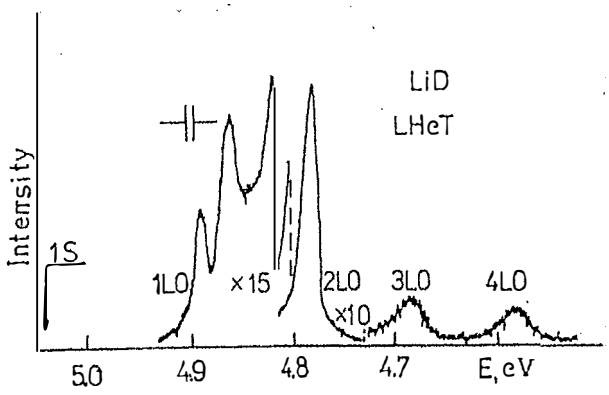

Fig. 9. Resonant Raman scattering of a LiD crystals at the excitation E = 4.992 eV at 4.2 K.

To pay attention the large half - width of observable lines in the RRS spectrum. As was shown in the paper [20] their half - width are always larger than of the excitation line. The proximity of the exciting light frequency to the energy of exciton transitions leads to an essential modification of the selection rules for light scattering. The presence of the second - order TO (Γ) ($\hbar\omega_{TO(\Gamma)}$ = 76 meV for LiH) in the RRS spectrum may be explained by a relatively strong scattering deformation mechanism in these crystals, where, however the main mechanism, as was seen from both figures, is Frőchlich mechanism of intraband scattering. The longwavelength displacement of the excitation line frequency relatively exciton resonance a monotonic decrease the intensity of RRS spectrum as whole more than 60 - fold in both LiH and LiD crystals [15].

The X - Ray diffraction investigaions show [21] that LiH_xD_{1-x} mixed crystals form a continuos row a variable lattice constant (and exciton radius, respectively) that obeys Vegard's law [16].

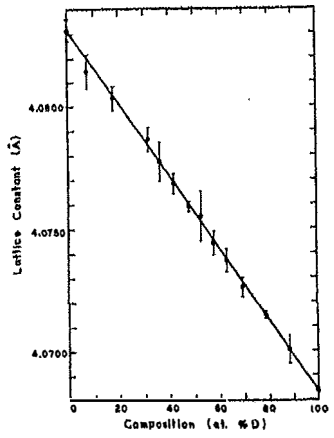

Fig. 10. Lattice constant in the ^{7}Li(H, D) crystals plotted against the isotopic concentrtion (after [21]).

Taking into account linear dependence on the lattice constant (Fig. 10) we have build the dependent of the band gap energy on the distance between nucleons in deuterium nuclei. Fig. 11 shows the concentration dependence of the energy of interband transition E_g (force of strong interaction between proton and neutron) (see Fig. 2). As can be seen from Fig. 11, VCA method (the straight dashed line) cannot describe observed experimental results. This dependence has a nonlinear character. Here r_H and r_D are radius of hydrogen and deuterium nuclei according to CODATA data.

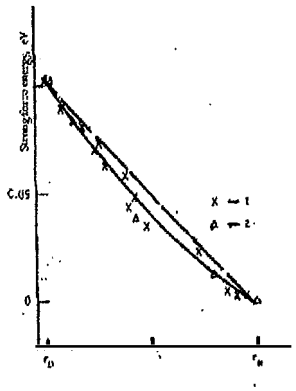

Fig. 11. The long – range part of the force of strong nuclear interaction dependence on the distance between nucleons in deuterium nucleus. The straight dashed line is the linear dependence of the force dependence F_s in the virtual model. The solid line corresponds to calculation using the polynom of second degree $F_s = f(r_d)$. Points derived from the reflection spectra indicated by crosses, and those from luminescence spectra by triangles.

Comparison the all experimental results on the luminescence (reflection) and light scattering in the crystals which differ by a term of one neutron only is allowed to the next conclusions;

1. At the adding one neutron (using LiD crystals instead LiH ones) is involved the increase exciton energy on 103 meV.
2. At the addition one neutron the energy of LO phonons is decreased on the 36 meV, that is direct seen from luminescence and scattering spectra.
3. In the isotope effect, the energy of acoustic phonons does not depend on the replacement of H by D [20] , which is proved by identical structure of the light scattering spectra [15, 22]. Along with this, a small change in the energy of optical (LO) phonons (36 meV) observed in the luminescence and light scattering spectra indicates a non - electron - phonon renormalization mechanism of the energy of zero - phonon line of free excitons in LiD crystals.

Both characteristics are macroscopic. As will be shown below these experimental results are very useful for nuclear and physics of high energy physics.

IV. Discussion.

Traditionally nuclear - electron interaction (in our case neutron - electron interaction) taking into account the solving Schrödinger equation using Born - Oppenheimer (adiabatic) approximation [23]. Below we consider the essence of the Born - Oppenheimer approximation of the nuclear - electron interaction on the molecule example. The Schrödinger equation for the molecule

$$\hat{H}\Psi(\vec{r}, \vec{R}) = E\Psi(\vec{r}, \vec{R}) \qquad (4)$$

here $\Psi(\vec{r}, \vec{R})$ is an eigenfunction and E the corresponding eigenvalue, $\hat{H}$ the Hamiltonian operator of molecule and $\vec{r}$ is electron and $\vec{R}$ is nuclear distance. The simplest approximate method for solving the Schrödinger equation (4) uses, as indicated above, the so - called Born - Oppenheime approximation [23]. This approximation is used that the nuclei are much heavier than an electron and, consequently, move very slowly in comparison with the electronic motion.

If the nucleus to be fixed in some configuration for this particular $\vec{R}$ (distance between nuclei) we get the next differential equation

$$-\frac{\hbar^2}{2m}\sum_i \Delta_i^2\Psi(\vec{r}, \vec{R}) - \frac{\hbar^2}{2}\sum_\alpha \frac{\Delta_\alpha}{M_\alpha}\Psi(\vec{r}, \vec{R}) + V(\vec{r}, \vec{R})\Psi(\vec{r}, \vec{R}) = E\Psi(\vec{r}, \vec{R}), \quad (5)$$

where Δ is Laplasian [24], m and M electron and nucleus mass, index i for electrons and α is index for nuclei.

Further we put

$$\Psi(\vec{r}, \vec{R}) = \chi(\vec{r}, \vec{R})\varphi(\vec{R}) \qquad (6)$$

here $\varphi(\vec{R})$ is the nuclear wavefunction, which depends on nuclear distance $\vec{R}$ and on electronic state.

After substitution (6) in (5) we have

$$-\frac{\hbar^2}{2m}\varphi(\vec{R})\sum_i \Delta_i\chi(\vec{r}, \vec{R}) - \frac{\hbar^2}{2}\sum_\alpha \frac{\Delta_\alpha}{M_\alpha}\chi(\vec{r}, \vec{R})\varphi(\vec{R}) + V(\vec{r}, \vec{R})\chi(\vec{r}, \vec{R})\varphi(\vec{R}) = E\,\chi(\vec{r}, \vec{R})\varphi(\vec{R}). \qquad (7)$$

Further we neglect the next members in (7)

$$\hat{L}\Psi(\vec{r}, \vec{R}) = -\frac{\hbar^2}{2}\sum_\alpha \frac{1}{M_\alpha}[\varphi(\vec{R})\Delta_\alpha\chi(\vec{r}, \vec{R}) + 2\nabla_\alpha\varphi(\vec{R})\nabla_\alpha\chi(\vec{r}, \vec{R})]. \qquad (8)$$

Operator $\hat{L}$ is call the non - adiabatic operator, which describe the nuclear - electron interaction. After the last operation the equation (8) splits on two equations:

$$-\frac{\hbar^2}{2m}\sum_i \Delta_i\chi(\vec{r}, \vec{R}) + V(\vec{r}, \vec{R})\chi(\vec{r}, \vec{R}) = E_l(\vec{R})\chi(\vec{r}, \vec{R}); \qquad (9)$$

and

$$-\frac{\hbar^2}{2}\sum_\alpha \frac{\Delta_\alpha}{M_\alpha}\varphi(\vec{R}) + E_l(\vec{R})\varphi(\vec{R}) = W\varphi(\vec{R}). \qquad (10)$$

Where $E_l(\vec{R})$ is electronic energy and W is the nuclear energy. Every equation have the view of the Schrödinger equation. The first equation (9) describes the electron stationary state in adiabatic approximation. Equation (10) is an equation for a wavefunction of the nuclei alone. Note, please that Equation (9) contains the nuclear charges through the Coulomb potential, but is doesn't include any reference to nuclear mass. Thus $E_l(\vec{R})$, the eigenvalue (energy) of the electronic Schrödinger equation (9) is the same for all isotopes, and consequently, is isotopically independent. The independent $E_l(\vec{R})$ on isotopic substitution is the essence of the Born - Oppenheimer approximation. However, we must repeat, that the Born - Oppenheimer approximation

[23] is the standard anzatz to the description of the interaction between electrons and nuclei in solids (see, e.g. [25]). Moreover, comparison the non - accelerator experimental results on the luminescence (reflection) and light scattering [15] in the crystals which differ by a term of one neutron only is allowed to the next conclusions;

1. At the adding one neutron (using LiD crystals instead LiH ones) is involved the increase exciton energy on 103 meV.

2. At the addition one neutron the energy of LO phonons is decreased on the 36 meV that is direct seen from luminescence and scattering spectra [20].

3. In the isotope effect, the energy of acoustic phonons does not depend on the replacement of H by D [15, 20], which is proved by the identical structure of the light scattering spectra [15, 19, 22]. Along with this, a small change in the energy of optical (LO) phonons (36 meV) observed in the luminescence and light scattering spectra indicates a non - electron - phonon renormalization mechanism of the energy of zero - phonon emission line of free excitons in LiD crystals. The same results have been obtained for diamond.

The X - ray diffraction investigations show that the LiH_xD_{1-x} mixed crystals [21] form a continuos row of the solid solution and testify themselves like a virtual crystal with a variable lattice constant (and exciton radius, respectively) that obeys Vegard's law (see Fig. 10).

The measurements of the low temperature of reflection [15, 19, 22] and luminescence spectra of the whole series of mixed crystals is permitted to obtain the dependence of the interband transition (the long - range force dependence of strong nuclear interaction on the distance between nucleons in deuterium nucleus) energy on the deuterium concentration (see below Fig. 11). Taking into account that the concentration of the isotopes is vary directly the lattice constant (see Fig. 36) we are plotting the dependence of the power of the force strong interaction on the distance between nucleons depicted on Fig. 11. This dependence has a nonlinear character. As can be seen from Fig. 11, VCA method (the straight dashed line) cannot describe observed experimental results.

The independent of the potential energy (the eigenvalue of the Schrödinger equation) is the essence adiabatic approximation. However, we must repeat, that the Born - Oppenheimer approximation [20] is the standard anzatz to the description of the interaction between electrons and nuclei in solids [25]. Now we should take into account a small contribution to isotopic shift through reduced electron mass $\mu = ((m_e M_{Nucl})/(m_e + M_{Nucl}))$ so far as M_{Nucl} is different for the hydrogen and deuterium nucleus. In this case the contribution equals $\Delta E \simeq 6$ meV. Contribution to isotope shift of the zero - phonon line in luminescence spectra of LiD crystals as well as Lamb shift

and specific Coulomb potential approximately equal 1, and 1 meV, respectively. This values is less then isotope shift in our experiments on the two order and more. These all last results force us to search for new models and mechanisms of nuclear (neutron) - electron interaction including the results of subatomic physics, e.g. hadron - lepton interaction.

Out of four known interactions, three are described by SM - the electromagnetic, weak and strong ones. The first two of them have a common electroweak gauge interaction behind them. The symmetry of this interaction $SU(2)_L$ X $U(1)_Y$ manifests itself at energies higher than ~ 200 GeV. At lower energies, this symmetry is broken down to $U(1)_{EM} \neq U(1)_Y$ (the electroweak symmetry breaking): in SM this breaking is related to the vacuum expectation value of a scalar field [26]. The strong interaction in SM is described by the QCD, a theory with the gauge group $SU(3)_C$. The effective coupling constant of this theory grows when the energy decreased [1]. As a result, particles which feel this interaction cannot exist as free states and appear only in the form of bound states called hadrons (see, also [26]). Most of modern methods of quantum field theory work at small values of coupling constant,α_s, [27 - 31], that is, for QCD, at high energies. Quarks and leptons, the so - called SM matter fields, are described by fermionic fields. Quarks take part in strong interactions and compose observable bound state hadrons. Both quarks and leptons participate in the electroweak interaction. The matter fields constitute three generation: particles from different generation interact identically but have different masses (see, e.g. [4]). For the case of neutrino, Yukawa [7] interactions are forbidden as well, so neutrinos are strictly massless in SM (see, however [32]). The gauge bosons, which are carriers of interactions, are massless for unbroken gauge groups $U(1)_{EM}$ (electromagnetism - photons) and $SU(3)_C$ (QCD - gluons), masses of $W^{\pm}$ and Z^0 bosons are determined by the mechanism of electroweak symmetry breaking. It should noted that the forces between the quarks must be long - range, because the gluons have zero mass. This does not imply that forces between hadrons are also long range, because hadrons have zero color charges overall. The forces between the colorless hadrons are the residues of the forces between their quark constituents, and cancel when the hadrons are far apart.

Returning to our non - accelerator experimental results, we should underline that in this paper we measure the strong coupling strength in crystals which differ by term of one neutron from each other. When we add one neutron in the hydrogen nucleus, we artificial activation of the strong interaction. As far as the gravitation, electromagnetic and weak interactions are the same in both kind crystals (LiH and LiD), it only changes the strong interaction. Therefore a logical conclusion is made that the

renormalization of the energy of electromagnetic excitations (isotopic shift equals 0.103 eV) is carried out by strong nuclear interaction. The short - range character of the strong interaction of nucleons does not possess direct mechanism of the elementary excitation (electrons, excitons, phonons) energy renormalization, which was observed in our low temperature experiments. Second reason that the interpretation of our experimental results is very difficult task because they are first demonstration of the violation of the strong conclusion in nuclear and particles physics that the strong nuclear force does not act on the colorless leptons (see, e.g. [4, 1]). Moreover we have some contradictions taking into account that the forces between quarks must be long - range, because the gluons have zero mass. But as was mentioned above, the short range when forces between the colorless hadrons are the residues of the forces between their quark constituents, and cancel when the distance between hadrons is more than nuclear size [5]. We can see that the nuclear size transforms long - range interaction in the short - range strong one. It is very old question which up to present time has not any theoretical explanation.

In spite of above discussion, at present time we can distinguish the following mechanisms of the isotopic shift zero phonon line:

1. Long - range electric field of the neutron's quarks. This mechanism owing to the confinement quarks is limited by the boundary of the neutron.

2. The possible new structure of the quarks and leptons - so - called preons [1, 33 - 38].

3. The most likely mechanism of the neutron - lepton interaction is connected to the magnetic - like strong field of neutron 's quarks. Taking into account anomalous magnetic moment of the neuron in the paper [39] was obtained the value of strong coupling constant $\alpha_s = 2.4680$ (see, also[40]). Quite large value in comparison with the accelerator technique value $\alpha_s(M_Z) = 0.1198$ [28]. The large value α_s is thus justified to think that residual strong forces acting beyond nucleon could exist. A possible interpretation is to assume that in addition to the 8 gluons predicted by QCD $SU(3)_c$ group there is a ninth gluon color singlet [4]

$$g_9 = \frac{1}{\sqrt{3}} (r\bar{r} + g\bar{g} + b\bar{b}) \qquad (11)$$

This massless photon - like gluon may be strongly interacts between nucleons (neutrons) and leptons (electrons) (see, also [2, 4]. Returning to Fig. 11 we can note that our measurements permit to obtain value of strong coupling constant from α_s =

2.4680 (pure LiD crystals) to $\alpha_s = 0$ (pure LiH crystals). Moreover, in Fig. 12 we show the dependence of α_s on neutron's number in different substances. We can see as early in the case of pure LiD crystals we have non - linear character of α_s on the neutron's number in different substances. Deviation from nonlinearity may indicate the emergence of a new force not taken int account in the SM and requiring a more fundamental, including theoretical analysis.

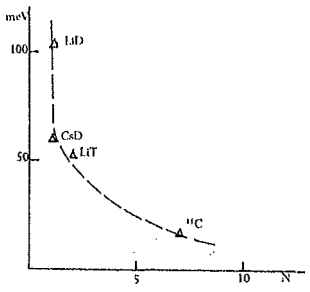

Fig. 12. The dependence of the strong force on the number of neutrons in different substances.

Thus, the tentative interpretation of describing non - accelerator experimental results does not find consisted explanation at the change of strong interaction leaving to another mystery of SM. We should remind that intrinsic contradiction of Standard Model is already well - known. Really, the Lagrangian of QCD (theory of the strong interaction) has the next form (see, e.g. [41]):

$$L = i\sum_q \bar{\Psi}^a_q(\nabla_\mu\gamma_\mu + im_q)\Psi^a_q - \tfrac{1}{4}G^n_{\mu\nu}G^n_{\mu\nu}, \quad (12)$$

where

$$\nabla_\mu = \partial_\mu - ig\frac{\lambda^n}{2}A^n_\mu,$$

$$G^n_{\mu\nu} = \partial_\mu A^n_\mu - \partial_n A^n_\mu + gf^{nml}A^n_\mu A^l_\nu. \qquad (13)$$

Ψ^a_q and A^n_μ are quark and gluon fields, a=1,2,3,...8 are color indices , λ^n and f^{nml} are Gell - Mann matrices and f symbols, m_q - are bare (current) masses, q = u, d, s, c, ... different quarks. It is common place [2, 4] that the Lagrangian (12) contains the members which describe both free motion and interaction between quarks and gluons, which is defined by the strength couple g. Spacing of which it is necessary to remark that although the Lagrangian (12) possesses rather attractive peculiarities (see, also [2, 4]), its eigenstates are the quarks and the gluons which are not observed in free states [42, 43]. The observed hadrons in the experiment don't eigenstates in QCD. It is obvious to expect that the modern theory of QCD should finally overcome these difficulties.

The next step our discussion is devoted to the neutron - electron binding energy. From our non - accelerator experimental results is followed that this value equals 0.106 eV on LiH_xD_{1-x} and 0.107 eV on the diamond (see, also [44]). In electrostatic model, it is shown [45] the neutron - electron binding energy is less than analogous proton with an electron (13,6 eV) by approximately 128 times. Hence it follows that the theoretical value of the binding energy of a neutron with an electron is 106, 7 meV. Our experimental value of a neutron - electron binding energy is in excellent agreement with theoretical value.

The remarkable properties of the graphene promise unheard of applications, especially in the semiconductor state. Especially graphene nanostructures are promising candidates for future nanoelectronics and solid - state quantum information technology. As was shown above, in the vicinity of K - points (Fig. 5 in Chapter 5 [1]), the low - energy electron/hole dispersion relation is proportional to momentum, rather than its square (see, e.g. [46, 47]). This is analogous to the energy dispersion relation of massless relativistic electrons, so the electrons/holes of graphene are described as Dirac fermions having no mass. In a simple neighbor model graphene is a semimetal with zero - overlap between valence and conduction bands. In order to make graphene a real technology, a special issue must be solved: creating an energy gap at K - points in the Brillouin zone (see, Fig. 5 in Chapter 5 [1]).

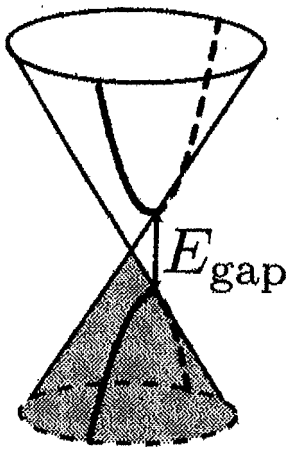

Fig. 13. The energy dispersion of semimetal (solid line) and semiconductor (dashed line).

Different attempts have been made by researches, such as patterning graphene into nanoribbon, forming graphene quantum dots, making use of multilayer graphene sheet and applying an external electric field (see, e.g [47]. It was shown that the uniaxial strain can open a band - gap in a metallic carbon nanotubes as well as carbon nanoribbon . As an example Fig. 40 shows the dependence of the energy of interband transition on the width of the graphene nanoribbons. The observed dependence is well described by the following expression $E_g = \alpha^*/ (W - W^*)$, where $\alpha^* = 0.38$ eV/nm, and $W^* = 16$ nm accounts for inactive edges [48]. This formula gives value of E_g equal to several eV, if W is reduced to a size , for example, ^{13}C, but it is impossible. The isotopic transformation of graphene, a semimetal into semiconductor deserves special attention [49, 50] This means of the cones dispersion pattern $E(\vec{k})$ at the K point of the Brillouin zone of graphene reformes into the usual parabolic dispersion of band structure pattern (see Fig. 13).

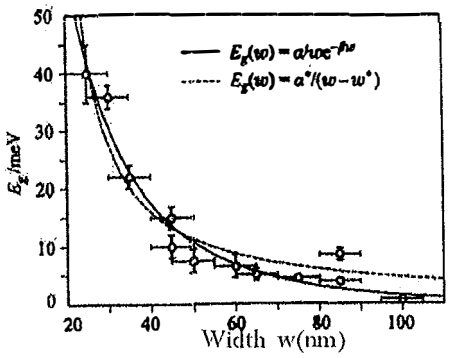

Fig. 14. The dependence of E_g as a function of width of the graphene nanoribbons (after [48]).

Taking into account Raman scattering spectra we have been obtained E_g in graphene of several hundred meV (up to 1 eV). Since value of E_g depends on the concentration of ^{13}C in graphene, this mechanism is easily realized either chemically or technologically. With the opening E_g of massless fermions (leptons = electrons) acquire mass. Estimates of different ways of opening E_g in graphene give the following equality: $E_g = 2m$ [50]. When $E_g = 1$ eV leptons acquire a mass equal 0.5 eV - the value is not large, but finite. One of the mechanisms of acquire mass in elementary particle physics is considered in the paper [51]. This paper predicts that both quarks and gluons acquire running mass distribution in QCD, which are large at infrared momenta. The current quark of perturbative QCD evolves into a constituent quark as its momentum becomes smaller. The constituent quark mass arises from a cloud of low - momentum gluons attaching then selves to the current quark. This is DCSB: an essentially nonperturbative effect that generates a quark mass from nothing; namely it occurs even in the chiral limit. DCSB namely the generation of mass from nothing is a theoretically established nonperturbative feature of QCD. The solution of a gap equation shows that gluons are cannibals: they are particle species whose members become massive by eating each other (the details see [49 - 520=]).

5. Conclusion.

The artificial activation of the strong nuclear interaction by adding one (two or more) neutrons in atomic nuclei leads it to the direct observation of the strong interaction in low - temperature optical spectra of solids. This conclusion opens new avenue in the investigation of the constant of strong nuclear interaction in the wide value range by means the condensed matter alike traditional methods. The observation of an isotopic shift (0.103 eV) of the zero-phonon line of free excitons in the luminescence spectra of LiH (without strong interaction in the hydrogen nucleus) and LiD (with strong interaction in the deuterium nucleus) crystals was the first and direct evidence of the long-range interaction of the Yukawa potential. Indeed, in both crystals, the lithium ions, the proton and the electron are the same and, therefore, the gravitational, electromagnetic and weak interactions are the same, and the addition of a neutron, according to Yukawa, a strong interaction appears, the influence of which manifests itself in the isotopic shift. These experimental results demonstrate the neutron-electron binding energy (0.106 eV) which is in excellent agreement with the theoretical Breit estimate of 0.1067 eV Experimental observation of the renormalization of the elementary excitation energy of solids by the strong nuclear interaction stimulates its count in the process of description of the elementary excitations dynamics in quantum electrodynamics. Present review continuous to develop between nuclear and condensed matter physics, and for the first time it was shown solid - state manifestation of quantum chromodynamics.

References.

1. V.G. Plekhanov, Hadron - Lepton Interaction (LAMBERT Academic Publishing, Germany, 2021)

2. D.H. Perkins, Introduction to High Energy Physics (CUP, Cambridge, 2000).

3. W.N. Cottingham, D.A. Greenwood, An Introduction to the Standard Model of Particle Physics (CUP, Cambridge, 2007).

4. G. Griffiths, Introduction to Elementary Particles (Wiley - VCH, Weinheim, 2008).

5. E.M. Henley, A. Garcia, Subatomic Physics (World Scientific Publishing Co., Singapore, 2007).

6. 6. M. Gell - Mann, Y. Neeman. The Eightfold Way (Benjamin, Reading,Mass., 1964).

7. Y. Yukawa, On the interaction of elementary particles, Proc. Phys. Math. Soc. **17** (1935) 48 - 57.

8. J.E. Field, The Properties of Natural and Synthetic Diamond (Academic Press, New York, 1982).

9. R.M. Santilli, The physics of new clean energy anf fuels according to hadronic mechanics, J. New Energy **1** (1998) 5 - 314; Scintia **151** (2024); R.M. Santilli, Hadronic Mechanics and Einstein Determenism: a New Paradigm in Nuclear Physics (Index of Sciences, London, 2025).

10. R.M. Santilli, aparent experimental confirmation of pseudoprotons and their application to new clean nuclear energies, Int. J. Appl. Math. **9** (2019) 72 - 100; A. Muktbodh, Santilli's recovering of Einstein's determinism, Prog. Phys. **20** (2024) 26 - 32; R.M. Santilli, Hadronc Mechanics and Einsrein's Determenism: A new Paradigm in Nuclear Physics (Index of Sciences, London, 2025).

11.V.G. Plekhanov, Experimental manifestation of the effect of disorder on exciton binding energy in mixed crystals, Phys. Rev. (1996) **B53** 9558 - 9560; V.G. Plekhanov, Isotope effects in lattice dynamics, Phys. - Uspekhi (Moscow) **46** (2003) 553 - 579.

12. V.G. Plekhanov, Renormalization the energy of elementary excitations in solids by the strong nuclear interaction, Universal J. Phys. and Appl. **11** (2017) 6 - 12.

13. R.S. Knox, Theory of Excitons (Academic Press, New York - London, 1963).

14. O.I. Tuytuynnik, V.I. Tuytuynnik, F.F. Gavrilov and G.I Pilipenko, Lithium hydride single crystal grow by Bridgmen - Stockbarge method using ultrosound, J. Crystal Growth **68** (1984) 741 - 749.

15. V.G. Plekhanov, Giant Isotope Effects in Solids (Stefan University Press, La Jola, CA, 2004).

16. I. Nordheim, Zur Elektrontheorie der metalle, Ann. Phys. (Leipzig) **401** (1931) 641 - 678.

17. S. Baroni, G. Pastori Parravichini, G. Pezzica, Quasiparticle band structure of lithium hydride, Phys. Rev. B**32** (1985) 4077 - 4083.

18. J.L. Verble, J.L Warren and J.L. Yarnell, Lattice dynamics of lithium hydride, ibid, **168** (1968) 980 - 989.

19. V.G. Plekhanov, Isotopic and disorder effects in large radis exciton spectroscopy, Phys. - Uspekhi **40** (1997) 553 - 568.

20. V.G. Plekhanov, V.I. Altukhov, Lihgt scattering in LiH crystas with LO phonon emission J. Raman Spectr. **16** (1985) 358 - 365.

21. W.B. Zimmerman, Lattice constant dependence on isotopic composition in the ^{7}Li(H,D) system, Phys. Rev. B**5** (1972) 4704 - 7.

22. V.G. Plekhanov, Fundamentals and applications of isotope effect in solids, **51** (2006) 287 - 426.

23. M.Born and J.R. Oppenheimer, On the quantum theory of molecules, in, Quantum Chemistry (Classic Scientific Paper) (World Sci. Publ. Co., Singapore, 2000).

24. G. Arfken, Mathematical Methods for Physicists (Academic Press, New York and London, 1968).

25. W.A. Harrison, Electronic Structure and Properties of Solids (W.F. Freeman and Co., San Fransicko, 1980); R.M. Martin, Electronic Structure - Basic Theory and Practical Methods (CUP, Cambridge, 2004).

26. F.I. Yndurain, The Theory of Quark and Gluon Interaction (Springer, Berlin, 2013).

27. G.M. Prosperi, M. Raciti, and C. Simolo, On the running coupling constant in QCD, Prog. Part. Nucl. Phys. **58** (2007) 387 - 438.

28. A. Deur, S.J. Brodsky and G.F. Toramond, The QCD running coupling, Progress in Particle and Nuclear Physics **90** (2016)1 - 74.

29. S. Bethke, World summary of α_s (2012), Eur. Phys. J. C**64** (2012) 689 - 695.

30. G. Altarelli, The QCD running coupling and its measurements, in, Proc. Corfu Summer Institute and Workshops on Elementary Particle Physics and Gravity, ArXiv: hep - ph/1303.6065 (2013).

31. G. Altarelli, Collider Physics within the Standard Model: a Primer, ArXiv: hep - ph/ 1303. 2842.

32. J. Jaeckel, A. Ringwad, The low - energy frontier of particle physics, Annu. Rev. Nucl. Part. Sci. **60** (2010) 405 - 450.

33. O.W. Greenberg, A new level of structure, Phys. Today, **38** (1985) 22 - 30.

34. B. Robson, The Generation model of particle physics, in, Particle Physics, E. Kennedy ed. (In Tech. Open Access Publisher, Rijeka, Croatia, 2012).

35. M. Aghirescu, The Cold Genesis of Matter and Fields (Science Publishing Group, New York, 2015).

36. C.S. Kalman and I. D'Souza, Preons: Models of Leptons, Quarks and Gauge Bosons as Composite Particles (World Scientific, Singapore, 1992).

37. C.S. Kalman, Why quarks cannot be fundamental particles, Nuclear Phys. B: Proceedings Supplements **142** (2005) 235 - 237.

38. O. Consa, The Helicon: A new preon model, Prog. Phys. **14** (2019) 215 - 219.

39. V.G. Plekhanov, J.G. Buitrago, Evidence of residual strong interaction in nuclear atomic level via isotopic shift in LiH - LiD crystals, Prog. Phys. **15** (2019) 68 - 71.

40. V.G. Plekhanov, Measurements of the wide value range of strong interaction coupling constant, SSRG - IJAP **6** (2019) 32 - 37.

41. I.M. Dremin, A.B. Kaidalov, Quantum chromodynamics and the phenomenology of strong interaction, Phys - Uspekhi **49** (2006) 263 - 273.

42. D. Vretenar and W. Weise, Exploring the nucleus in the context of low - energy QCD, Lecture Notes Phys. **641** (2004) 65 - 117.

43. V.G. Plekhanov, Direct observation of the strong nuclear interaction in the optical spectra of solids, Proceed. 3rd Conf. High Energy Phys. Rome, Italy, 2017, p.46.

44. V.G. Plekhanov, Phenomenology of the origin of isotope effect, PSIJ **18** (2018) 1 - 11.

45. G. Breit, Theory of isotope shift, Rev. Mod. Phys. **30** (1958) 507 - 517.

46. A.H. Castro Neto, F. Guinea, M.N. Peres et al., The electronic properties of graphene, Rev. Mod. Phys. **81** 109 - 162.

47. A.C. Ferrari, F. Fal'ko, Jari Kinaret et al., Science and technology road map for graphene, related two - dimensional crystals, and hybrid systems, Nanoscale **7** (2015) 4598 - 4810.

48. Ch. Stampfer, S. Fringe, J. Guttinger, Transport in graphene nanostructures, Front. Phys. **6** (2011) 271 - 293.

49. V.G. Plekhanov, Chapter 1 in, Understanding Quarks, Nova Science Publishers, Inc., New York, 2021, p.p. 1 - 92.

50. Ken - ichi Sasaki, Massive Dirac Fermions Signal in Raman Spectrum of Graphene, Phys. Rev. B**97** (2018)115413 - 6.

51. C.D. Roberts, Hadron physics and QCD: Just the basic facts, ArXiv: nucl - th/ 1501.06581.

52. C.D. Roberts, Empirical consequence of emergent mass, Symmetry **12** (2020) 1468 - 1506.

HADRONIC JOURNAL 48, 341 - 363 (2025)
DOI 10.29083/HJ.48.03.2025/SC341

A VARIATIONAL FORMULATION FOR A TWO PHASE MODEL IN SUPERCONDUCTIVITY AND A RESPECTIVE NUMERICAL EXAMPLE

Fabio Silva Botelho
Department of Mathematics
Federal University of Santa Catarina - UFSC
Florianópolis, SC, Brazil
fabio.botelho@ufsc.br

Received July 30, 2024
Revised August 15, 2025

Abstract

This short communication develops a variational formulation for modeling a two phase model in superconductivity. The results are based on standard tools of calculus of variations and optimization theory. Moreover, we emphasize the context here addressed is essentially an Euler-Bernoullian one.

AMS Classification 35Q70, 70S05, 76A02
Keywords. Ginzburg-Landau system, superconductivity, strong variational formulations, Lagrange multipliers, optimization.

Copyright © 2025 by Hadronic Press, Inc., Palm Harbor, FL 34684, USA

1 Introduction

The first part of this article develops a variational formulation for a model in superconductivity.

Such results are based on tools of calculus of variations and related Lagrange multipliers approach. It is worth emphasizing, in the model here presented, a particle system corresponding to a fluid phase a, as submitted to a decreasing in temperature, partially changes into a super-conducting phase b. We emphasize, in such a here presented model, the super-conducting phase b behaves somewhat like a "single particle field", with approximately a unique quantum energy level.

Hence, concerning such scenarios, the particle mass constraint functionals for the phases a e b stand for

$$J_{Aux_1^a} = \int_0^{t_f} \int_\Omega E_1^a(y,t) \left(\int_\Omega (|\phi_a(x,y,t)|^2 \, dx - m_p^a \right) \, dy \, dt, \tag{1}$$

where for such a phase a, the energy level $E_1^a(y,t)$ depends on y and t, and

$$J_{Aux_1^b} = \int_0^{t_f} E_1^b(t) \left(\int_\Omega (|\phi_b(x,t)|^2 \, dx - m_p^b \right) \, dt, \tag{2}$$

where for such a phase b, the energy level $E_1^b(t)$ does not depend on y, that is, depends only on t, qualitatively behaving as a single energy state at each t.

Furthermore, we highlight the two main fields for such a system are a position one and a velocity one, which we specify below in the next lines.

It is worth mentioning similar models in superconductivity (the standard Ginzburg-Landau ones) are addressed in [1, 2].

As standard references in theoretical fluid mechanics we would cite [3, 4, 5, 6, 7]. For related numerical methods we would mention [8, 9, 10, 11]. Concerning other similar models, we would cite [12, 13, 14, 15, 16, 17].

Finally, details on the Sobolev spaces involved may be found in [18].

Let $\Omega \subset \mathbb{R}^3$ be an open, bounded and simply connected set with a regular (Lipschitzian) boundary denoted by $\partial\Omega$.

Generically, we consider a electronic density motion initially modeled as a particle system one, through the field of position $\mathbf{r} : \Omega \times [0, t_f] \to \mathbb{R}^3$ and field of velocities $\mathbf{v}$ where $\mathbf{v}(\mathbf{r}(x,t),t)$ stands for the velocity at the position $\mathbf{r}(x,t)$ and time $t \in [0, t_f]$.

Moreover, the gravity field is denoted by

$$\mathbf{g} = -g\mathbf{k},$$

related to the $\mathbb{R}^3$ basis

$$\{\mathbf{i} = (1,0,0), \mathbf{j} = (0,1,0), \mathbf{k} = (0,0,1)\}.$$

2 The mathematical model

In this section, we develop in details the concerning variational formulation.

We emphasize such a set $\Omega \subset \mathbb{R}^3$ stands for a control volume, in which along a time interval $[0, t_f]$, where $t \in [0, t_f]$ denotes time, an electronic density develops a compressible motion.

For a particle system corresponding to a normal phase a, we start by defining the following electronic density field,

$$\hat{\rho}_a(x,y,t) = \left(|\phi_a(x,y,t)|^2 \frac{|\phi_a^M(y,t)|^2}{m_p^a} \right) \tag{3}$$

Here m_p^a denotes the mass of a single particle type a.

The macroscopic fluid density for such phase a, is defined by

$$\rho_a(y,t) = |\phi_a^M(y,t)|^2.$$

We recall that in the super-conducting phase b has approximately a unique energy level, which depends only on t but does not depend on the macroscopic variable y.

For such a particle system corresponding to the super-conducting phase b, we start by defining the following density field,

$$\hat{\rho}_b(x,y,t) = \left(|\phi_b(x,t)|^2 \frac{|\phi_b^M(y,t)|^2}{m_p^b} \right) \tag{4}$$

Here m_p^b denotes the mass of a single particle type b.

The macroscopic electronic fluid density for such phase b, is defined by

$$\rho_b(y,t) = |\phi_b^M(y,t)|^2.$$

It is worth highlighting that generically, we denote

$$L^2(\Omega \times [0,t_f]) =$$
$$\left\{ h : \Omega \times [0,t_f] \to \mathbb{R} \text{ measurable } : \int_0^{t_f} \int_\Omega |h(x,t)|^2 \, dxdt < +\infty \right\}, \quad (5)$$

$$L^2(\Omega \times [0,t_f];\mathbb{R}^3) = \left\{ h = (h_1,h_2,h_3) : \Omega \times [0,t_f] \to \mathbb{R}^3 \right.$$
$$\left. : \; h_k \in L^2(\Omega \times [0,t_f]),\ \forall k \in \{1,2,3\} \right\}, \quad (6)$$

$$W^{1,2}(\Omega \times [0,t_f]) = \left\{ h : \Omega \times [0,t_f] \to \mathbb{R} \; : \; h \in L^2(\Omega \times [0,t_f]) \right.$$
$$\left. \text{and } h_t,\ h_{x_j} \in L^2(\Omega \times [0,t_f]),\ \forall j \in \{1,2,3\} \right\}, \quad (7)$$

where the partial derivatives h_t, h_{x_j} are understood in a distributional sense, $\forall j \in \{1,2,3\}$.

Moreover,

$$W^{1,2}(\Omega \times [0,t_f];\mathbb{R}^3) = \left\{ h = (h_1,h_2,h_3) : \Omega \times [0,t_f] \to \mathbb{R}^3 \right.$$
$$\left. : \; h_k \in W^{1,2}(\Omega \times [0,t_f]),\ \forall k \in \{1,2,3\} \right\}. \quad (8)$$

Similar notations are valid for other sets and other related complex and vectorial cases.

With such notations in mind, we define the concerning function spaces

$$V_1^a =$$
$$\left\{ \phi_a \in W^{1,2}(\Omega \times \Omega \times [0,t_f];\mathbb{C}) \; : \; \nabla_x \phi_a \cdot \mathbf{n} = \text{ on } \partial\Omega \times \Omega \times [0,t_f], \right.$$
$$\nabla_y \phi_a \cdot \mathbf{n} = \text{ on } \Omega \times \partial\Omega \times [0,t_f], \frac{\partial \phi_a(x,y,0)}{\partial t} = 0$$
$$\left. \text{and } \frac{\partial \phi_a(x,y,t_f)}{\partial t} = 0 \text{ in } \Omega \times \Omega \right\} \quad (9)$$

and

$$V_2^a = \left\{ \phi_a^M \in W^{1,2}(\Omega \times [0,t_f];\mathbb{C}) \; : \; \phi_a^M = 0 \text{ on } \partial(\Omega_1 \cup \Omega_2) \times [0,t_f], \right.$$
$$\left. \phi_a^M(z,t) = \phi_{in}(z,t) \text{ on } \partial\Omega_{in} \times [0,t_f] \text{ and } \phi_a^M(z,0) = \phi_0 \text{ in } \Omega \right\}, \quad (10)$$

where

$$\partial\Omega = \partial\Omega_{in} \cup \partial\Omega_1 \cup \partial\Omega_2 \cup \partial\Omega_{out}.$$

Moreover we suppose such a union is quasi-disjoint and through $\partial\Omega_{in}$ and $\partial\Omega_{out}$ are allowed the entering and exiting of fluid mass, respectively.

We define also,

$$V_1^b = \left\{\phi_b \in W^{1,2}(\Omega \times [0,t_f];\mathbb{C}) \ : \ \nabla_x \phi_b \cdot \mathbf{n} = \text{ on } \partial\Omega \times [0,t_f], \right. \\ \left. \frac{\partial \phi_b(x,0)}{\partial t} = 0 \text{ and } \frac{\partial \phi_b(x,t_f)}{\partial t} = 0 \text{ in } \Omega \right\} \tag{11}$$

and

$$V_2^b = \left\{\phi_b^M \in W^{1,2}(\Omega \times [0,t_f];\mathbb{C}) \ : \ \phi_b^M = 0 \text{ on } \partial(\Omega_1 \cup \Omega_2) \times [0,t_f], \right. \\ \left. \phi_b^M(z,t) = \phi_{in}(z,t) \text{ on } \partial\Omega_{in} \times [0,t_f] \text{ and } \phi_b^M(z,0) = \phi_0 \text{ in } \Omega \right\}, \tag{12}$$

Observe that, we may denote

$$\rho(y,t) = \rho_a(y,t) + \rho_b(y,t).$$

2.1 The position fields

For the phase a, we start by denoting the macroscopic electronic position field as

$$\mathbf{r}_a : \Omega \times [0,t_f] \to \mathbb{R}^3,$$

where

$$\mathbf{r}_a(x,t) = ((X_a)_1(x,t),(X_a)_2(x,t),(X_a)_3(x,t)).$$

In an internal variable and relativistic context, the particle position field for such a phase a, is defined by

$$\hat{\mathbf{r}}_a(x,t) = (\mathbf{r}_a(x,t),t) + \tilde{\mathbf{r}}_a^p(\mathbf{r}_a(x,t),t) = (\mathbf{r}_a(x,t),t) + (ct,\tilde{\mathbf{r}}_a(\mathbf{r}_a(x,t)).$$

Here $c > 0$ denotes the speed of light.

For the phase b, we start by denoting the macroscopic electronic position field as

$$\mathbf{r}_b : \Omega \times [0,t_f] \to \mathbb{R}^3,$$

where

$$\mathbf{r}_b(x,t) = ((X_b)_1(x,t),(X_b)_2(x,t),(X_b)_3(x,t)).$$

In an internal variable and relativistic context, the particle position field for such a phase a, is defined by

$$\hat{\mathbf{r}}_b(x,t) = (\mathbf{r}_b(x,t),t) + \tilde{\mathbf{r}}_b^p(\mathbf{r}_b(x,t),t) = (\mathbf{r}_b(x,t),t) + (ct,\tilde{\mathbf{r}}_b(\mathbf{r}_b(x,t)).$$

We define also the following function space

$$V_3^a = \{\mathbf{r}_a \in W^{1,2}(\Omega \times [0,t_f];\mathbb{R}^3) \ : \ \mathbf{r}_a = \mathbf{0} \text{ on } (\partial\Omega_1 \cap \partial\Omega_2) \times [0,t_f] \text{ and } \mathbf{r}_a(z,0) = \mathbf{r}_0 \text{ in } \Omega\}, \tag{13}$$

and assume

$$\tilde{\mathbf{r}}_a \in V_4 = W^{1,2}(\mathbb{R}^3;\mathbb{R}^3).$$

For the phase b, we define the following corresponding space

$$V_3^b = \{\mathbf{r}_b \in W^{1,2}(\Omega \times [0,t_f];\mathbb{R}^3) \ : \ \mathbf{r}_b = \mathbf{0} \text{ on } (\partial\Omega_1 \cap \partial\Omega_2) \times [0,t_f] \text{ and } \mathbf{r}_b(z,0) = \mathbf{r}_0 \text{ in } \Omega\}, \tag{14}$$

and assume

$$\tilde{\mathbf{r}}_b \in V_4 = W^{1,2}(\mathbb{R}^3;\mathbb{R}^3).$$

2.2 About the system constraints

Denoting by $m_T = m_a(0) + m_b(0)$ the total system mass at $t = 0$, we have the following constraint

$$\begin{aligned} m_T &= m_a(0) + m_b(0) \\ &= m_a(t) + \int_0^t \int_{\partial\Omega} \rho_a(y,\tau)\mathbf{v}_a \cdot \mathbf{n} \, dS \, d\tau \\ &\quad + m_b(t) + \int_0^t \int_{\partial\Omega} \rho_b(y,\tau)\mathbf{v}_b \cdot \mathbf{n} \, dS \, d\tau \end{aligned} \tag{15}$$

where

$$\mathbf{v}_a = \mathbf{v}_a(\mathbf{r}_a(x,t),t),$$
$$\mathbf{v}_b = \mathbf{v}_b(\mathbf{r}_b(x,t),t).$$

and where

$$m_a(t) = \int_\Omega \rho_a(y,t) \, dt$$

and

$$m_b(t) = \int_\Omega \rho_b(y,t) \, dt,$$

on $[0,t_f]$.

Here $\mathbf{n}$ denotes outward normal field to $\partial\Omega = S$.

Relating the internal kinetics energy, in a relativistic context, we define the following functional

$$
\begin{aligned}
& E^a_{C_1} \\
= \; & -\frac{1}{2}\int_0^{t_f}\int_\Omega\int_\Omega \frac{\hat\rho_a(x,y,t)\, d\tilde{\mathbf{r}}^p_a}{\sqrt{1-\frac{\tilde v_a^2}{c^2}}\, dt}\cdot\frac{d\tilde{\mathbf{r}}^p_a}{dt}\sqrt{-g^a}|\det X'_a|\, dx\, dy\, dt \\
= \; & \frac{1}{2}\int_0^{t_f}\int_\Omega\int_\Omega \frac{\hat\rho_a(x,y,t)}{\sqrt{1-\frac{\tilde v_a^2}{c^2}}}(c^2-\tilde v_a^2)\sqrt{-g^a}|\det X'_a|\, dx\, dy\, dt \\
= \; & \frac{1}{2}\int_0^{t_f}\int_\Omega\int_\Omega c\hat\rho_a(x,y,t)\sqrt{c^2-\tilde v_a^2}\sqrt{-g^a}|\det X'_a|\, dx\, dy\, dt \\
= \; & \frac{1}{2}\int_0^{t_f}\int_\Omega\int_\Omega c\hat\rho_a(x,y,t)\sqrt{c^2-\hat g^a_{jk}\frac{\partial(X_a)_j}{\partial t}\frac{\partial(X_a)_k}{\partial t}}\sqrt{-g^a}|\det X'_a|\, dx\, dy\, dt \\
= \; & \frac{1}{2}\int_0^{t_f}\int_\Omega e^a_C\, dy\, dt, \qquad (16)
\end{aligned}
$$

where generically, we have denoted, $(X_a)_0 = t$,

$$
g^a_{jk} = \frac{\partial\tilde{\mathbf{r}}^p_a}{\partial(X_a)_j}\cdot\frac{\partial\tilde{\mathbf{r}}^p_a}{\partial(X_a)_k}, \forall j,k\in\{0,1,2,3\}
$$

$$
\{\hat g^a_{jk}\} = \{g^a_{jk}\}_{(j,k\in\{1,2,3\})},
$$

$g^a = \det\{g^a_{jk}\}$, where

$$
w\cdot v = -w_0v_0 + \sum_{k=1}^{3} w_kv_k
$$

for

$$
w = (w_0, w_1, w_2, w_3)
$$

and

$$
v = (v_0, v_1, v_2, v_3)\in\mathbb{R}^4,
$$

and

$$
e^a_C = \int_\Omega c\hat\rho_a(x,y,t)\sqrt{c^2-\hat g^a_{jk}\frac{\partial(X_a)_j}{\partial t}\frac{\partial(X_a)_k}{\partial t}}\sqrt{-g^a}|\det X'_a|\, dx.
$$

With analogous notation, the corresponding functional for the phase b is defined by

$$
\begin{aligned}
& E^b_{C_1} \\
= \; & \frac{1}{2}\int_0^{t_f}\int_\Omega\int_\Omega c\hat\rho_b(x,y,t)\sqrt{c^2-\hat g^b_{jk}\frac{\partial(X_b)_j}{\partial t}\frac{\partial(X_b)_k}{\partial t}}\sqrt{-g^b}|\det X'_b|\, dx\, dy\, dt \\
= \; & \frac{1}{2}\int_0^{t_f}\int_\Omega e^b_C\, dy\, dt, \qquad (17)
\end{aligned}
$$

where,

$$e_C^b = \int_\Omega c\hat{\rho}_b(x,y,t)\sqrt{c^2 - \hat{g}_{jk}^b \frac{\partial (X_b)_j}{\partial t}\frac{\partial (X_b)_k}{\partial t}}\sqrt{-g^b}|\det X_b'|\,dx.$$

For the interacting and self-interacting energies, in a non-linear Schrödinger equation context, we define the following functional,

$$\begin{aligned} E_{in} &= \frac{\alpha_1^a}{2}\int_0^{t_f}\int_\Omega\int_\Omega \rho_a(y,t)^2\,dy\,dt \\ &\quad -\frac{\beta_1^a}{2}\int_0^{t_f}\int_\Omega\int_\Omega \rho_a(y,t)\,dy\,dt \\ &\quad +\frac{\alpha_1^b}{2}\int_0^{t_f}\int_\Omega\int_\Omega \rho_b(y,t)^2\,dy\,dt \\ &\quad -\frac{\beta_1^b}{2}\int_0^{t_f}\int_\Omega\int_\Omega \rho_b(y,t)\,dy\,dt \end{aligned} \tag{18}$$

for appropriate $\alpha_1^a > 0$, α_1^b and β_1^a, $\beta_1^b > 0$.

On the other hand, we define

$$\begin{aligned} E_M &= \frac{1}{2}\int_0^{t_f}\int_\Omega\int_\Omega \left(\frac{\gamma_1^a}{m_p^a}|\nabla\phi_a(x,y,t) - iw_a\mathbf{A}\phi_a(x,y,t)|^2\right)|\phi_a^M(y,t)|^2\,dx\,dy\,dt \\ &= \frac{1}{2}\int_0^{t_f}\int_\Omega\int_\Omega \left(\frac{\gamma_1^b}{m_p^b}|\nabla\phi_b(x,t) - iw_b\mathbf{A}\phi_b(x,t)|^2\right)|\phi_b^M(y,t)|^2\,dx\,dy\,dt, \end{aligned} \tag{19}$$

for appropriate constants γ_1^a, $\gamma_1^b > 0$ and w_a, $w_b \in \mathbb{R}$.

Concerning the restrictions, already including the respective Lagrange multipliers, we define also the following functionals,

$$\begin{aligned} &J_{Aux_1^a} = \\ &\int_0^{t_f}\int_\Omega E_1^a(y,t)\left(\int_\Omega(|\phi_a(x,y,t)|^2\,dx - m_p^a\right)\,dy\,dt, \end{aligned} \tag{20}$$

$$\begin{aligned} &J_{Aux_1^b} = \\ &\int_0^{t_f} E_1^b(t)\left(\int_\Omega(|\phi_b(x,t)|^2\,dx - m_p^b\right)\,dt, \end{aligned} \tag{21}$$

$$J_{Aux_2} = \int_0^{t_f} E_2(t) \left(m_T - \int_\Omega \rho_a(y,t)\, dy - \int_0^t \int_{\partial\Omega} \rho_a(y,\tau)\mathbf{v}_a \cdot \mathbf{n}\, dS\, d\tau \right.$$
$$\left. - \int_\Omega \rho_b(y,t)\, dy - \int_0^t \int_{\partial\Omega} \rho_b(y,\tau)\mathbf{v}_b \cdot \mathbf{n}\, dS\, d\tau \right) dt. \tag{22}$$

$$J_{Aux_3^a} = \int_0^{t_f} \int_\Omega E_3^a(x,t) \left(\mathbf{v}_a(\mathbf{r}_a(x,t),t) - \frac{\partial \mathbf{r}_a(x,t)}{\partial t} \right) dx\, dt,$$

$$J_{Aux_3^b} = \int_0^{t_f} \int_\Omega E_3^b(x,t) \left(\mathbf{v}_b(\mathbf{r}_b(x,t),t) - \frac{\partial \mathbf{r}_b(x,t)}{\partial t} \right) dx\, dt,$$

$$J_{Aux_4} = -\int_0^T \int_\Omega \hat{P} \left(\frac{d\rho}{dt} + \rho_a \text{ div } \mathbf{v}_a + \rho_b \text{ div } \mathbf{v}_b \right) dy\, dt, \tag{23}$$

Moreover, considering the pressure and temperature scalar fields, we define

$$P_a = \frac{d(\hat{P}\rho_a)}{dt},$$

$$P_b = \frac{d(\hat{P}\rho_b)}{dt},$$

where

$$\hat{P} \in V_5$$

$$V_5 = \{\hat{P} \in W^{1,2}(\Omega \times [0,t_f]) \ : \ P = P_a + P_b = P(\hat{P},\rho) = P_0, \text{ on } \partial\Omega \times [0,t_f]\}.$$

and the temperature fields, T_a, T_b through the equations

$$(C_v)_a \rho_a T_a = e_C^a \tag{24}$$

so that

$$(C_v)_b \rho_b T_b = e_C^b \tag{25}$$

for an appropriate real constant $C_v > 0$.

At this point, we define the entropy differentials

$$dS_a = -\hat{K}_a \frac{\rho_a}{\rho} \ln\left(\frac{\rho_a}{e\,\rho}\right) dydt,$$

$$dS_b = -\hat{K}_b \frac{\rho_b}{\rho} \ln\left(\frac{\rho_b}{e\,\rho}\right)\, dydt,$$

and the functional

$$E^S = \int_0^{t_f} \int_\Omega (T_a\, dS_a + T_b\, dS_b).$$

Moreover, we also define

$$e^S = T_a S_a + T_b S_b,$$

where

$$S_a = -\hat{K}_a \frac{\rho_a}{\rho} \ln\left(\frac{\rho_a}{e\,\rho}\right)$$

and

$$S_b = -\hat{K}_b \frac{\rho_b}{\rho} \ln\left(\frac{\rho_b}{e\,\rho}\right).$$

With such results in mind, neglecting the effect of electromagnetic fields on the temperature ones, we define the restriction

$$\begin{aligned} & (C_v)_a \rho_a \frac{dT_a}{dt} + (C_v)_b \rho_b \frac{dT_b}{dt} \\ = \;& K_a \nabla^2 T_a + K_b \nabla^2 T_b \\ & -P_a \text{ div } \mathbf{v}_a - P_b \text{ div } \mathbf{v}_b + \frac{de^S}{dt}, \end{aligned} \tag{26}$$

for an appropriate real constants $K_a > 0,\ K_b > 0$.

At this point, we define the following function space

$$V_6^a = \{T_a \in W^{1,2}(\Omega \times [0,t_f]) \ :\ T_a(z,t) = T_1^a(z,t) \text{ on } \partial\Omega \times [0,t_f] \text{ and } T_a(z,0) = T_0^a(z) \text{ in } \Omega\},$$

$$V_6^b = \{T_b \in W^{1,2}(\Omega \times [0,t_f]) \ :\ T_b(z,t) = T_1^b(z,t) \text{ on } \partial\Omega \times [0,t_f] \text{ and } T_b(z,0) = T_0^b(z) \text{ in } \Omega\},$$

and

$$\begin{aligned} V_7^a \;=\; & \{\mathbf{v}_a \in W^{1,2}(\mathbb{R}^3;\mathbb{R}^3) \ :\ \mathbf{v}_a = \mathbf{0} \text{ on } (\partial\Omega_1 \cup \partial\Omega_2) \times [0t_f T] \\ & \text{and } \mathbf{v}_a(z,0) = \mathbf{v}_0^a \text{ on } \Omega\}. \end{aligned} \tag{27}$$

$$\begin{aligned} V_7^b \;=\; & \{\mathbf{v}_b \in W^{1,2}(\mathbb{R}^3;\mathbb{R}^3) \ :\ \mathbf{v}_b = \mathbf{0} \text{ on } (\partial\Omega_1 \cup \partial\Omega_2) \times [0,t_f] \\ & \text{and } \mathbf{v}_b(z,0) = \mathbf{v}_0^b \text{ on } \Omega\}. \end{aligned} \tag{28}$$

With such restrictions and definitions in mind, we define also the following functionals,

$$J_{Aux_5^a} = \int_0^{t_f} \int_\Omega E_5^a(y,t)\left((C_v)_a \rho_a T_a - e_C^a\right)\, dydt \tag{29}$$

$$J_{Aux_5^b} = \int_0^{t_f} \int_\Omega E_5^b(y,t)\left((C_v)_b \rho_b T_b - e_C^b\right)\, dydt \tag{30}$$

and

$$\begin{aligned} J_{Aux_6} = \int_0^{t_f} \int_\Omega E_6(y,t) \Bigg(& (C_v)_a\, \rho_a \frac{dT_a}{dt} + (C_v)_b\, \rho_b \frac{dT_b}{dt} \\ & -K_a \nabla^2 T_a - K_b \nabla^2 T_b \\ & +P_a \text{ div } \mathbf{v}_a + P_b \text{ div } \mathbf{v}_b - \frac{de^S}{dt}\Bigg)\, dy\, dt. \end{aligned} \tag{31}$$

Finally, we define the following functional,

$$J_{Aux_7^a} = \int_0^{t_f} \int_\Omega E_{50}^a(y,t)\left(\rho_a(y,t) - \int_\Omega \left(\frac{|\phi_a(x,y,t)|^2}{m_p^a}\right) dx\, |\phi_a^M(y,t)|^2\right) dy\, dt \tag{32}$$

$$J_{Aux_7^b} = \int_0^{t_f} \int_\Omega E_{50}^b(y,t)\left(\rho_b(y,t) - \int_\Omega \left(\frac{|\phi_b(x,y,t)|^2}{m_p^b}\right) dx\, |\phi_b^M(y,t)|^2\right) dy\, dt \tag{33}$$

3 The main functional

Here we define the functional J, by

$$\begin{aligned} J = & \frac{1}{2}\int_0^{t_f} \int_\Omega \rho_a \mathbf{v}_a \cdot \mathbf{v}_a\, dy\, dt - \int_0^{t_f} \int_\Omega \rho_a \mathbf{g} \cdot \mathbf{r}_a\, dy\, dt \\ & +\frac{1}{2}\int_0^{t_f} \int_\Omega \rho_b \mathbf{v}_b \cdot \mathbf{v}_b\, dy\, dt - \int_0^{t_f} \int_\Omega \rho_b \mathbf{g} \cdot \mathbf{r}_b\, dy\, dt \\ & -K_1 \int_0^{t_f} \int_\Omega \rho_a \mathbf{A} \cdot \frac{\partial \mathbf{r}_a}{\partial t}\, dxdt \\ & -K_1 \int_0^{t_f} \int_\Omega \rho_b \mathbf{A} \cdot \frac{\partial \mathbf{r}_b}{\partial t}\, dxdt, \end{aligned} \tag{34}$$

for an appropriate real constant K_1.

Moreover, for $\varepsilon > 0$ small, we define the functional J_1, by

$$\begin{aligned} J_1 &= -\int_0^{t_f}\int_\Omega V(x,t)K_1(\rho_a+\rho_b)\,dxdt \\ &+\frac{1}{8\pi}\int_0^{t_f}\int_\Omega |\ \mathrm{Curl}\ \mathbf{A}-\mathbf{B}_0|^2_{\mathbb{R}^3}\,dx\,dt \\ &-\frac{1}{8\pi}\int_0^{t_f}\int_\Omega \varepsilon_0(\rho(\mathbf{r}_a,\mathbf{r}_b),\mathbf{r}_a,\mathbf{r}_b)\left|\nabla V+\frac{1}{c}\frac{\partial \mathbf{A}}{\partial t}\right|^2_{\mathbb{R}^3}\,dxdt \\ &+\int_0^{t_f}\int_0^{t_f}\rho_a\mathbf{B}\times\frac{\partial \mathbf{r}_a}{\partial t}\cdot(\mathbf{r}_a(x,\varepsilon t)-\mathbf{r}_a(x,0))\,dx\,dt \\ &+\int_0^{t_f}\int_0^{t_f}\rho_b\mathbf{B}\times\frac{\partial \mathbf{r}_b}{\partial t}\cdot(\mathbf{r}_b(x,\varepsilon t)-\mathbf{r}_b(x,0))\,dx\,dt, \end{aligned} \tag{35}$$

where $c > 0$ in atomic units denotes the speed of light,

$$\mathbf{B} = \mathbf{B}_0 - \ \mathrm{Curl}\ \mathbf{A},$$

denotes the total magnetic field, $\mathbf{A}$ denotes a magnetic potential and $\mathbf{B}_0$ stands for an external magnetic field.

Furthermore, V is an external electric potential and

$$\mathbf{E} = \left(\nabla V + \frac{1}{c}\frac{\partial \mathbf{A}}{\partial t}\right),$$

is the electric field resulting from the charged particles.

Defining

$$(V,\mathbf{A}) \in V_8 = W^{1,2}(\Omega\times[0,t_f])\times W^{1,2}(\Omega\times[0,t_f];\mathbb{R}^3)$$

and

$$\tilde{V} = V_1^a\times V_1^b\times V_2^a\times V_2^b\times V_3^a\times V_3^b\times V_5\times V_6^a\times V_6^b\times V_7^a\times V_7^b\times V_8,$$

the final variational formulation $J_{total}:\tilde{V}\to\mathbb{R}$ stands for

$$\begin{aligned} J_{total} &= -J+J_1 \\ &E_{C_1}^a+E_{C_1}^b+E_{in} \\ &+E_M+J_{Aux_1^a}+J_{Aux_1^b}+J_{Aux_2}+J_{Aux_3^a}+J_{Aux_3^b} \\ &J_{Aux_4}+J_{Aux_5^a}+J_{Aux_5^b} \\ &+J_{Aux_6}+J_{Aux_7^a}+J_{Aux_7^b}-E^S. \end{aligned} \tag{36}$$

The variation of J_{total} in $\mathbf{r}_a$ which lead us to the correct Euler-Lagrange equation is defined by

$$\begin{aligned}
&\hat{\delta}(J_{total})_{\mathbf{r}_a}(\mathbf{r}_a, \mathbf{r}_a(x,\varepsilon t),\ \cdots,\mathbf{A}, V;\varphi)\\
=\ &\lim_{h\to 0}\left[J_{total}(\mathbf{r}_a + h\varphi, \mathbf{r}_a(x,\varepsilon t) + h\varphi,\ \cdots,\mathbf{A}, V)\right.\\
&\left.-J_{total}(\mathbf{r}_a, \mathbf{r}_a(x,\varepsilon t),\ \cdots,\mathbf{A}, V)\right]/h\\
=\ &\mathbf{0},\ \forall\varphi\in C_c^\infty(\Omega\times[0,T];\mathbb{R}^3).
\end{aligned}\tag{37}$$

We highlight the solution of the concerned system including such an Euler-Lagrange equation is computable, through the Newton's method for example, by expanding J_{total} as a quadratic approximate function in φ about $(\mathbf{r}_a(x,t), \mathbf{r}_a(x,\varepsilon t))$ in each iteration.

A similar remark is valid for the variation of J_{total} in $\mathbf{r}_b$.

Remark 3.1. *Generically denoting*

$$V = V(x,t) = \hat{V}(\mathbf{r}_a, \mathbf{r}_b),$$

the variation of J_{total} in $\mathbf{A}$ stands for

$$\begin{aligned}
&curl\ (\ curl\ \mathbf{A} - \mathbf{B}_0) + \frac{1}{c}\frac{\partial}{\partial t}\left(\varepsilon_0\left(\nabla\hat{V}(\mathbf{r}_a,\mathbf{r}_b) + \frac{1}{c}\frac{\partial\mathbf{A}}{\partial t}\right)\right)\\
&+\mathcal{O}(\varepsilon) + 4\pi K_1\rho_a\frac{\partial\mathbf{r}_a}{\partial t} + +4\pi K_1\rho_b\frac{\partial\mathbf{r}_b}{\partial t}\\
=\ &\mathbf{0}.
\end{aligned}\tag{38}$$

Letting $\varepsilon\to 0$, we have the following Maxwell equation

$$curl\ \mathbf{B} - \frac{1}{c}\frac{\partial(\varepsilon_0\,\mathbf{E})}{\partial t} - 4\pi\tilde{J} = \mathbf{0},$$

where

$$\tilde{J} = K_1\rho_a\frac{\partial\mathbf{r}_a}{\partial t} + K_1\rho_b\frac{\partial\mathbf{r}_b}{\partial t}\tag{39}$$

The variation of J_{total} in V stands for

$$-4\pi K_1(\rho_a+\rho_b) + \ div\ \left(\varepsilon_0\left(\nabla\hat{V}(\mathbf{r}_a,\mathbf{r}_b) + \frac{1}{c}\frac{\partial\mathbf{A}}{\partial t}\right)\right) = \mathbf{0},$$

so that we obtain another Maxwell equation

$$div\ (\varepsilon_0\,\mathbf{E}) = 4\pi K_1(\rho_a+\rho_b).$$

Moreover, from

$$\mathbf{B} = -\ curl\ \mathbf{A} + \mathbf{B}_0$$

and assuming $div\,(\mathbf{B}_0) = 0$, *we have got*

$$div\ \mathbf{B} = -\ div\ (\ curl\ \mathbf{A}) = 0,$$

which is a third Maxwell equation.

Finally, the fourth Maxwell equation is obtained recalling that

$$\mathbf{E} = \nabla \hat{V}(\mathbf{r}_a, \mathbf{r}_b) + \frac{1}{c}\frac{\partial \mathbf{A}}{\partial t},$$

so that

$$curl\ \mathbf{E} = \ curl\,(\nabla V) + \frac{1}{c}\ curl\ \left(\frac{\partial \mathbf{A}}{\partial t}\right),$$

and therefore,

$$curl\ \mathbf{E} - \frac{1}{c}\left(\frac{\partial\ curl\ \mathbf{A}}{\partial t}\right) = \mathbf{0},$$

that is,

$$curl\ \mathbf{E} - \frac{1}{c}\left(\frac{\partial(-\mathbf{B} + \mathbf{B}_0)}{\partial t}\right) = \mathbf{0}.$$

Thus, if $\mathbf{B}_0$ *is time independent, that is,*

$$\frac{\partial \mathbf{B}_0}{\partial t} = \mathbf{0},$$

we have

$$curl\ \mathbf{E} + \frac{1}{c}\left(\frac{\partial \mathbf{B}}{\partial t}\right) = \mathbf{0}.$$

In summary, we have got all the four Maxwell equations as necessary conditions for a extremal point of J_{total}.

The objective of this section is complete.

4 A numerical example

In this section, we develop a numerical example which models the phase transition of a super-conducting straight bar corresponding to a domain $\Omega = [0, 1] \subset \mathbb{R}$, from a normal phase a to a superconductive phase b.

Here we highlight for this one dimensional example we have generically denoted

$$\nabla \phi_a = \frac{d\phi_a}{dx}$$

and

$$\nabla^2\phi_a = \frac{d^2\phi_a}{dx^2}.$$

For such a model, already including a Lagrange multiplier E related to the mass constraint

$$\int_\Omega (|\phi_a|^2 + |\phi_b|^2)dx = 1,$$

we define the simplified functional $J : V_1 \to \mathbb{R}$, where

$$\begin{aligned} J(\phi_a, \phi_b, \mathbf{r}_a, \mathbf{r}_b, E) \;=\; & -\frac{1}{2}\int_0^{t_f}\int_\Omega |\phi_a|^2 \frac{\partial \mathbf{r}_a}{\partial t}\cdot\frac{\partial \mathbf{r}_a^*}{\partial t}\,dx\,dt \\ & +\frac{\gamma_1}{2}\int_\Omega \nabla\phi_a\cdot\nabla\phi_a\,dx + \frac{\alpha_1}{4}\int_\Omega |\phi_a|^4\,dx \\ & -\frac{\beta_1}{2}\int_\Omega |\phi_a|^2\,dx \\ & -\frac{1}{2}\int_0^{t_f}\int_\Omega |\phi_b|^2 \frac{\partial \mathbf{r}_b}{\partial t}\cdot\frac{\partial \mathbf{r}_b^*}{\partial t}\,dx\,dt \\ & +\frac{\gamma_1}{2}\int_\Omega \nabla\phi_b\cdot\nabla\phi_b\,dx + \frac{\alpha_1}{4}\int_\Omega |\phi_b|^4\,dx \\ & -\frac{\beta_1}{2}\int_\Omega |\phi_b|^2\,dx \\ & -\frac{E}{2}\left(\int_\Omega (|\phi_a|^2 + |\phi_b|^2)dx - 1\right). \end{aligned} \tag{40}$$

where

$$V_1 = W_0^{1,2}(\Omega;\mathbb{C}^2)\times W^{1,2}(\Omega\times[0,t_f];\mathbb{R}^2)\times\mathbb{R}.$$

In such a numerical example, we set, for the normal phase, $\gamma_1 = 1$ $\alpha_1 = 1000$ (higher self-interacting level), and initially $\beta_1 = \beta_1(T) = 1050$, where T denotes the sample Ω temperature.

For the super-conducting phase b, we define $\gamma_2 = 1$, $\alpha_2 = 1.0$ (much lower self-interacting level) and $\hat{\beta}_2 = \hat{\beta}_2(T) = 60$, where $\hat{\beta}_2$ will be specified in the next lines.

Setting

$$\mathbf{r}_a(x,t) = \mathbf{C}_a e^{i\,w_a\,t}$$

$$\mathbf{r}_b(x,t) = \mathbf{C}_b e^{i\,w_b\,t}$$

where $i \in \mathbb{C}$ denotes the imaginary unit and $\mathbf{C}_a$ and $\mathbf{C}_b$ are appropriate vectors.

We also assume

$$\mathbf{C}_a \approx \mathbf{0}.$$

From the variation of J in ϕ_a, we obtain the following Euler-Lagrange equation,

$$\begin{aligned} & -\phi_a|\mathbf{C}_a|^2 w_a^2 - \gamma_1 \nabla^2 \phi_a + \alpha_1 |\phi_a|^2 \phi_a - \beta_1 \phi_a - E\phi_a \\ \approx & -\gamma_1 \nabla^2 \phi_a + \alpha_1 |\phi_a|^2 \phi_a - \beta_1 \phi_a - E\phi_a \\ \approx & \ 0. \end{aligned} \tag{41}$$

Moreover, from the variation of J in ϕ_b, we obtain the following Euler-Lagrange equation,

$$\begin{aligned} & -\phi_b|\mathbf{C}_b|^2 w_b^2 - \gamma_2 \nabla^2 \phi_b + \alpha_2 |\phi_b|^2 \phi_b - \beta_2 \phi_b - E\phi_b \\ = & -\gamma_2 \nabla^2 \phi_b + \alpha_2 |\phi_a|^2 \phi_a - \hat{\beta}_2 \phi_b - E\phi_b \\ = & \ 0, \end{aligned} \tag{42}$$

where $\hat{\beta}_2 = |\mathbf{C}_b|^2 w_b^2 + \beta_2$.

We have numerically solved such a system of equations.

Here, we define

$$v_a = \frac{|\phi_a|^2}{|\phi_a|^2 + |\phi_b|^2}$$

and

$$v_b = \frac{|\phi_b|^2}{|\phi_a|^2 + |\phi_b|^2}.$$

For the solutions v_a obtained for the values corresponding to a decreasing in temperature from T_1 to T_3, $\beta_1(T_1) = 1050$, $\beta_1(T_2) = 500$ and $\beta_1(T_3) = 100$, please see figures 1, 2 and 3, respectively.

For the corresponding solutions v_b, please see figures 4, 5 and 6, respectively.

We may observe that for such solutions, we start at T_1 with a normal phase corresponding to $v_a \approx 1$ and $v_b \approx 0$, in Ω and, as the temperature decreases to T_3, we obtain a super-conducting phase b, corresponding to $v_a \approx 0$ and $v_b \approx 1$, in Ω, as expected.

Finally, we highlight at T_3 and below T_3, we may increase a lot w_b (which corresponds to increase $\hat{\beta}_2$) without qualitatively changing the solution, obtaining, for such a higher level of w_b, a much higher kinetics energy, the so-called super electric currents.

Here we present the software "SuperCond-July-2025" in MAT-LAB through which we have obtained such numerical results.

****

1. clear all

   m8=1000;

   d=1/m8;

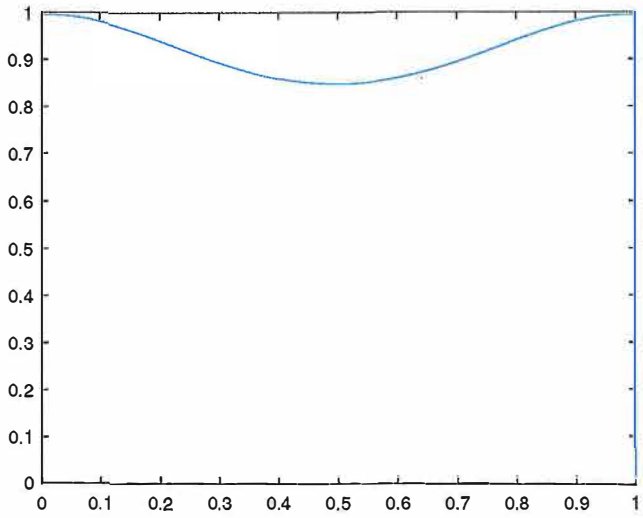

Figure 1: Graph for the normal phase $v_a(x)$ for the temperature T_1.

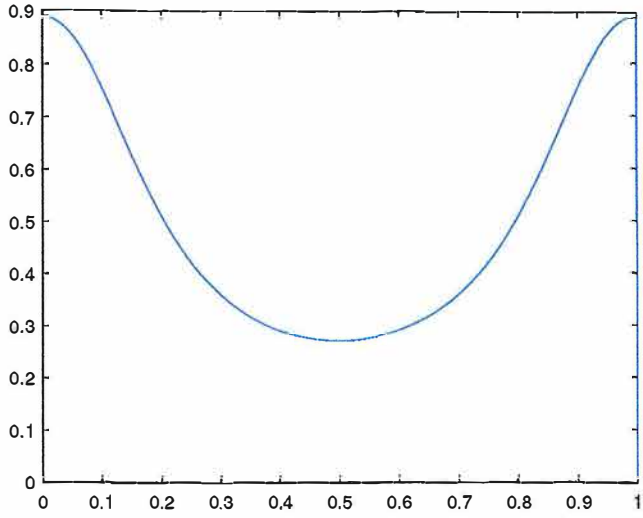

Figure 2: Graph for the normal phase $v_a(x)$ for the temperature $T_2 < T_1$.

K1=50;

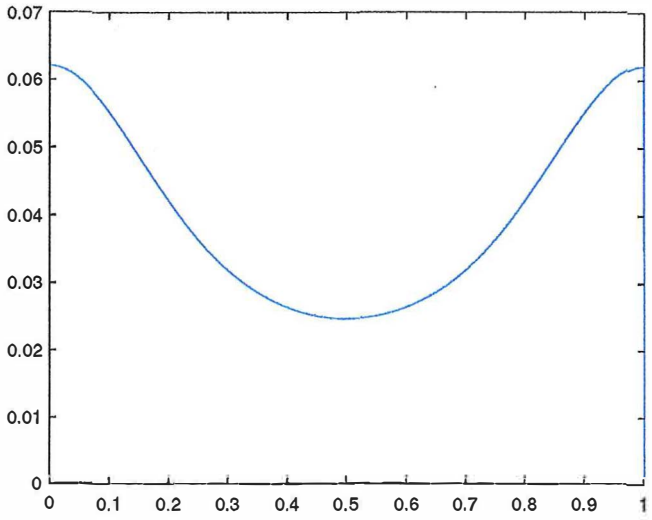

Figure 3: Graph for the normal phase $v_a(x)$ for the temperature $T_3 < T_2$.

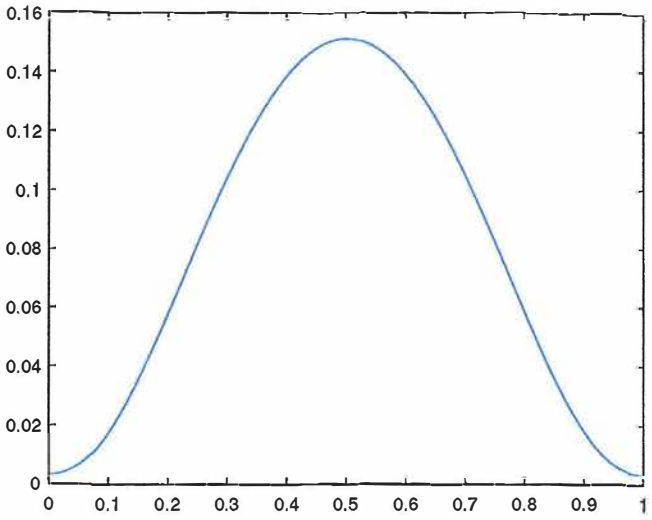

Figure 4: Graph for the super-conducting phase $v_b(x)$ for the temperature T_1.

$e1 = 10^{-10}$;

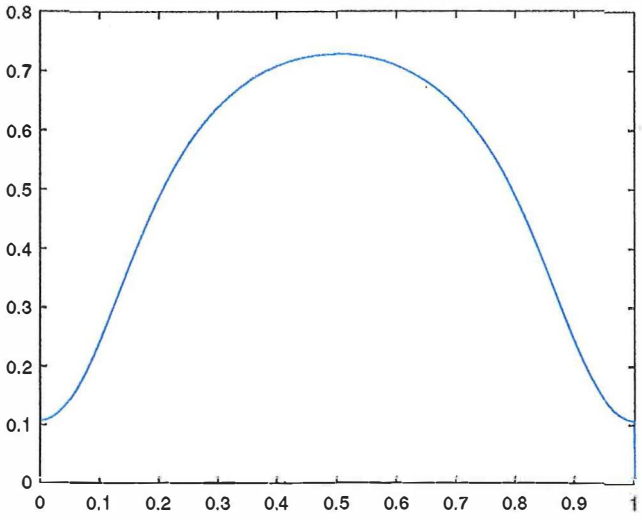

Figure 5: Graph for the super-conducting phase $v_b(x)$ for the temperature $T_2 < T_1$.

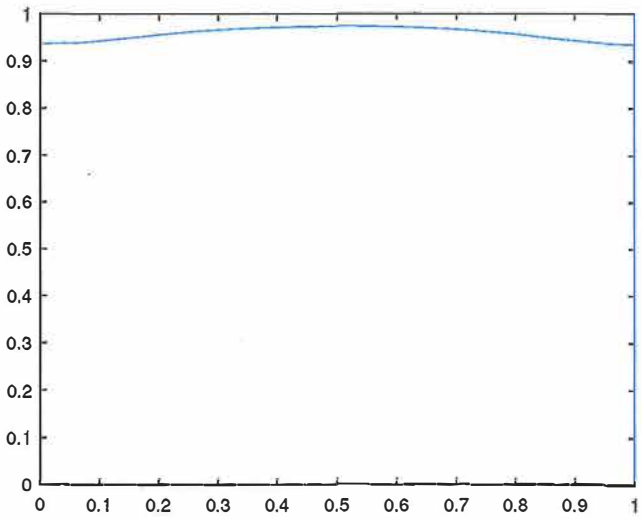

Figure 6: Graph for the super-conducting phase $v_b(x)$ for the temperature $T_3 < T_2$.

A1=1000;

A2=1.0;

B1=100;

B2=60.0;

for i=1:m8

ua(i,1)=10;

ub(i,1)=10;

end;

b12=1.0;

k=1;

while $(b12 > 10^{-4})$ && $(k < 9500)$

k

k=k+1;

S=0;

for i=1:m8

$S = S + ua(i,1)^2 * d + ub(i,1)^2 * d;$

end;

S1=sqrt(S+e1);

i=1;

$m12 = 2 + 3 * A1 * ua(i,1)^2 * d^2/S1^2 + K1 * d^2 - B1 * d^2;$

$m14 = 2 + 3 * A2 * ub(i,1)^2 * d^2/S1^2 + K1 * d^2 - B2 * d^2;$

m50(i)=1/m12;

m70(i)=1/m14;

$z1(i) = m50(i) * (ua(i,1) * d^2/S1 + 2 * A1 * ua(i,1)^3/(S1^2) * d^2);$

$z2(i) = m70(i) * (ub(i,1) * d^2/S1 + 2 * A2 * ub(i,1)^3/(S1^2) * d^2);$

for i=2:m8-1

$m12 = 2 + 3 * A1 * ua(i,1)^2 * d^2/(S1^2) + K1 * d^2 - B1 * d^2 - m50(i-1);$

$m14 = 2 + 3 * A2 * ub(i,1)^2 * d^2/(S1^2) + K1 * d^2 - B2 * d^2 - m70(i-1);$

m50(i)=1/m12;

m70(i)=1/m14;

$z1(i) = m50(i) * (ua(i,1) * d^2/S1 + 2 * A1 * ua(i,1)^3 * d^2/S1^2 + z1(i-1));$

$z2(i) = m70(i) * (ub(i,1) * d^2/S1 + 2 * A2 * ub(i,1)^3 * d^2/S1^2 + z2(i-1));$

end;

u1(m8,1)=0;

u2(m8,1)=0;

for i=1:m8-1

u1(m8-i,1)=m50(m8-i)*u1(m8-i+1,1)+z1(m8-i);

u2(m8-i,1)=m70(m8-i)*u2(m8-i+1,1)+z2(m8-i);

end;

b12=max(abs(u1-ua))+max(abs(u2-ub));

ua=u1;

ub=u2;

end;

for i=1:m8

$va(i,1) = ua(i,1)^2/(ua(i,1)^2 + ub(i,1)^2 + e1);$

$vb(i,1) = ub(i,1)^2/(ua(i,1)^2 + ub(i,1)^2 + e1);$

x1(i,1)=i*d;

end;

plot(x1,va);

****

5 Conclusion

In this article, we have presented a functional which the variation leads to a system of partial differential equations intended to model a phase transition from a normal to a superconductive electronic state.

In a near future research we intend to address similar models in superfluidity.

References

[1] J.F. Annet, Superconductivity, Superfluids and Condensates, 2nd edn. (Oxford Master Series in Condensed Matter Physics, Oxford University Press, Reprint, 2010)

[2] L.D. Landau L.D. and E.M. Lifschits, A Course of Theoretical Physics, Vol. 5- Statistical Physics, part 1. (Butterworth-Heinemann, Elsevier, reprint 2008).

[3] P. Constantin, C. Foias, Navier-Stokes equation, University of Chicago Press, Chicago, 1989.

[4] C. De Lellis , E. Brué, D. Albritton, M. Colombo, V. Giri , M. Janisch and H. Kwon, Instability and Non-uniqueness for the 2D Euler Equations, after M. Vishik (AMS-219) Volume 219 in the series Annals of Mathematics Studies, Princeton University Press, New Jersey, 2024. https://doi.org/10.1515/9780691257846

[5] M. Hamouda M, D. Han, C-Y. Jung , R. Temam, Boundary layers for the 3D primitive equations in a cube: the zero-mode, Journal of Applied Analysis and Computation. 2018; 8, No. 3, (873-889), DOI:10.11948/2018.873.

[6] A. Giorgini, A. Miranville A, R. Temam, Uniqueness and regularity for the Navier-Stokes-Cahn-Hilliard system, SIAM J. of Mathematical Analysis (SIMA).2019; 51, 3, (2535-2574), https://doi.org/10.1137/18M1223459.

[7] C. Foias, R.M. Rosa, R. Temam, Properties of stationary statistical solutions of the three-dimensional Navier-Stokes equations, J. of Dynamics and Differential Equations, Special issue in memory of George Sell. 2019; 31, 3, 1689-1741, https://doi.org/10.1007/s10884-018-9719-2.

[8] R. Temam, Navier-Stokes Equations, AMS Chelsea, reprint (2001).

[9] J.C. Tannehill, D.A. Anderson, R.H. Pletcher, *Computational Fluid Mechanics and Heat Transfer,* 2nd edn., Taylor and Francis, Philadelphia, PA, 1997.

[10] J.C. Strikwerda, finite difference cchemes and partial differential equations, second edition Philadelphia, SIAM, 2004.

[11] F.S. Botelho, "Approximate numerical procedures for the Navier-Stokes system through the generalized method of lines" Nonlinear Engineering, vol. 13, no. 1, 2024, pp. 20220376. https://doi.org/10.1515/nleng-2022-0376

[12] F. Botelho, Existence of solution for the Ginzburg-Landau system, a related optimal control problem and its computation by the generalized method of lines, Applied Mathematics and Computation, 2012; 218 (11976-11989).

[13] F.S. Botelho, An approximate proximal numerical procedure concerning the generalized method of lines. Mathematics 2022, 10(16), 2950; https://doi.org/10.3390/math10162950.

[14] F. Botelho Functional Analysis and Applied Optimization in Banach Spaces, (Springer Switzerland, 2014).

[15] F.S. Botelho, Functional analysis, calculus of variations and numerical methods in physics and engineering. Boca Raton, Florida, USA CRC Taylor and Francis; 2020.

[16] F.S. Botelho, Advanced Calculus and its Applications in Variational Quantum Mechanics and Relativity Theory, CRC Taylor and Francis, Florida, 2021.

[17] S. Sheng and Z. Shao, Concentration of mass in the pressureless limit of the Euler equations of one-dimensional compressible fluid flow, Nonlinear Analysis, Real world applications, 52, (2020), 103039. https://doi.org/10.1016/j.nonrwa.2019.103039

[18] R.A. Adams and J.F. Fournier, Sobolev Spaces, 2nd edn. (Elsevier, New York, 2003).

ISSN: 0162-5519

Established in 1978 by Prof. R. M. Santilli at Harvard University Hadronic Journal and Algebras, Groups and Geometries have been regularly published since 1978 without publication charges and are among the few remaining independent refereed journals.

This Journal publishes advances research papers and Ph. D. theses in any field of mathematics without publication charges.

For subscription, format and any other information please visit the website http://www.hadronicpress.com

HADRONIC PRESS INC.
35246 U. S. 19 North Suite 215
Palm Harbor, FL 34684, U.S.A.
http://www.hadronicpress.com
Email: info@hadronicpress.com
Phone: +1-727-946-0427

HADRONIC JOURNAL Volume 48, Number 3, September 2025

H/P HADRONIC PRESS, INC.